

January 2009

# The Los Cabos Lectures

## Dark Matter Halos

*Simon White*

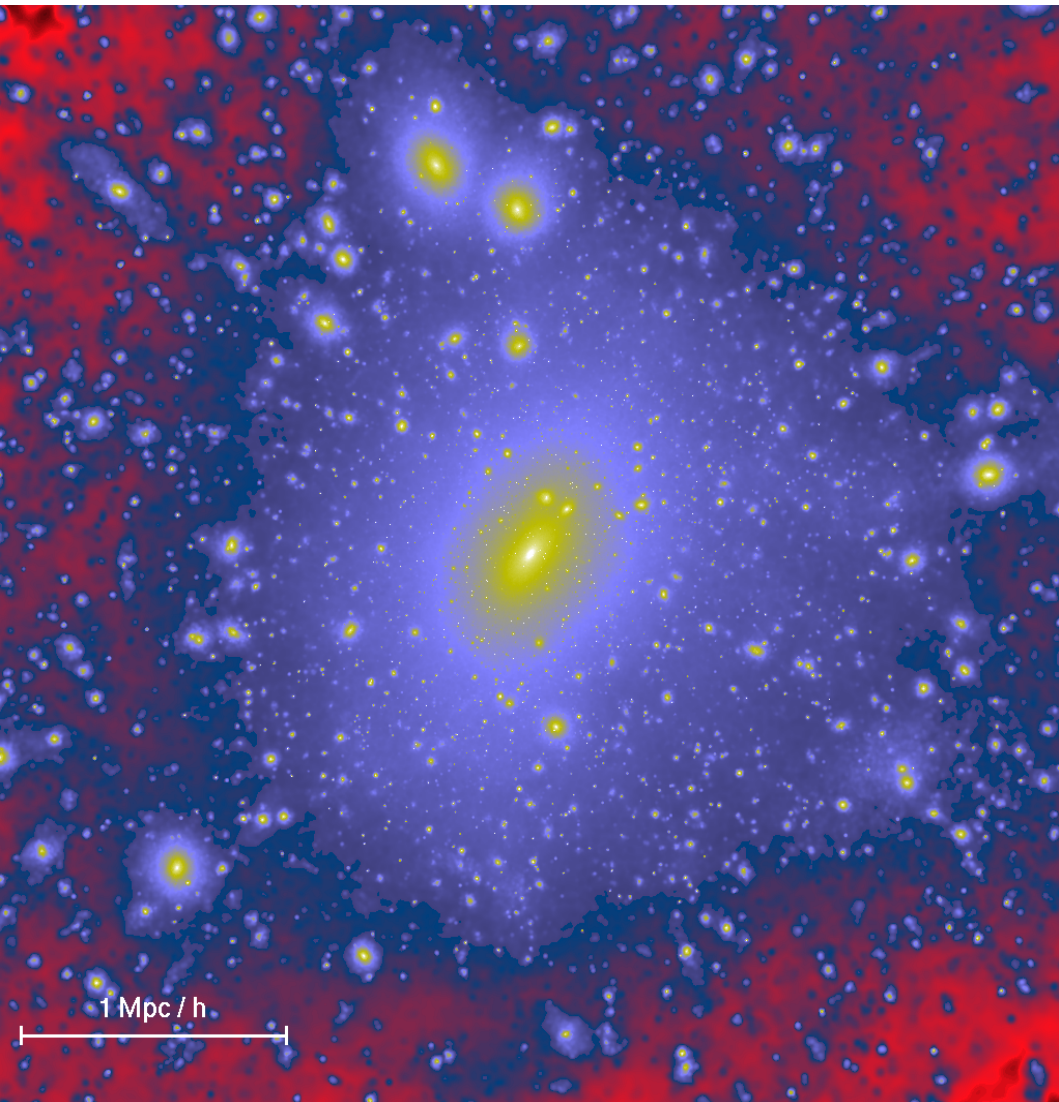
*Max Planck Institute for Astrophysics*

# Dark matter halos are the basic units of nonlinear structure

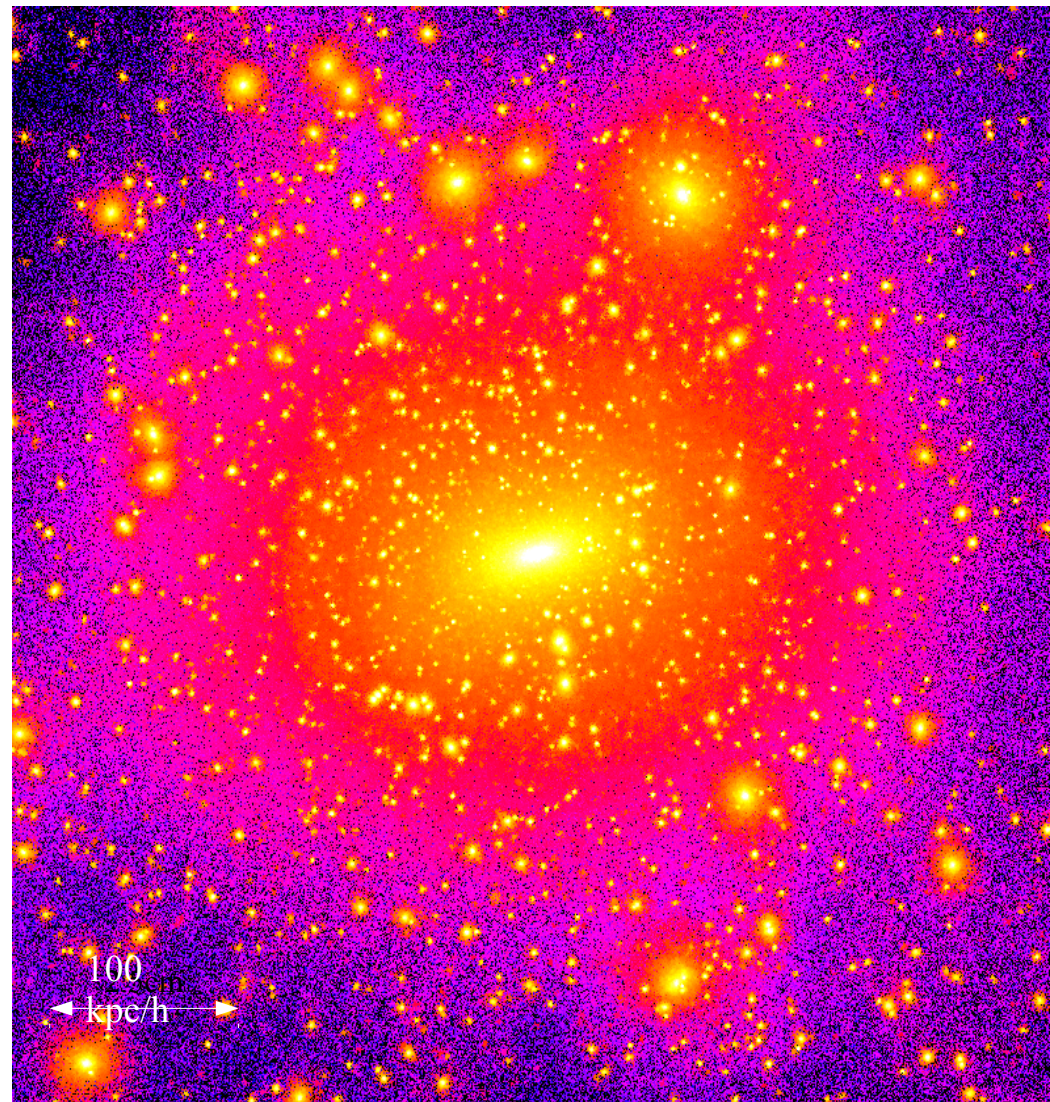
- Is all dark matter part of some halo?
- Was this always the case?
- How do halos grow? accretion? merging?
- How are they distributed?
- What is their internal structure?
  - density profile
  - shape
  - subhalo population – mass/radial distributions, evolution
  - caustics
- How do these properties affect DM detection experiments?
- How can they be used to test the standard paradigm?
- How do they affect/are they affected by the baryonic matter

# $\Lambda$ CDM halos

A rich galaxy cluster halo  
Springel et al 2001



A 'Milky Way' halo  
Power et al 2002



# A simple model for structure formation

In linear theory in a dust universe

$$\delta(\mathbf{x}, z) = D(z) \delta_o(\mathbf{x}) = (2\pi)^{-3/2} D(z) \int d^3k \delta_k \exp(-i \mathbf{k} \cdot \mathbf{x})$$

where we define  $D(0) = 1$

Consider the smoothed density field

$$\delta_s(\mathbf{x}, z; k_c) = (2\pi)^{-3/2} D(z) \int_{|\mathbf{k}| < k_c} d^3k \delta_k \exp(-i \mathbf{k} \cdot \mathbf{x})$$

and define  $\langle \delta_s(\mathbf{x}, z; k_c)^2 \rangle_x = D^2(z) \sigma_o^2(k_c)$ ,  $M_s = 6\pi^2 \rho_o k_c^{-3}$

As  $k_c$  grows from 0 to  $\infty$ , the smoothing mass decreases from  $\infty$  to 0, and  $\delta_s(\mathbf{x}, z; k_c)$  executes a random walk

For a gaussian linear overdensity field

$$\Delta \delta_s = \delta_s(\mathbf{x}, z; k_c + \Delta k_c) - \delta_s(\mathbf{x}, z; k_c)$$

is independent of  $\delta_s$  and has variance  $D^2 \Delta \sigma_o^2$

---- A Markov random walk ----

# The “Press & Schechter” Ansatz

A uniform spherical “top hat” perturbation virialises when its extrapolated linear overdensity is  $\delta_c \approx 1.69$

Assume that at redshift  $z$ , the mass element initially at  $\mathbf{x}$  is part of a virialised object with the largest mass  $M$  for which

$$\delta_s(\mathbf{x}, z; k_c(M)) \geq \delta_c$$

This is the Markov walk's first upcrossing of the barrier  $\delta_s = \delta_c$

The fraction of all points with first upcrossing below  $k_c$  is then the fraction of cosmic mass in objects with mass above  $M_s(k_c)$

$$\rightarrow n(M, z) dM = \frac{\rho_0}{\sqrt{(2\pi)M^2}} \frac{\delta_c}{D\sigma_0} \frac{d \ln \sigma_0^2}{d \ln M} \exp -\frac{1}{2} \left( \frac{\delta_c}{D\sigma_0} \right)^2$$

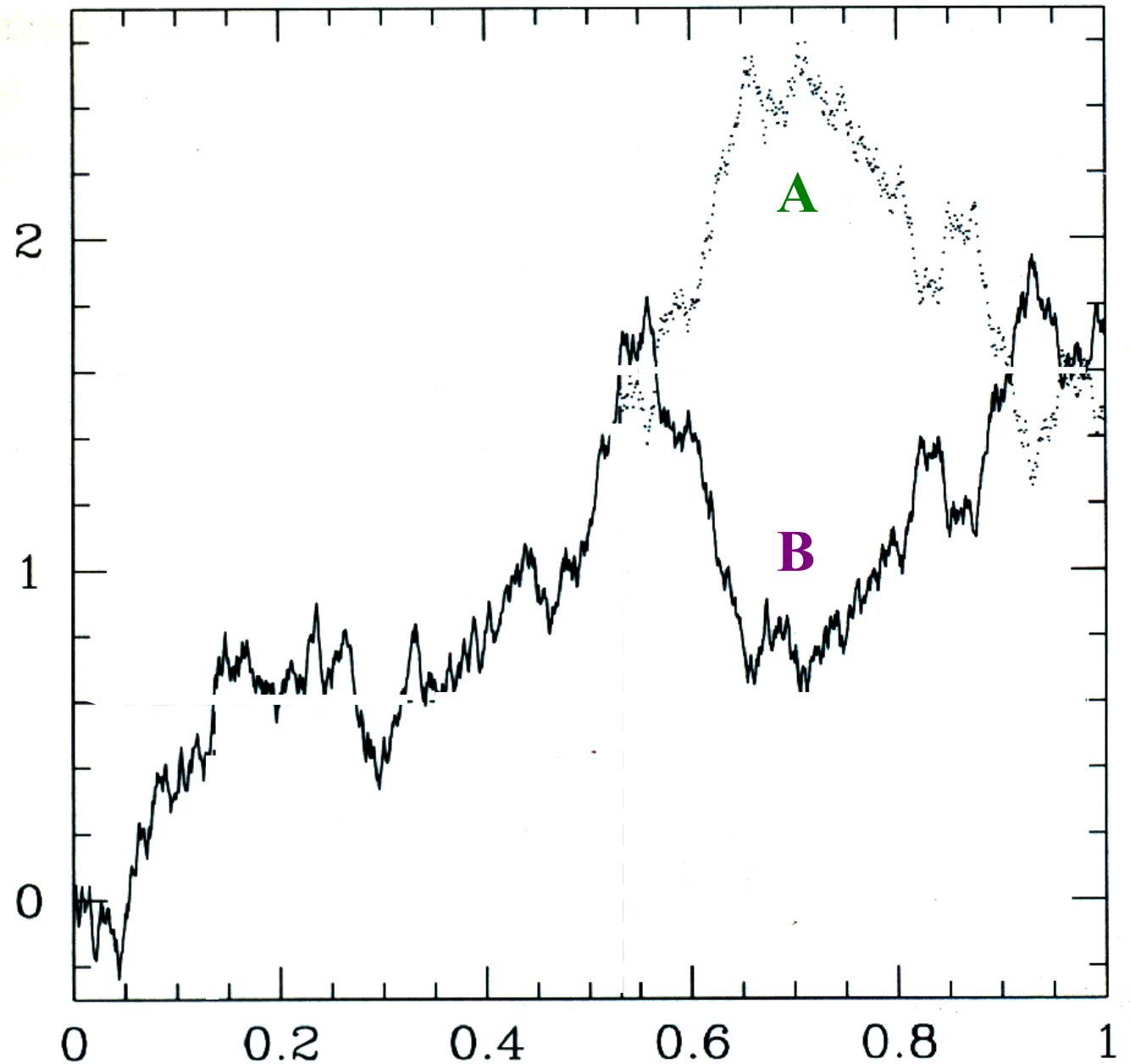
# Overdensity vs smoothing at a given position

If the density field is smoothed using a sharp filter in  $k$ -space, then each step in the random walk is independent of all earlier steps

A Markov process

The walks shown at positions **A** and **B** are equally probable

initial overdensity  $\delta_s/D(\tau)$



variance  $\sigma_0^2(k_c)$  of smoothed field

← mass

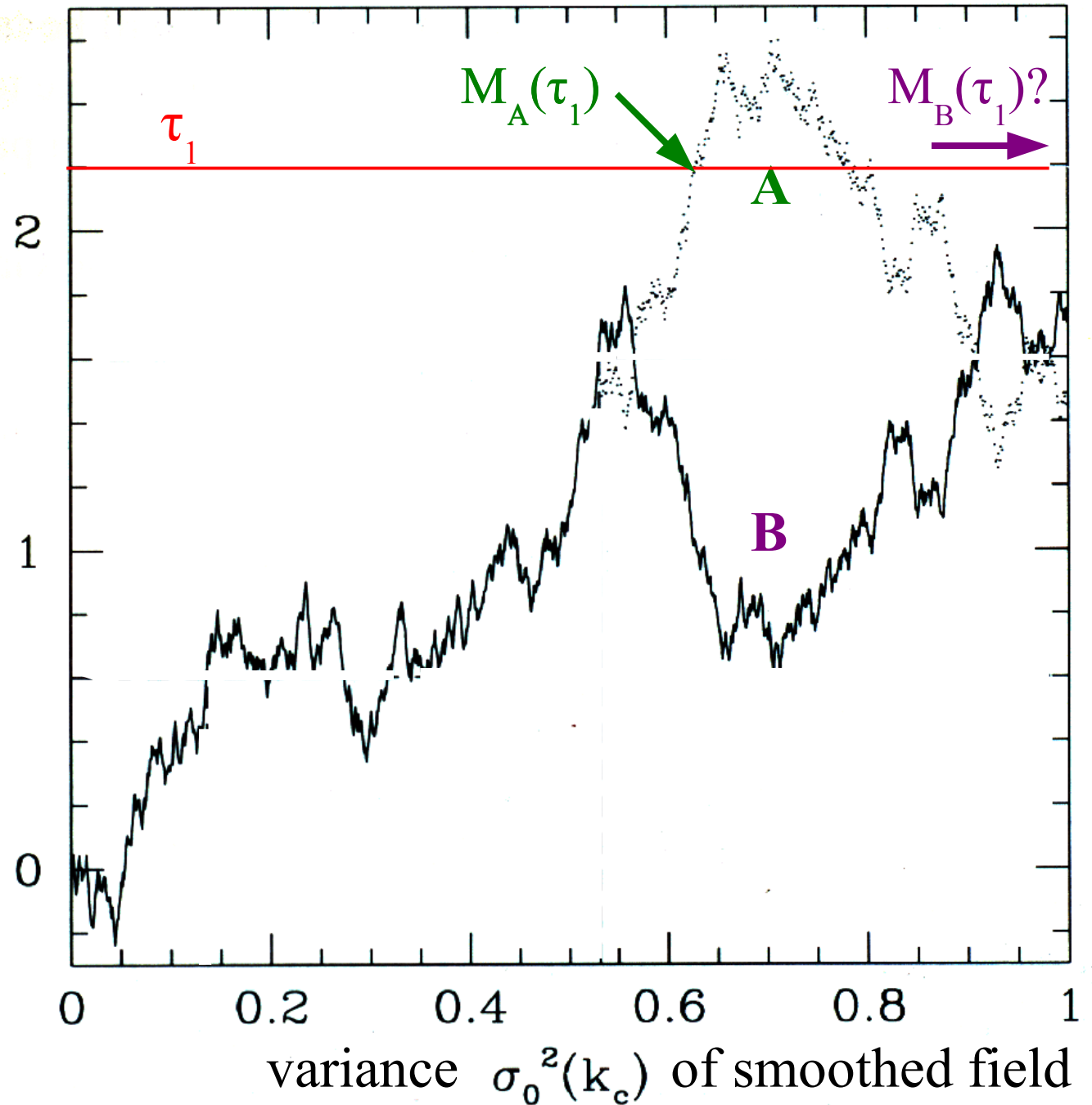
← spatial scale

# Overdensity vs smoothing at a given position

At an early time  $\tau_1$   
**A** is part of a quite massive halo

**B** is part of a very low mass halo or no halo at all

initial overdensity  $\delta_s/D(\tau)$



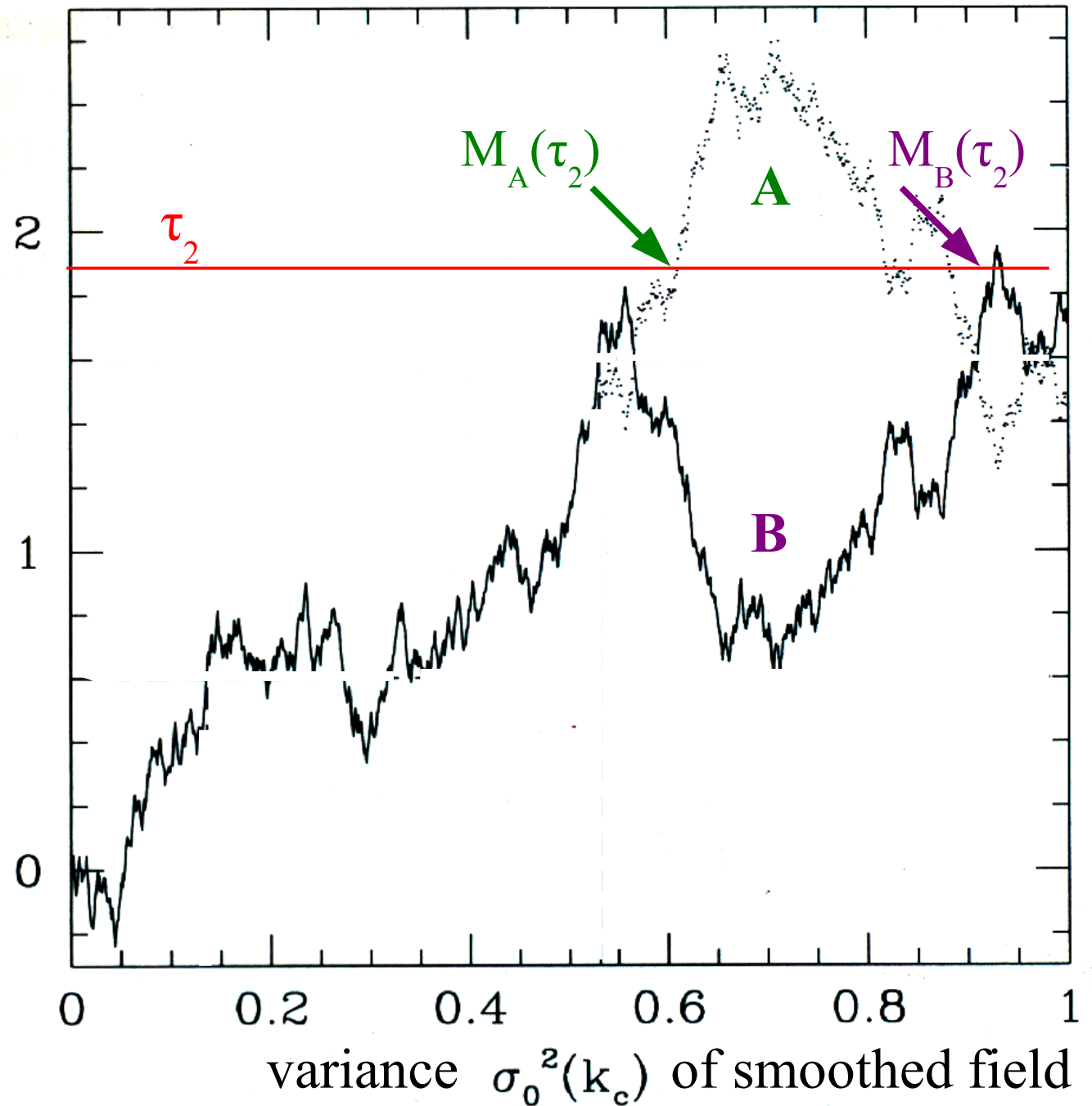
← mass

← spatial scale

# Overdensity vs smoothing at a given position

Later, at time  $\tau_2$   
**A**'s halo has grown slightly by accretion  
**B** is now part of a moderately massive halo

initial overdensity  $\delta_s/D(\tau)$



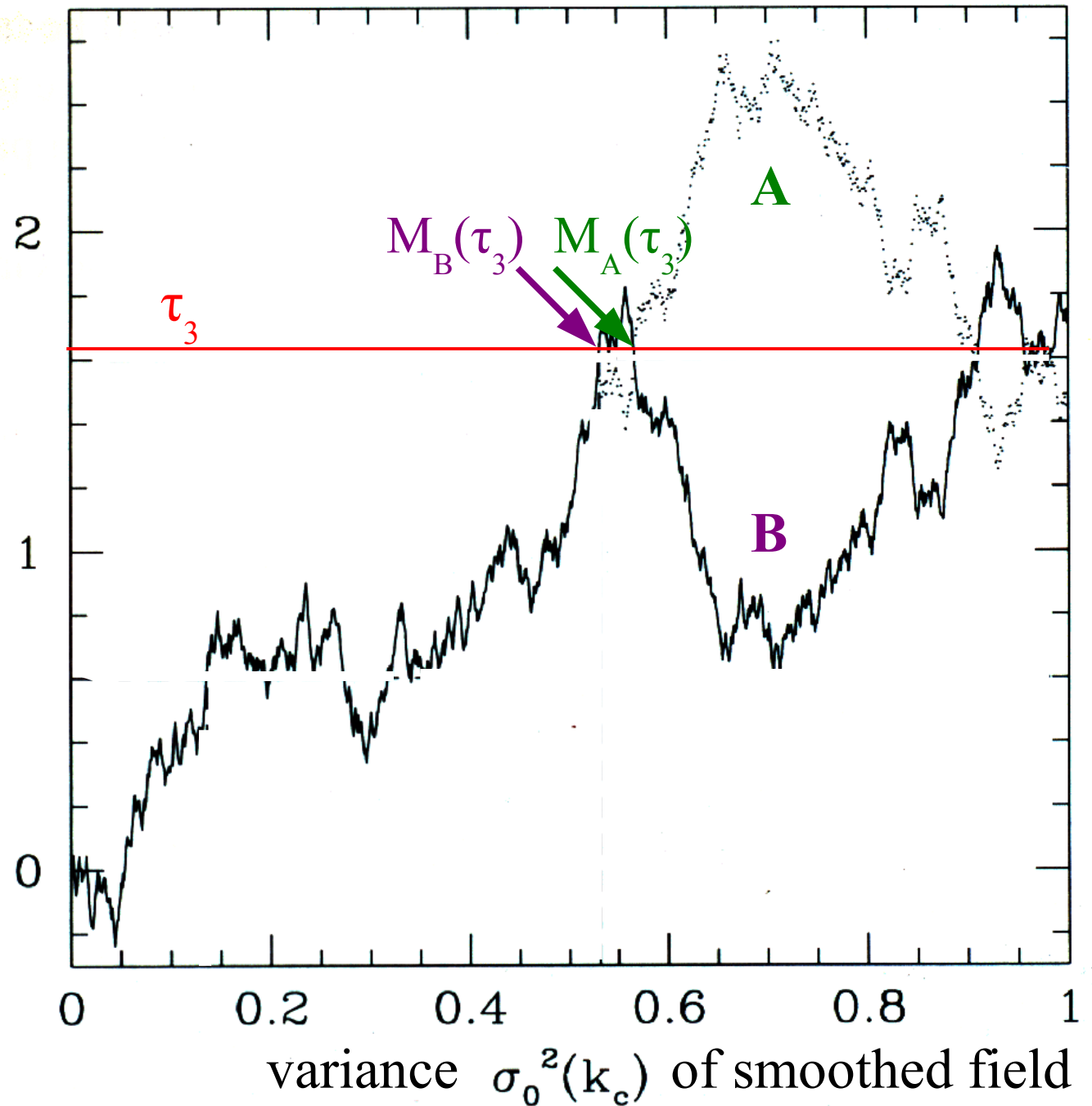
← mass  
← spatial scale

# Overdensity vs smoothing at a given position

A bit later, time  $\tau_3$   
**A**'s halo has grown further by accretion

**B**'s halo has merged again and is now more massive than **A**'s halo

initial overdensity  $\delta_s/D(\tau)$



← mass

← spatial scale

# Overdensity vs smoothing at a given position

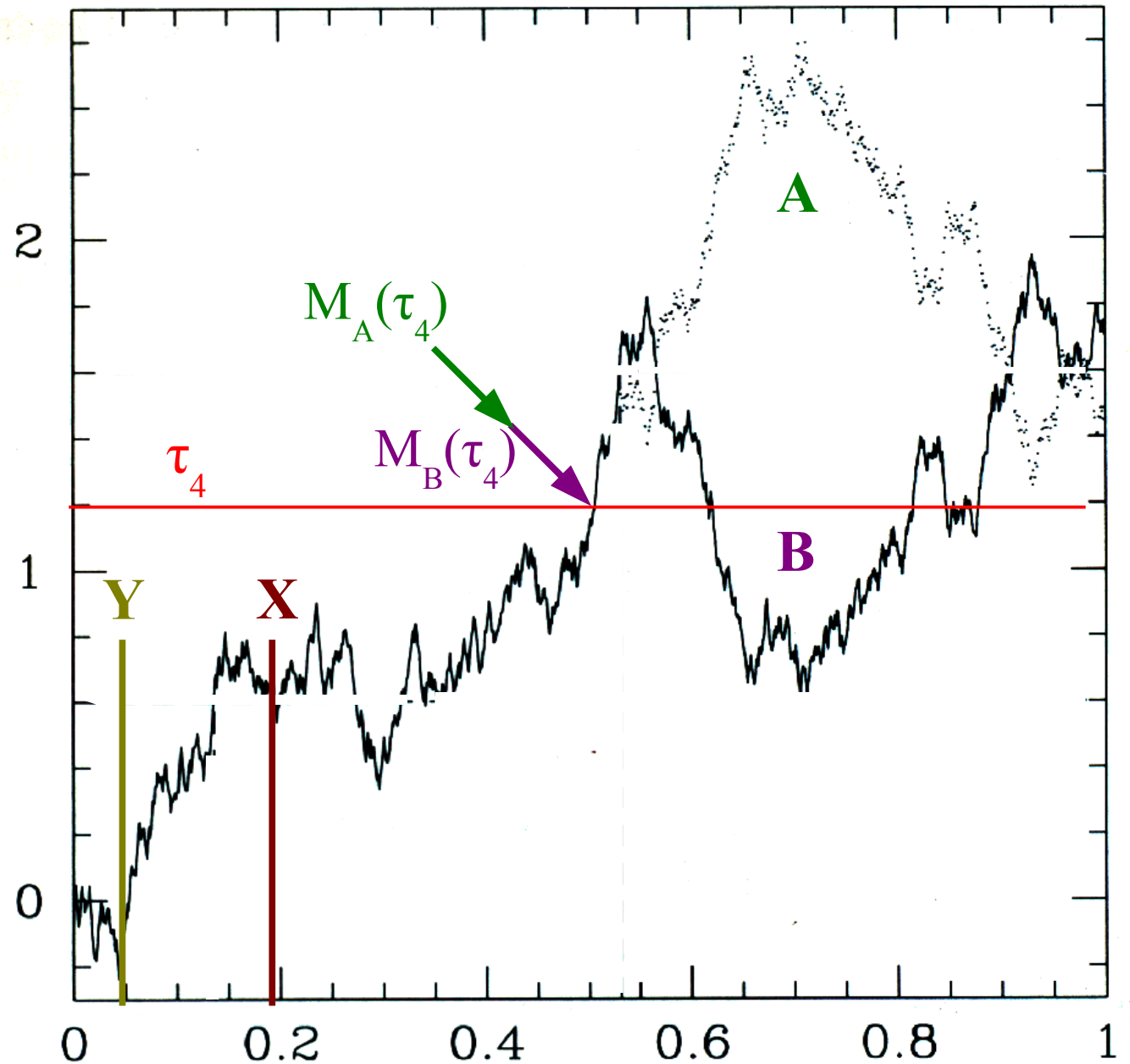
Still later, e.g.  $\tau_4$

**A** and **B** are part of halos which follow identical merging/accretion histories

On scale **X** they are embedded in a high density region.

On larger scale **Y** in a low density region

initial overdensity  $\delta_s/D(\tau)$



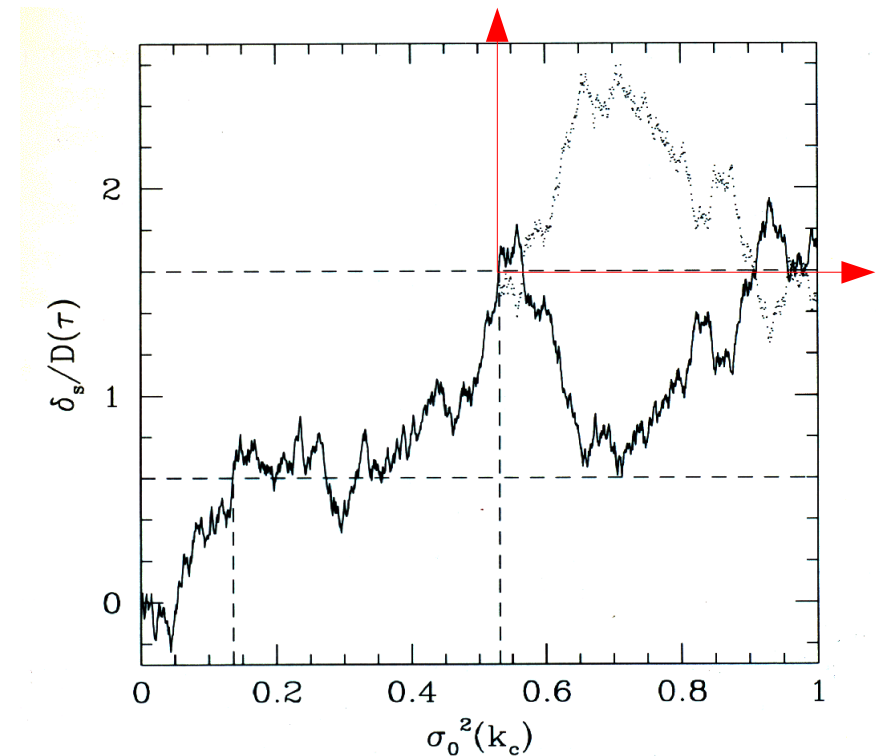
variance  $\sigma_0^2(k_c)$  of smoothed field

← mass

← spatial scale

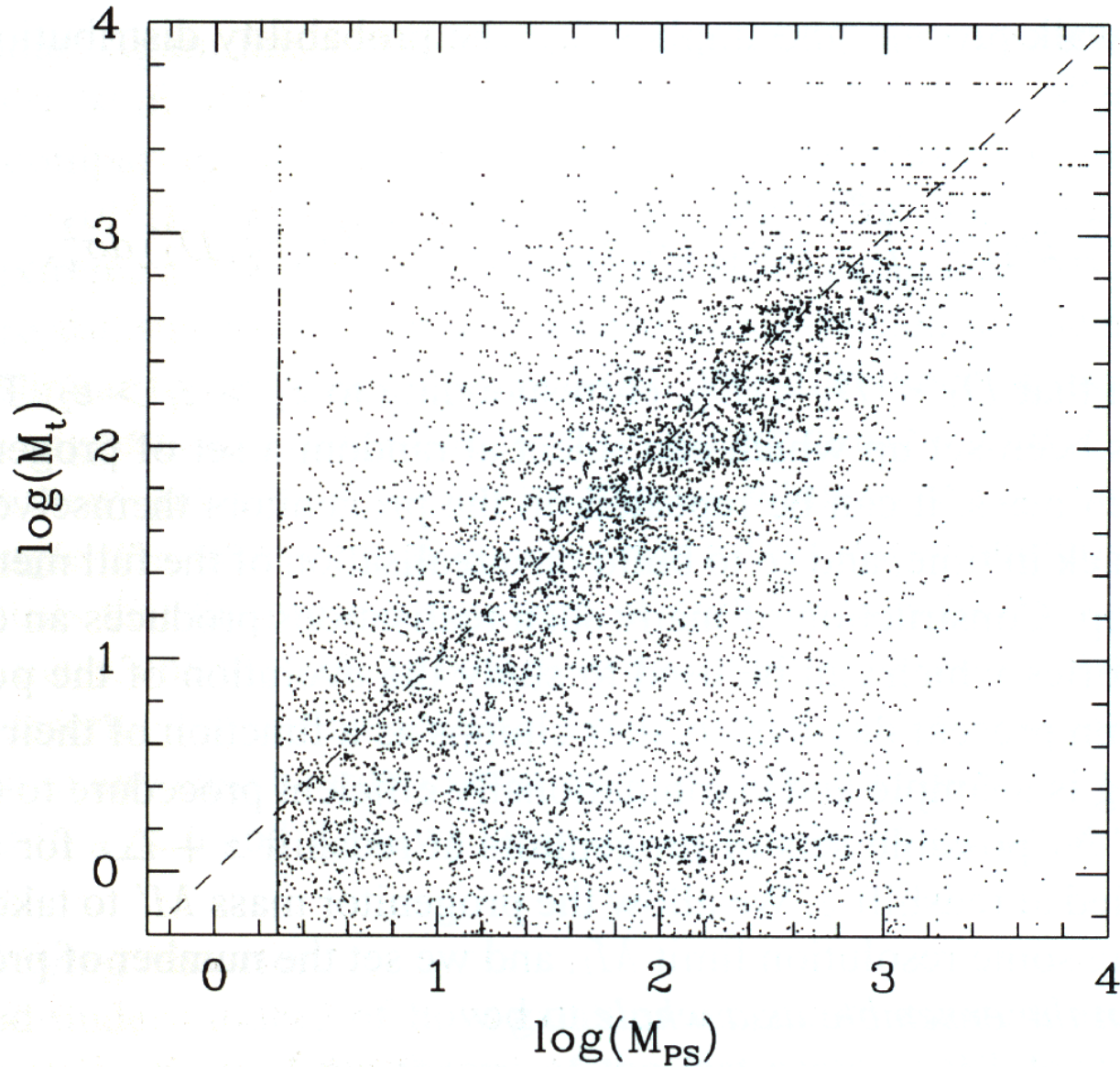
# Consequences of the Markov nature of EPS walks

- The assembly history of a halo is independent of its future
- The assembly history of a halo is independent of its environment
- The internal structure of a halo is independent of its environment
- The mass distribution of progenitors of a halo of given  $M$  and  $z$  is obtained simply by changing the origin to  $\sigma_0^2(M)$  and  $\delta_c/D(z)$
- The resulting formulae can be used to obtain descendant distributions and merger rates
- A similar argument gives formulae for the clustering bias of halos



# Does it work point by point?

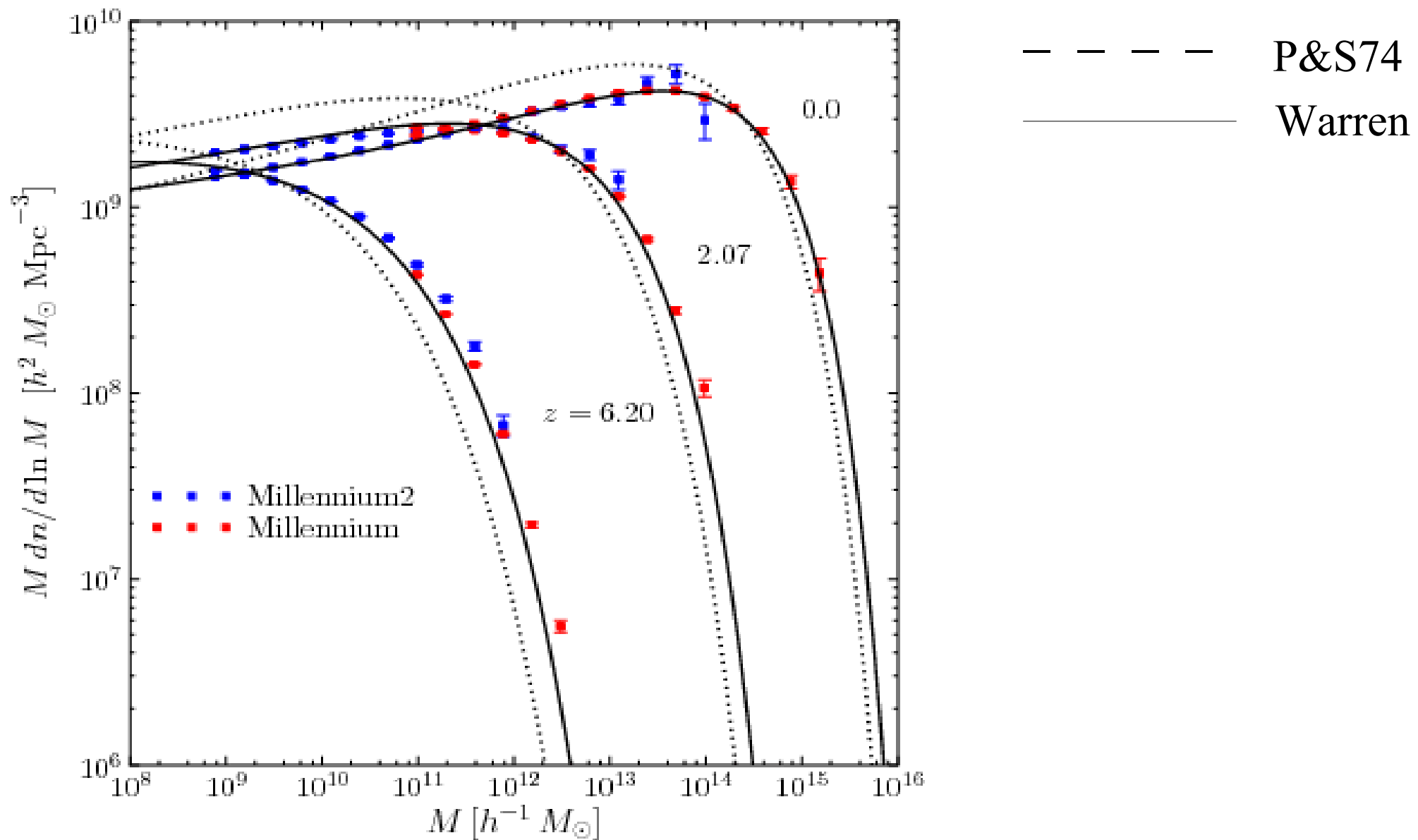
Mass of the halo in which the particle is actually found



Halo mass predicted for each particle by its own sharp k-space random walk

# Does it work statistically?

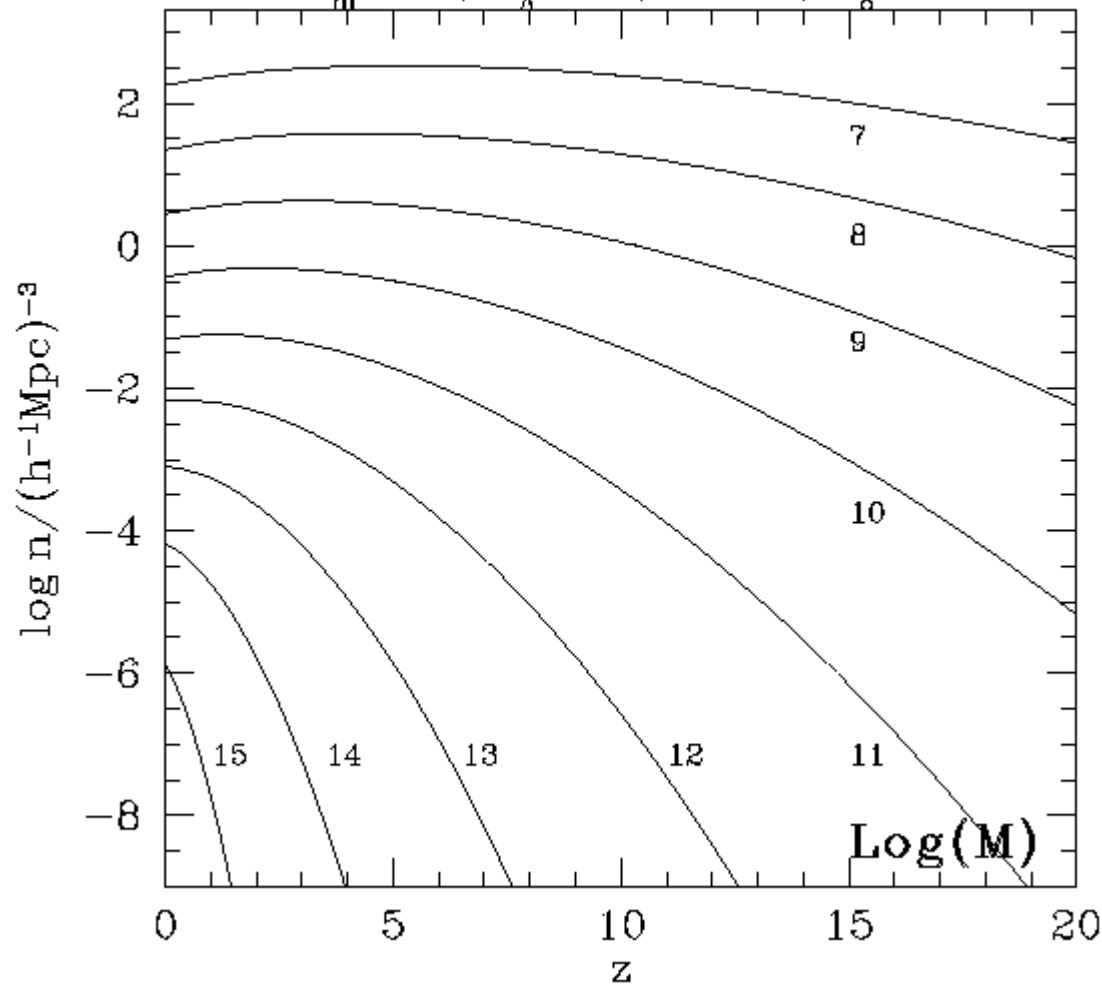
Boylan-Kolchin et al 2009



# Evolution of halo abundance in $\Lambda$ CDM

Mo & White 2002

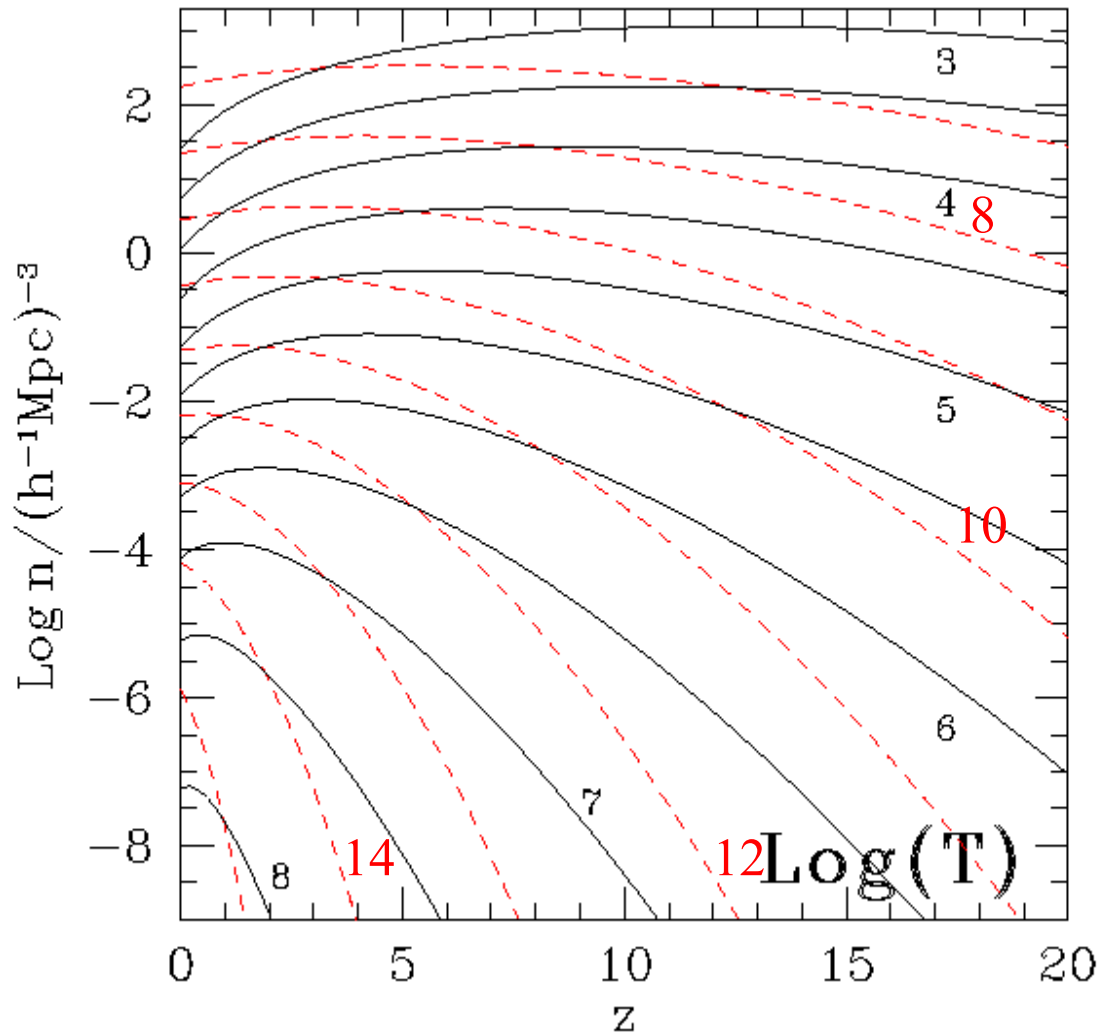
$\Omega_m=0.3, \Omega_\Lambda=0.7, h=0.7, \sigma_8=0.9$



- Abundance of rich cluster halos drops rapidly with  $z$
- Abundance of Milky Way mass halos drops by less than a factor of 10 to  $z=5$
- $10^9 M_\odot$  halos are almost as common at  $z=10$  as at  $z=0$

# Evolution of halo abundance in $\Lambda$ CDM

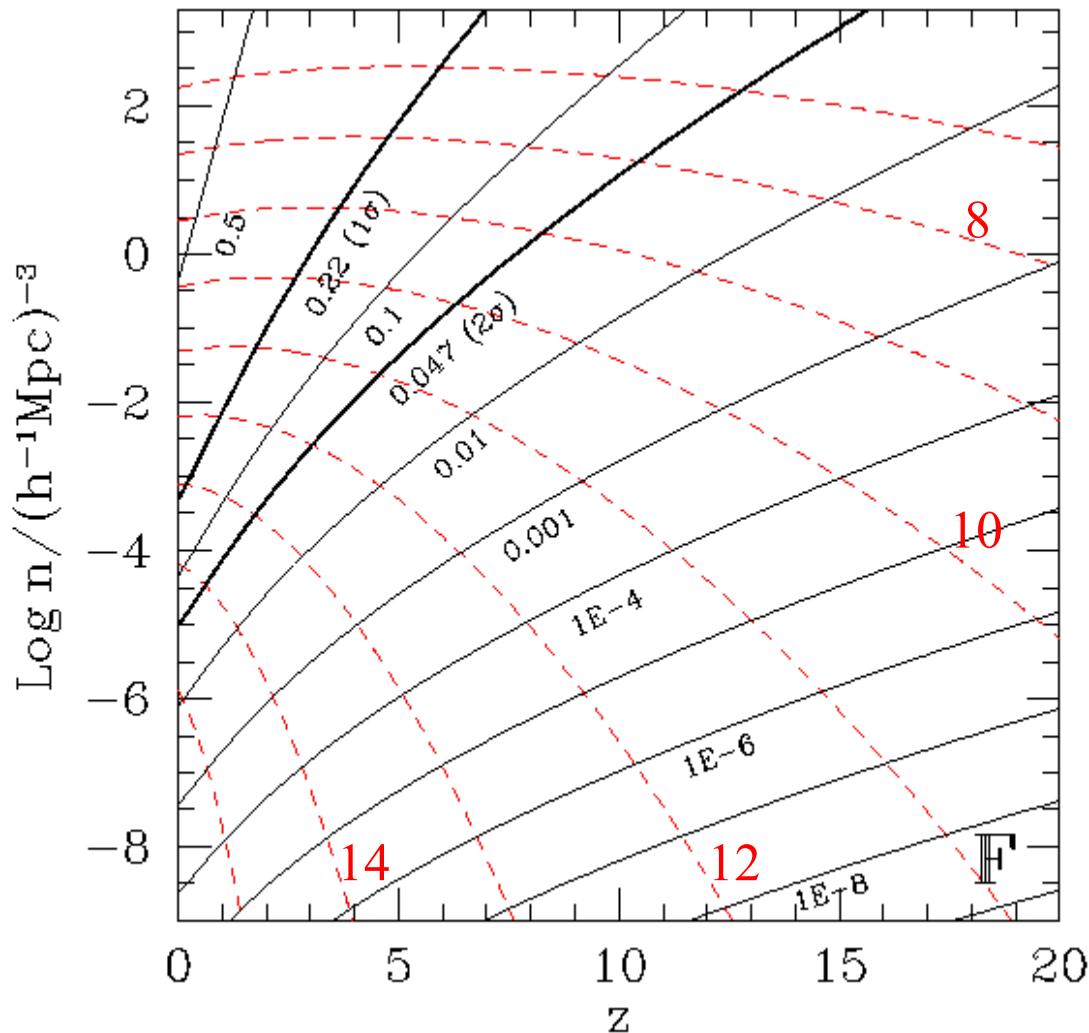
Mo & White 2002



- Temperature increases with both mass and redshift  
 $T \propto M^{2/3} (1+z)$
- Halos with virial temperature  $T = 10^7$  K are as abundant at  $z = 2$  as at  $z=0$
- Halos with virial temperature  $T = 10^6$  K are as abundant at  $z = 8$  as at  $z=0$
- Halos of mass  $> 10^{7.5} M_{\odot}$  have  $T > 10^4$  K at  $z=20$  and so can cool by H line emission

# Evolution of halo abundance in $\Lambda$ CDM

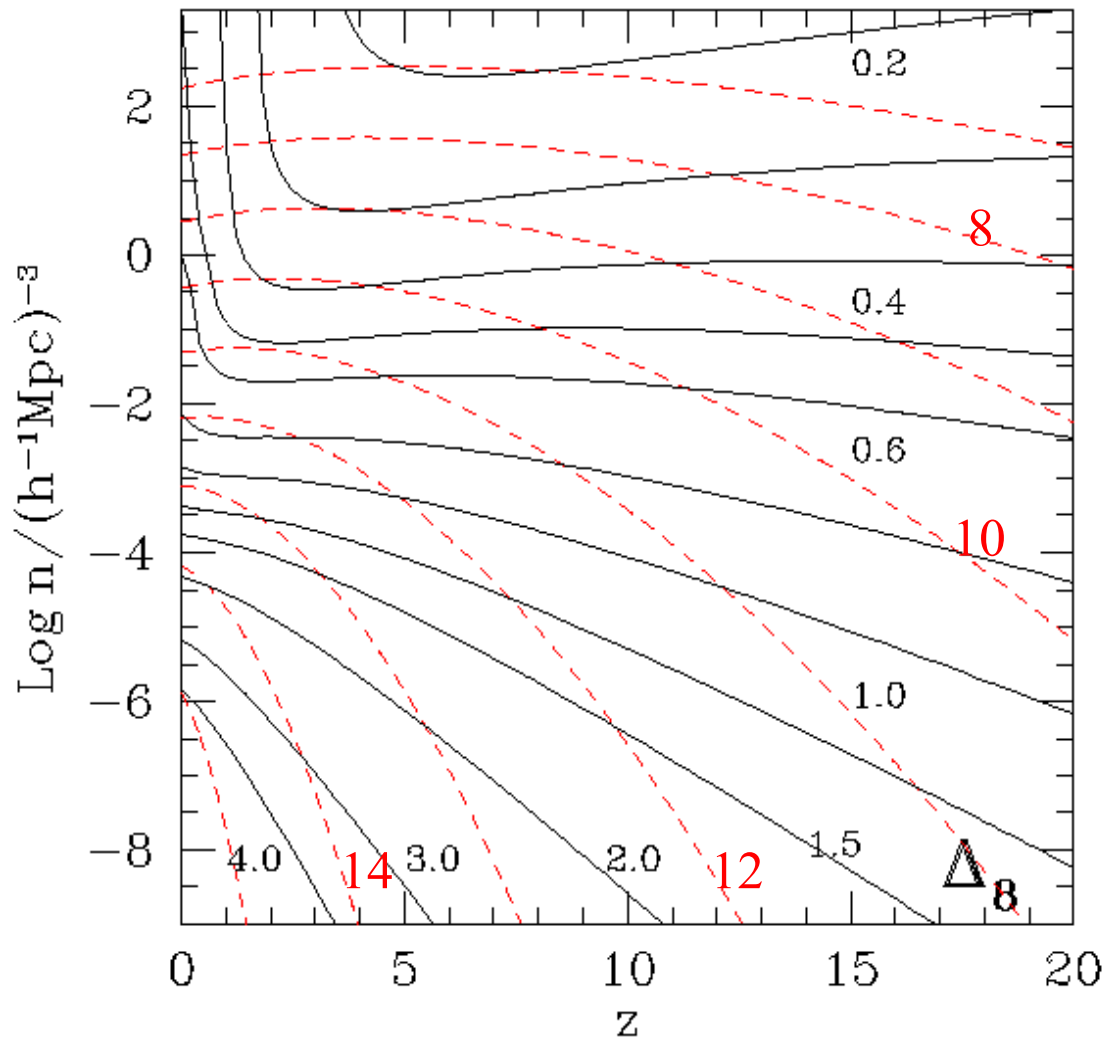
Mo & White 2002



- Half of all mass is in halos more massive than  $10^{10} M_{\odot}$  at  $z=0$ , but only 10% at  $z=5$ , 1% at  $z=9$  and  $10^{-6}$  at  $z=20$
- 1% of all mass is in halos more massive than  $10^{15} M_{\odot}$  at  $z=0$
- 40% of all mass at  $z=0$  is in halos which cannot confine photoionised gas
- 1% of all mass at  $z=15$  is in halos hot enough to cool by H line emission

# Evolution of halo abundance in $\Lambda$ CDM

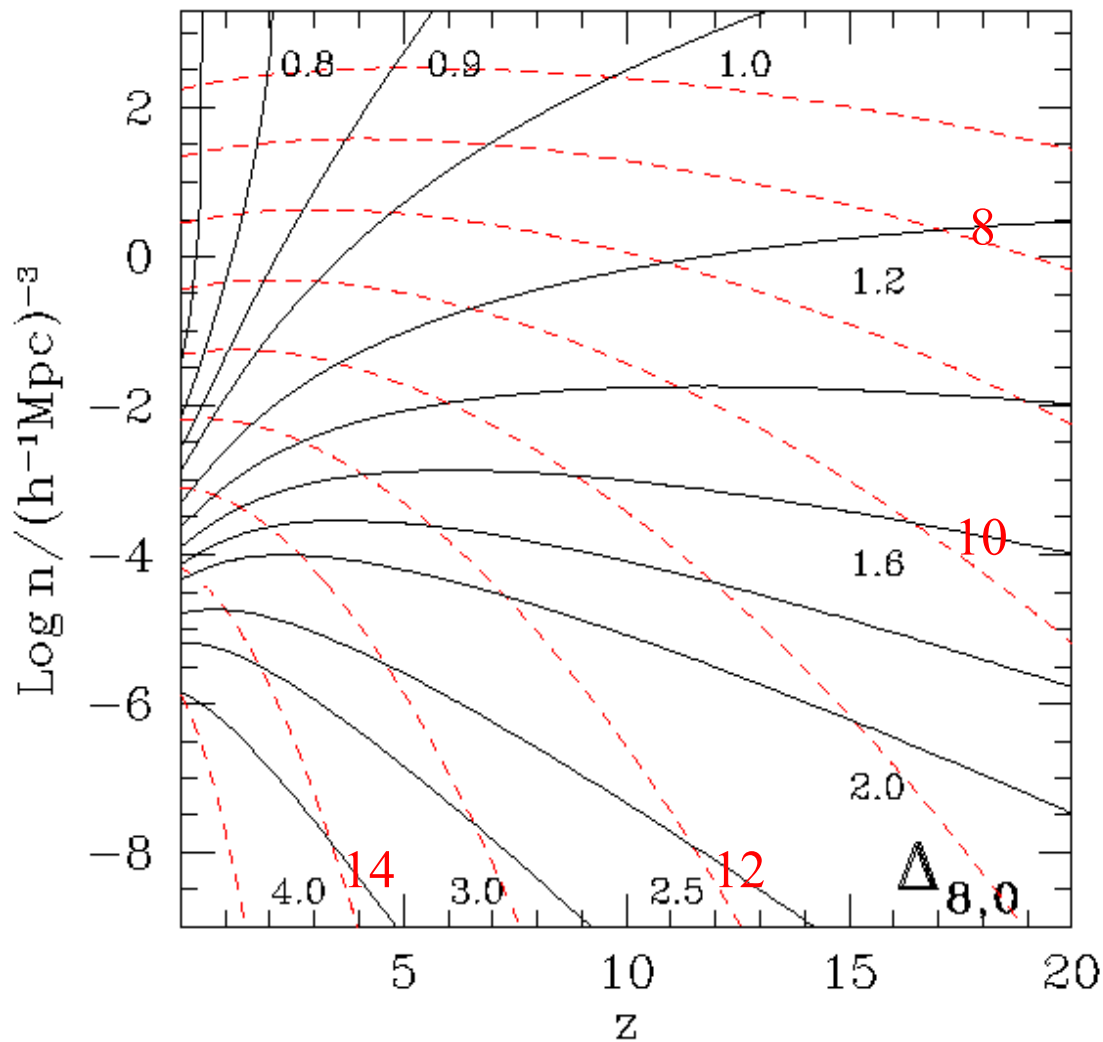
Mo & White 2002



- Halos with the abundance of  $L_*$  galaxies at  $z=0$  are equally strongly clustered at all  $z < 20$
- Halos of given mass or virial temperature are more clustered at *higher*  $z$

# Evolution of halo abundance in $\Lambda$ CDM

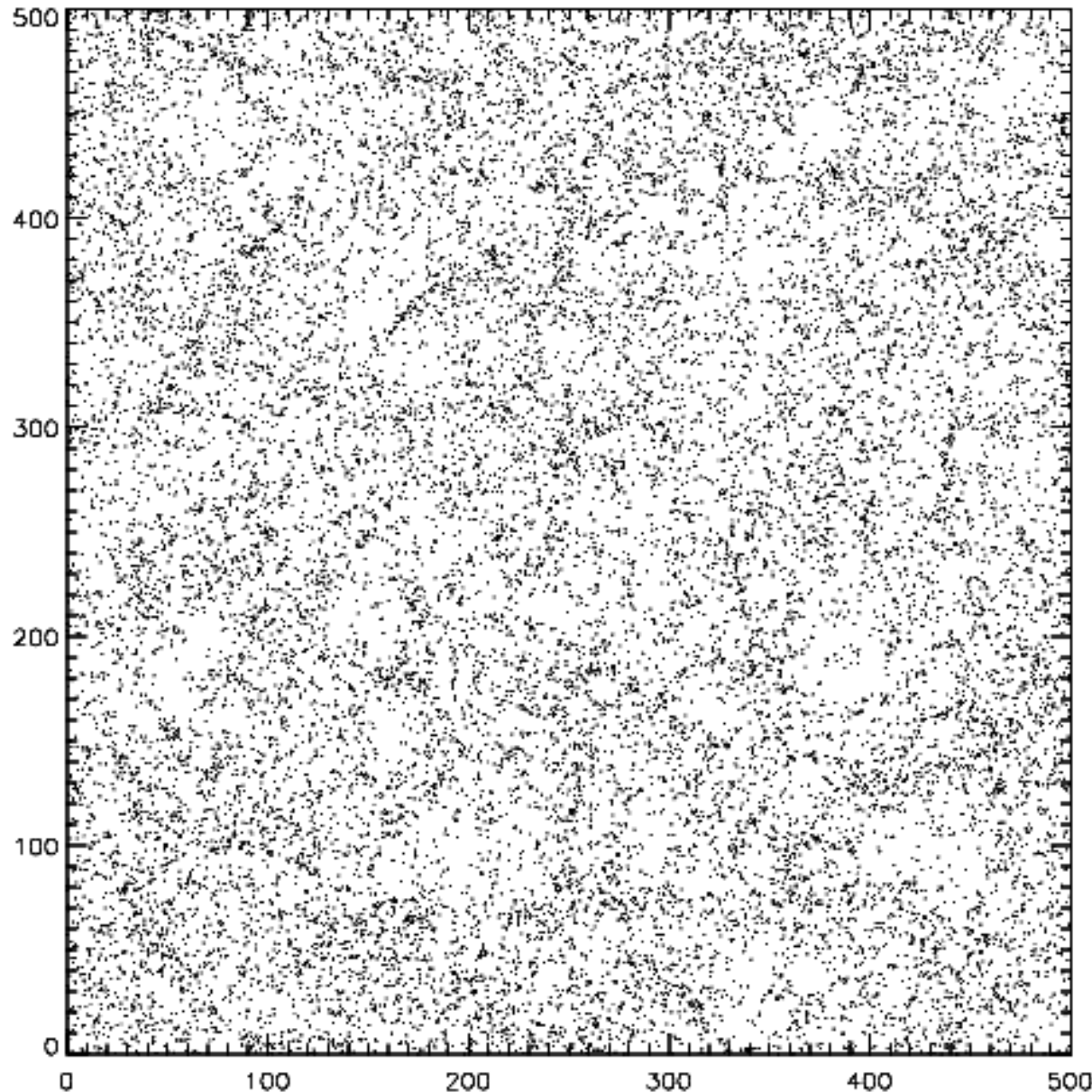
Mo & White 2002



- The remnants (stars and heavy elements) from all star-forming systems at  $z > 6$  are today more clustered than  $L_*$  galaxies
- The remnants of objects which at any  $z > 2$  had an abundance similar to that of present-day  $L_*$  galaxies are today more clustered than  $L_*$  galaxies

# Does halo clustering depend on formation history?

Gao, Springel & White 2005

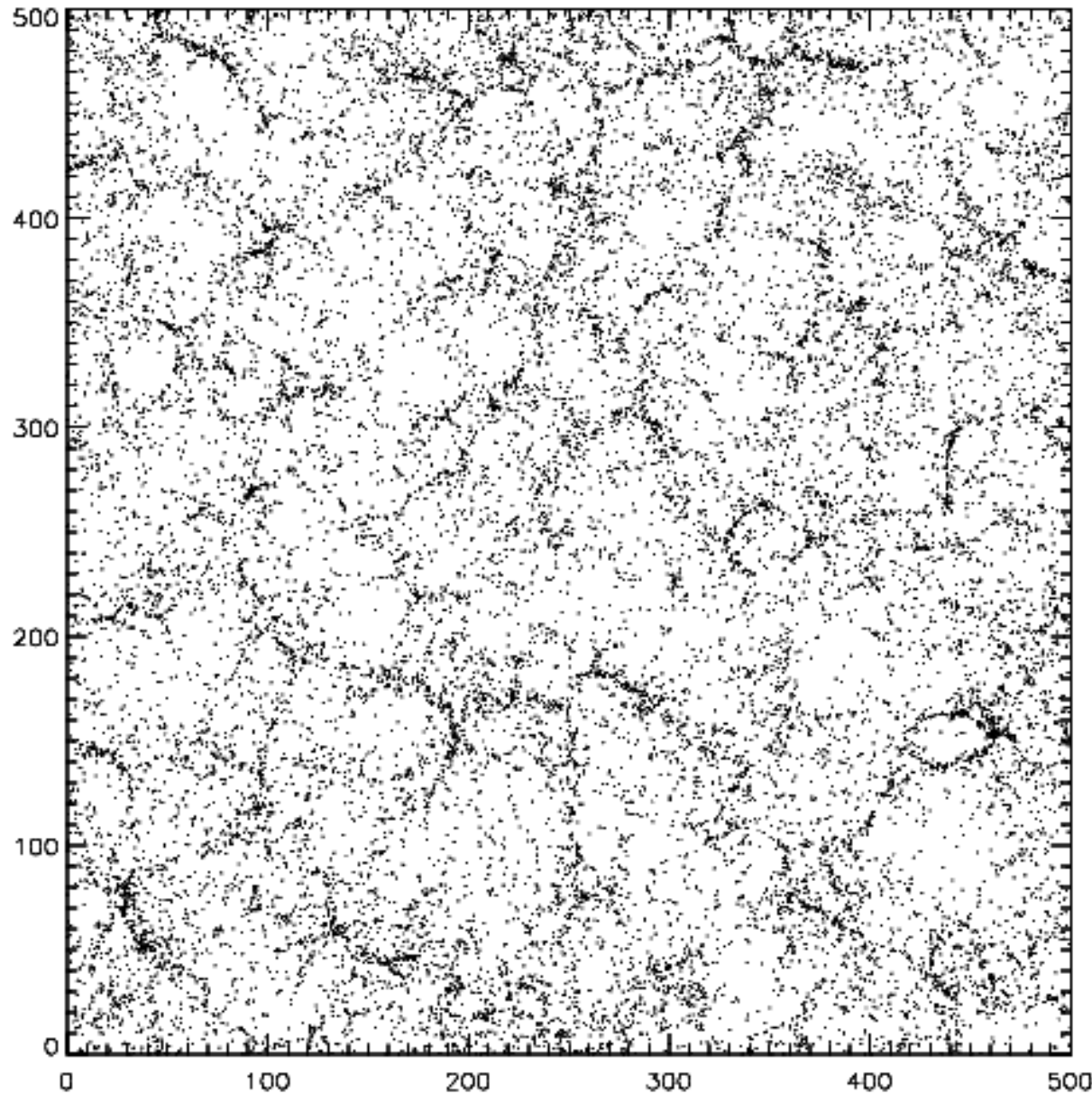


The 20% of halos with the *lowest* formation redshifts in a 30 Mpc/h thick slice

$$M_{\text{halo}} \sim 10^{11} M_{\odot}$$

# Does halo clustering depend on formation history?

Gao, Springel & White 2005

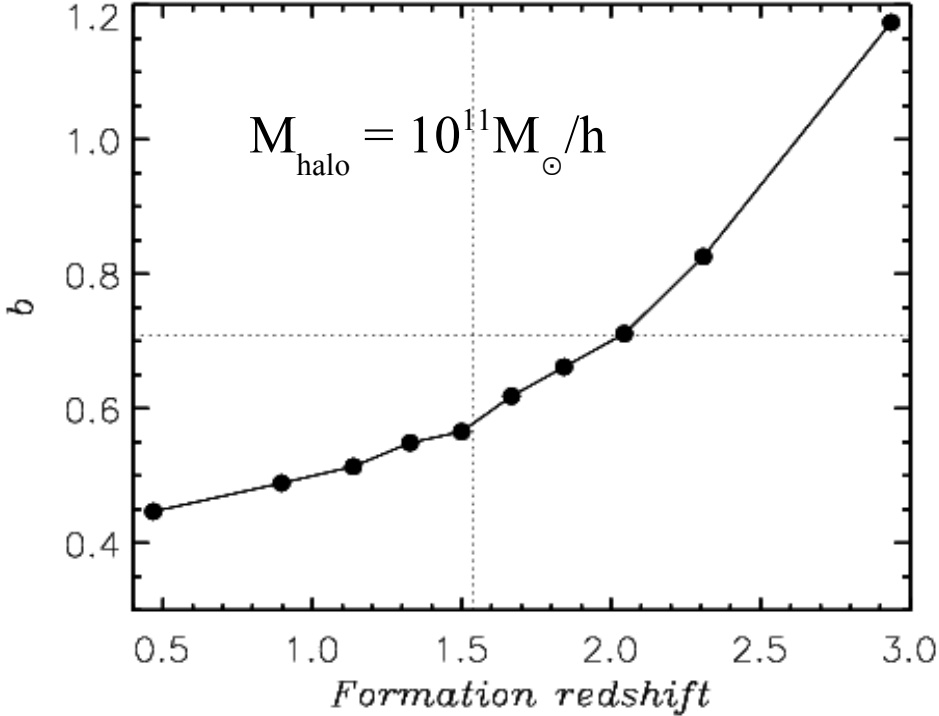


The 20% of halos with the *highest* formation redshifts in a 30 Mpc/h thick slice

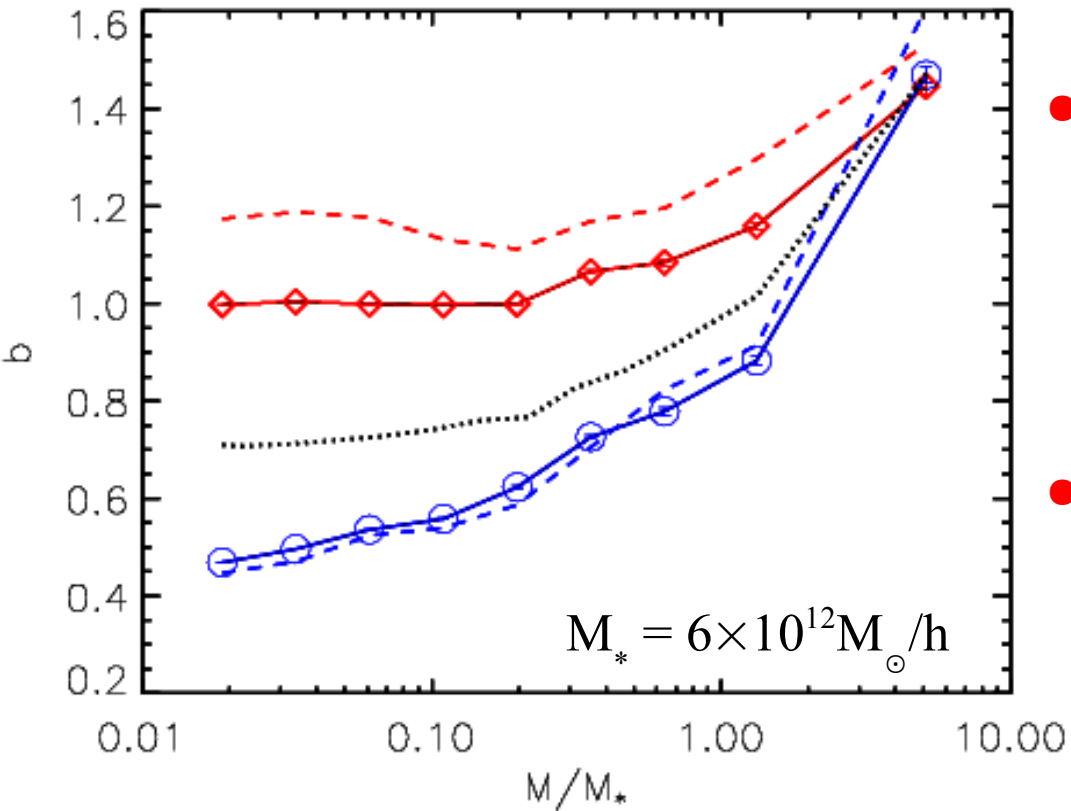
$$M_{\text{halo}} \sim 10^{11} M_{\odot}$$

# Halo bias as a function of mass and formation time

Gao, Springel & White 2005



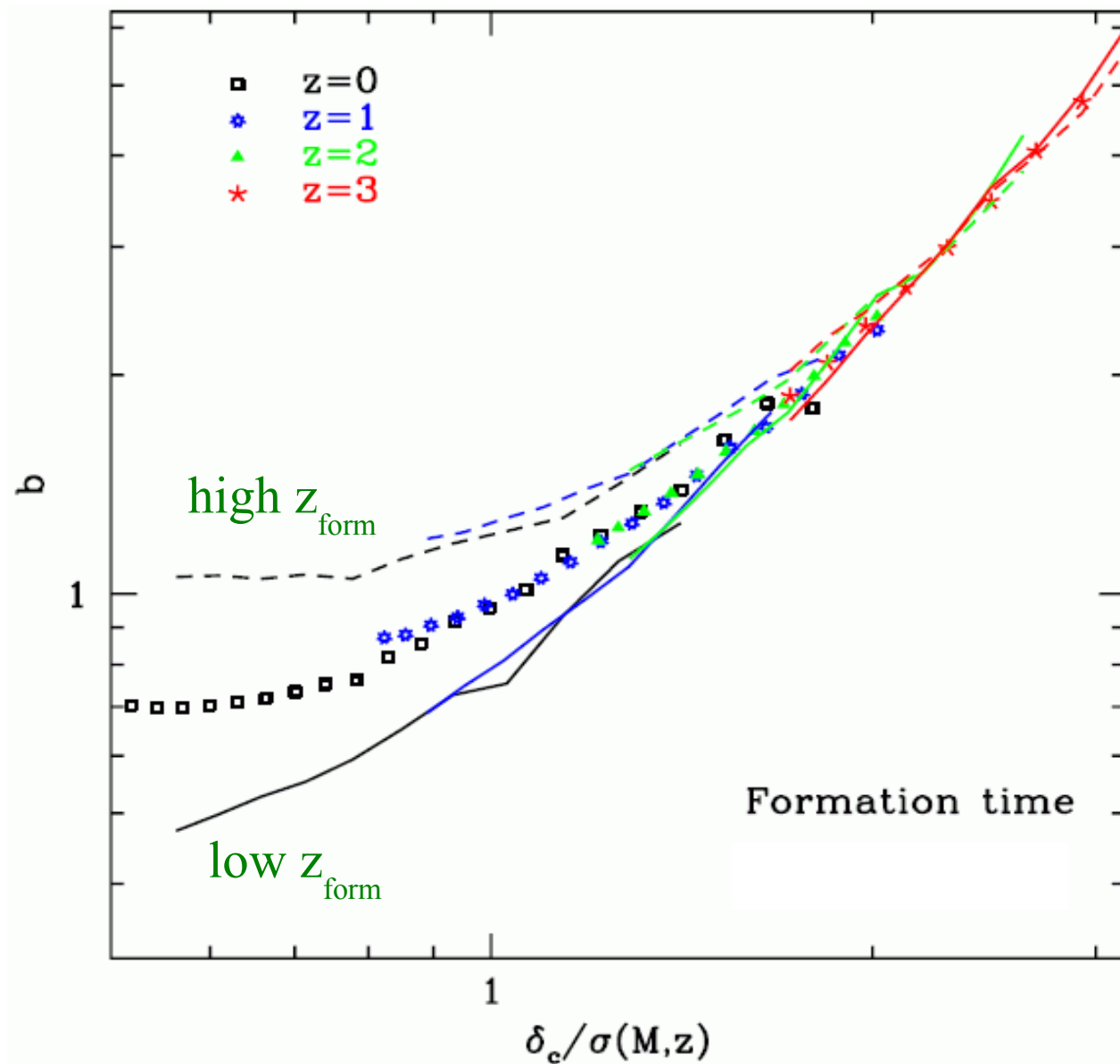
- Bias increases smoothly with formation redshift



- The dependence on formation redshift is strongest at low mass
- This dependence is consistent *neither* with excursion set theory *nor* with HOD models

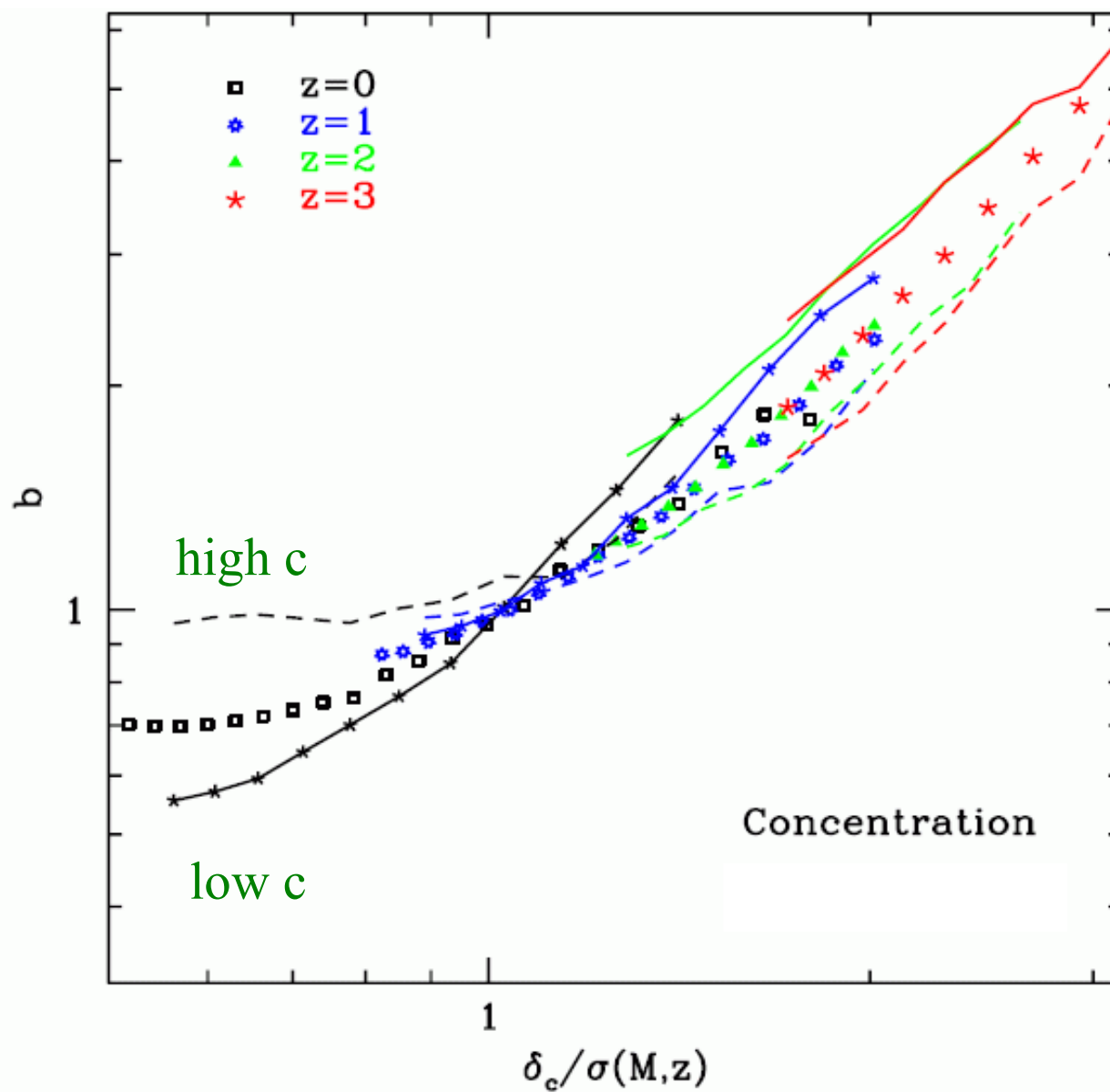
# Bias as a function of $\nu$ and formation time

Gao & White 2007



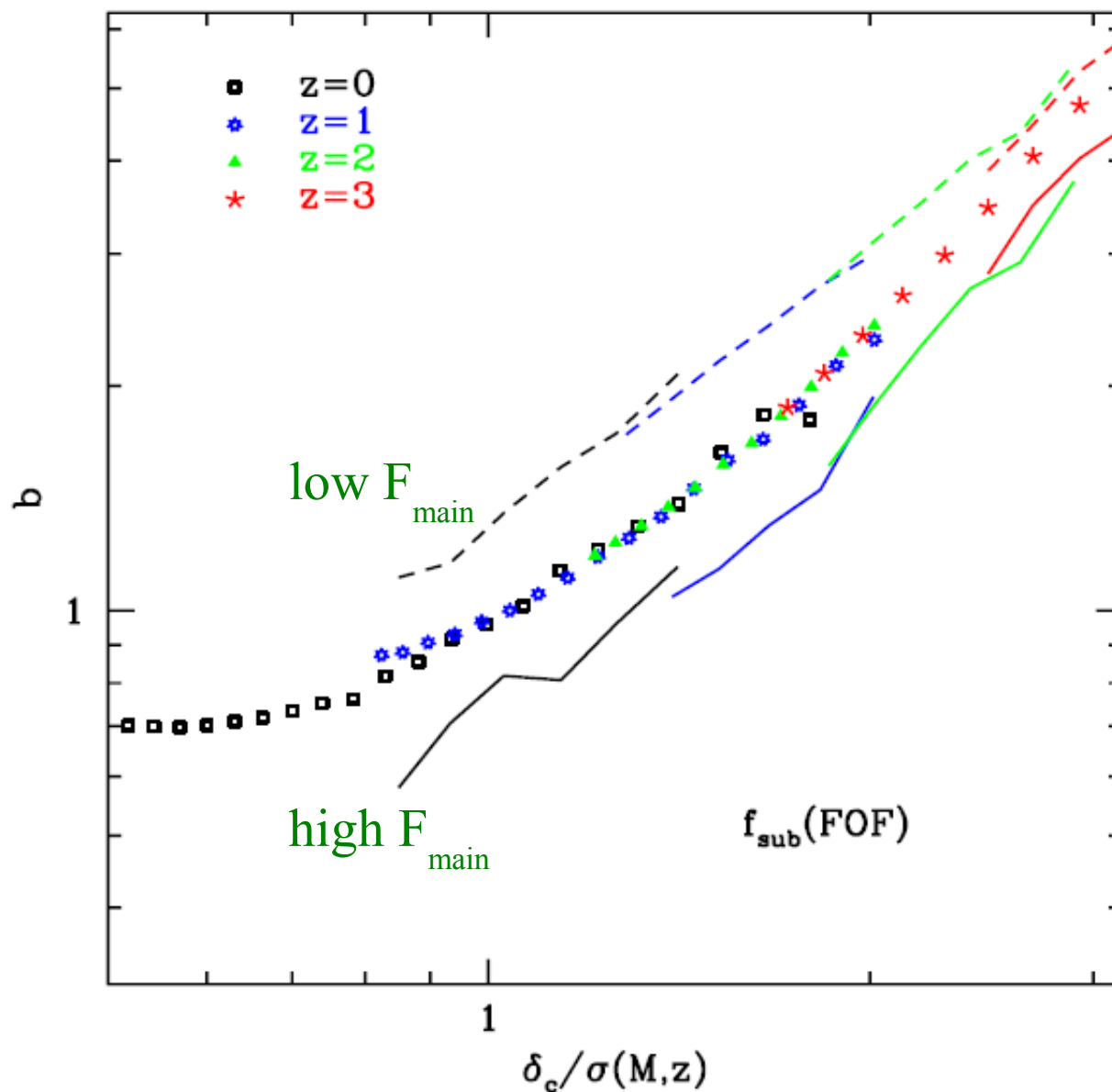
# Bias as a function of $v$ and concentration

Gao & White 2007



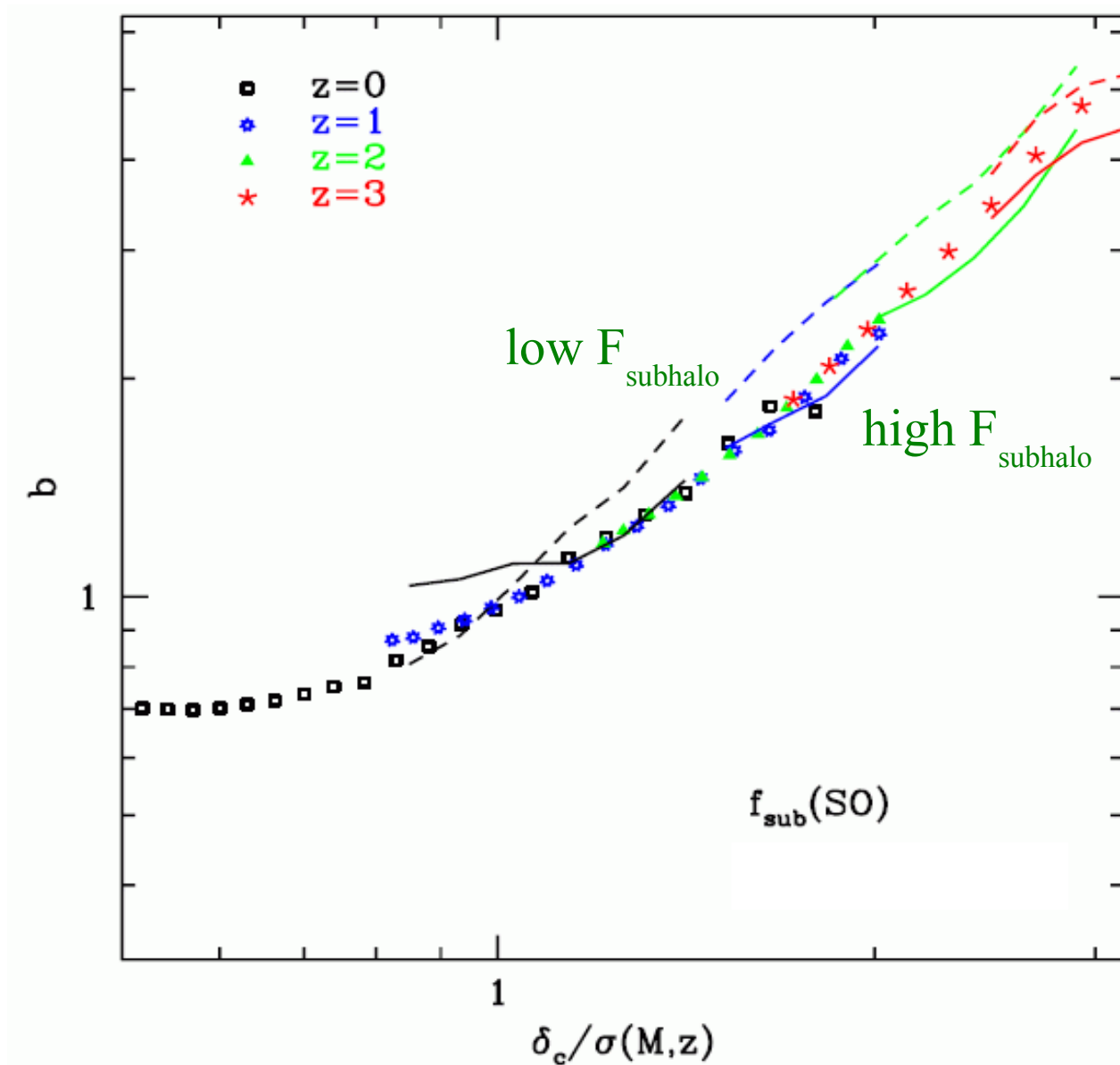
# Bias as a function of $\nu$ and main halo mass fraction

Gao & White 2007



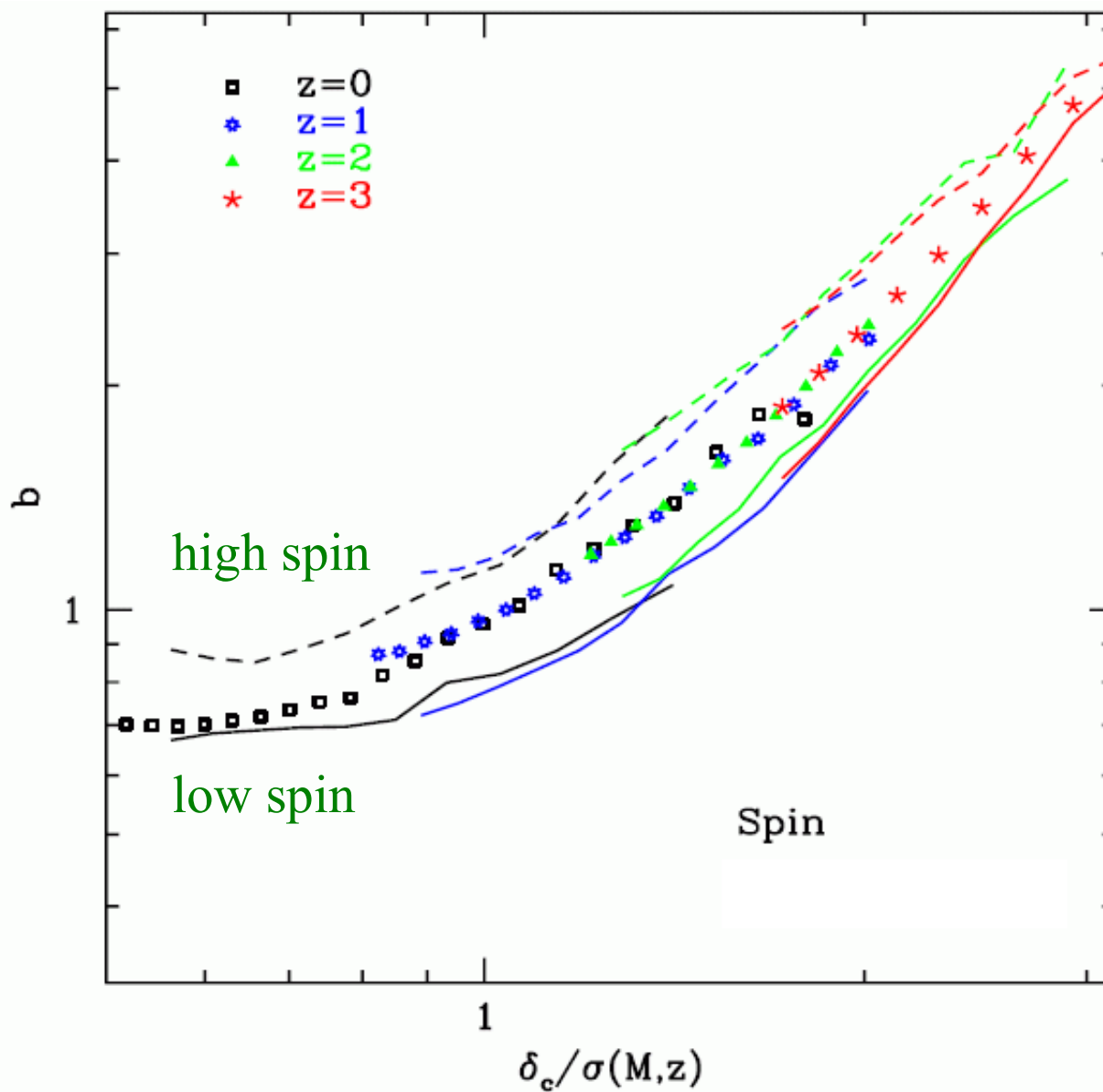
# Bias as a function of $\nu$ and subhalo mass fraction

Gao & White 2007



# Bias as a function of $v$ and spin

Gao & White 2007



# Halo assembly bias: conclusions

The large-scale bias of halo clustering relative to the dark matter depends on halo mass through  $\nu = \delta_c / D(z) \sigma_0(M)$  and also on

- formation time
- concentration
- substructure content
- spin

The dependences on these assembly variables are different and cannot be derived from each other, e.g. more concentrated halos are more strongly clustered at low mass but less strongly clustered at high mass; rapidly spinning halos are more strongly clustered by equal amounts at all masses.

These dependences are likely to be reflected in galaxy bias

January 2009

# The Los Cabos Lectures

## Dark Matter Halos: 2

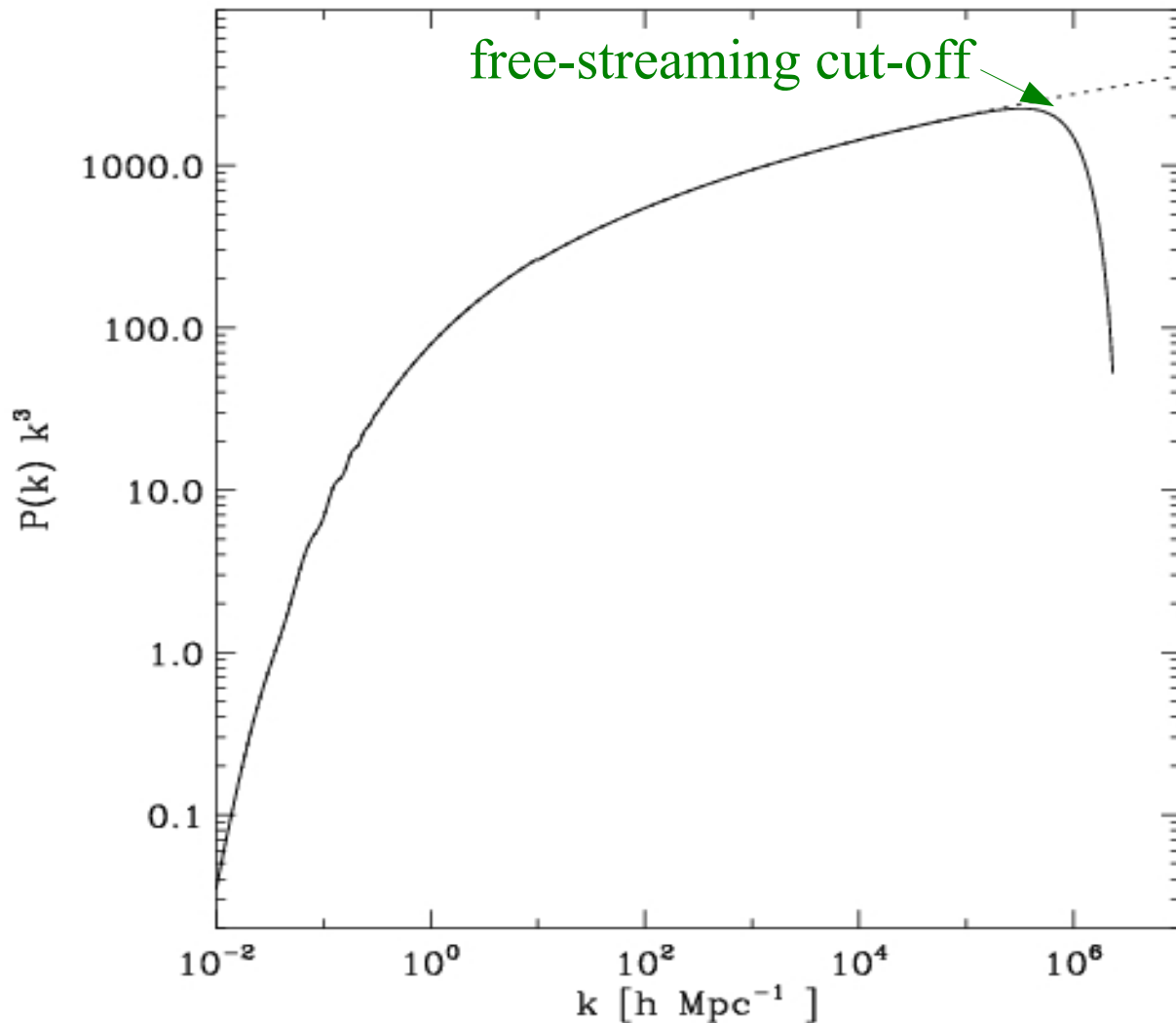
*Simon White*

*Max Planck Institute for Astrophysics*

# EPS statistics for the standard $\Lambda$ CDM cosmology

Millennium Simulation cosmology:  $\Omega_m = 0.25$ ,  $\Omega_\Lambda = 0.75$ ,  $n=1$ ,  $\sigma_8 = 0.9$

Angulo et al 2009



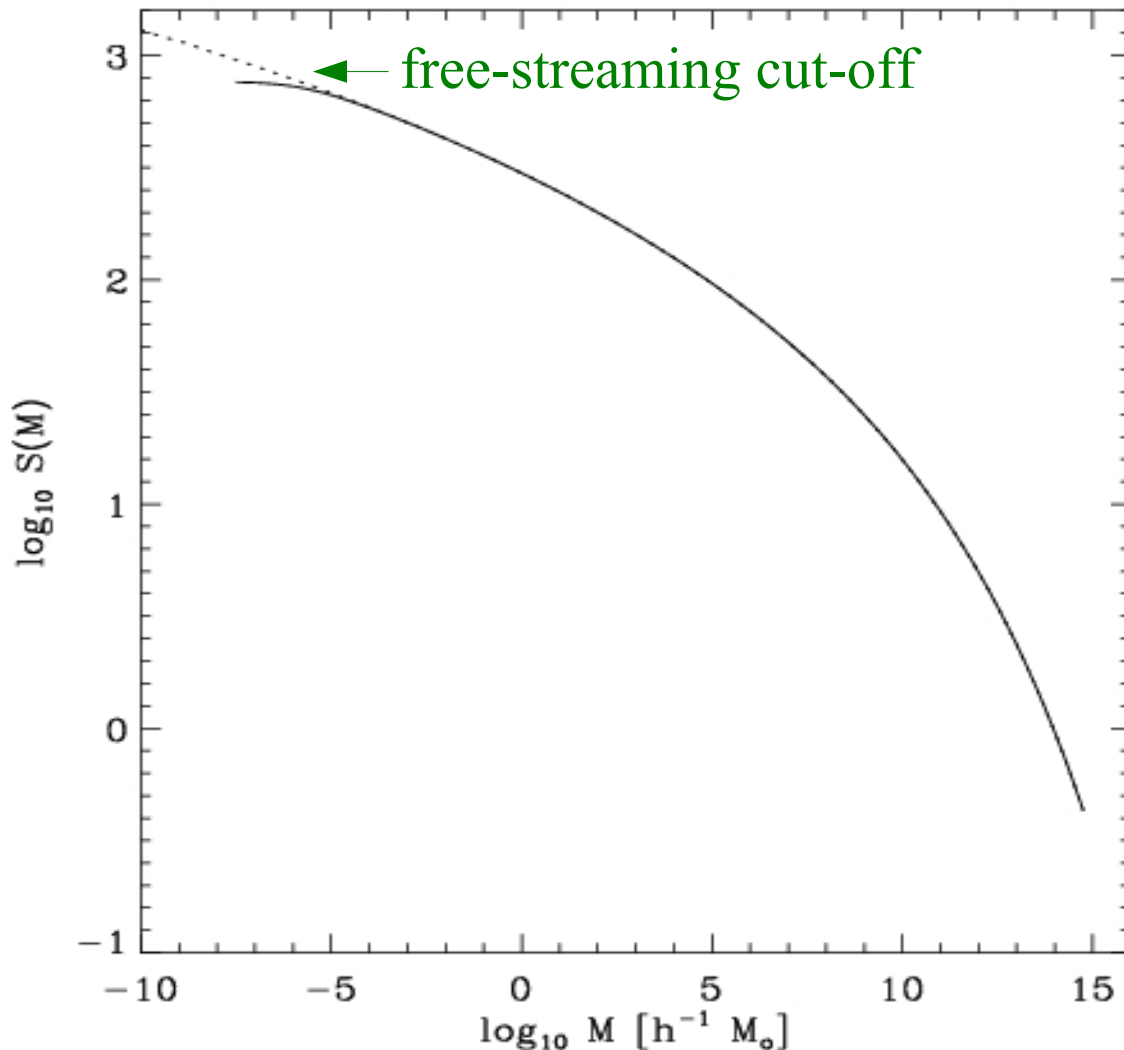
The linear power spectrum in “power per octave” form

Assumes a 100GeV wimp following Green et al (2004)

# EPS statistics for the standard $\Lambda$ CDM cosmology

Millennium Simulation cosmology:  $\Omega_m = 0.25$ ,  $\Omega_\Lambda = 0.75$ ,  $n=1$ ,  $\sigma_8 = 0.9$

Angulo et al 2009

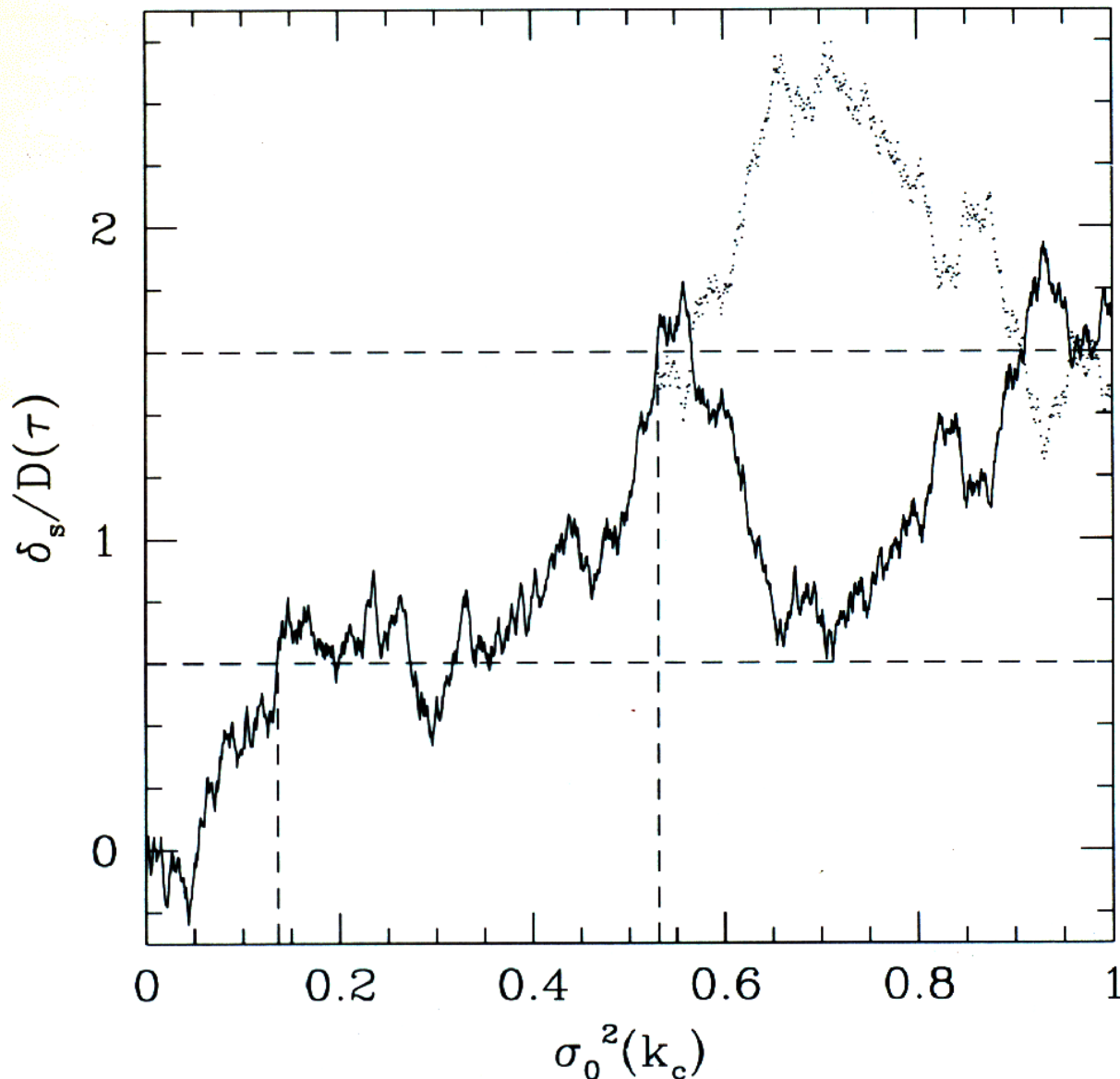


Variance of linear density fluctuation within spheres containing mass  $M$ , extrapolated to  $z = 0$

As  $M \rightarrow 0$ ,  $S(M) \rightarrow 720$

# EPS statistics for the standard $\Lambda$ CDM cosmology

Millennium Simulation cosmology:  $\Omega_m = 0.25$ ,  $\Omega_\Lambda = 0.75$ ,  $n=1$ ,  $\sigma_8 = 0.9$



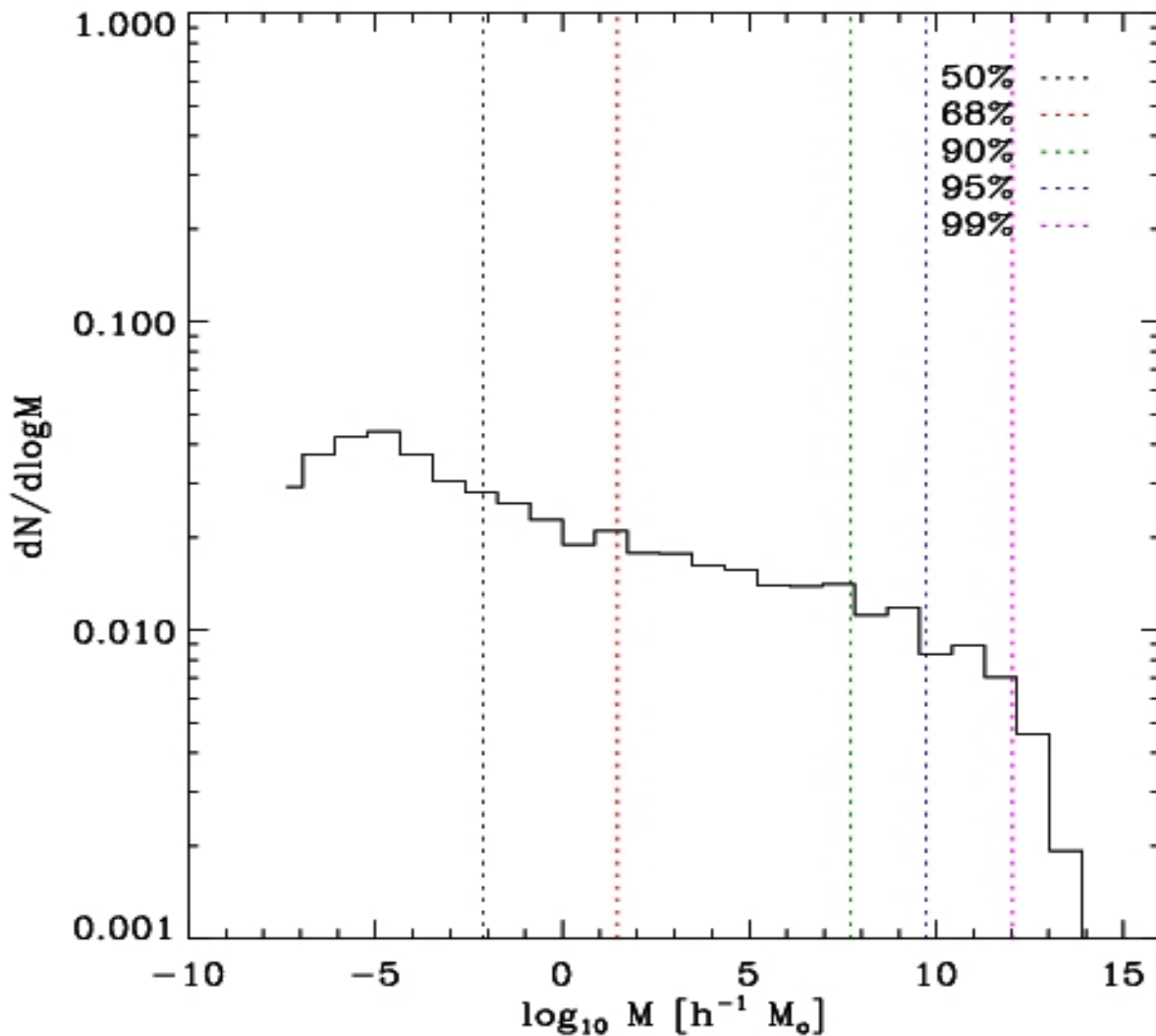
If these Markov random walks are scaled so the maximum variance is 720 and the vertical axis is multiplied by  $\sqrt{720}$ , then they represent complete halo assembly histories for random CDM particles.

An ensemble of walks thus represents the probability distribution of assembly histories

# EPS statistics for the standard $\Lambda$ CDM cosmology

Millennium Simulation cosmology:  $\Omega_m = 0.25$ ,  $\Omega_\Lambda = 0.75$ ,  $n=1$ ,  $\sigma_8 = 0.9$

Angulo et al 2009



Distribution of the masses of the first halos for a random set of dark matter particles

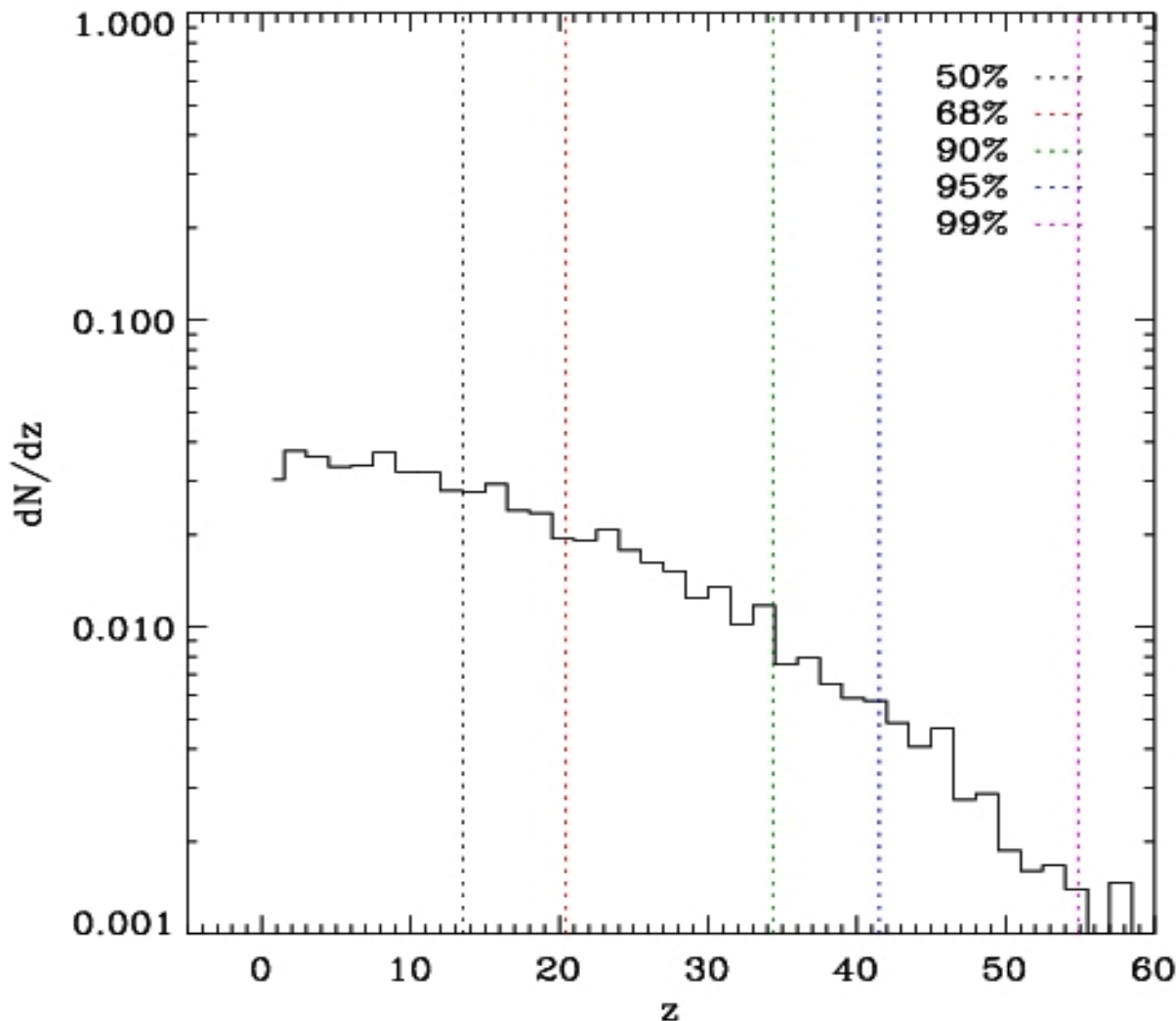
The median is  $10^{-2} M_\odot$

For 10% of the mass the first halo has  $M > 10^7 M_\odot$

# EPS statistics for the standard $\Lambda$ CDM cosmology

Millennium Simulation cosmology:  $\Omega_m = 0.25$ ,  $\Omega_\Lambda = 0.75$ ,  $n=1$ ,  $\sigma_8 = 0.9$

Angulo et al 2009



Distribution of the collapse redshifts of the first halos for a random set of dark matter particles

The median is  $z = 13$

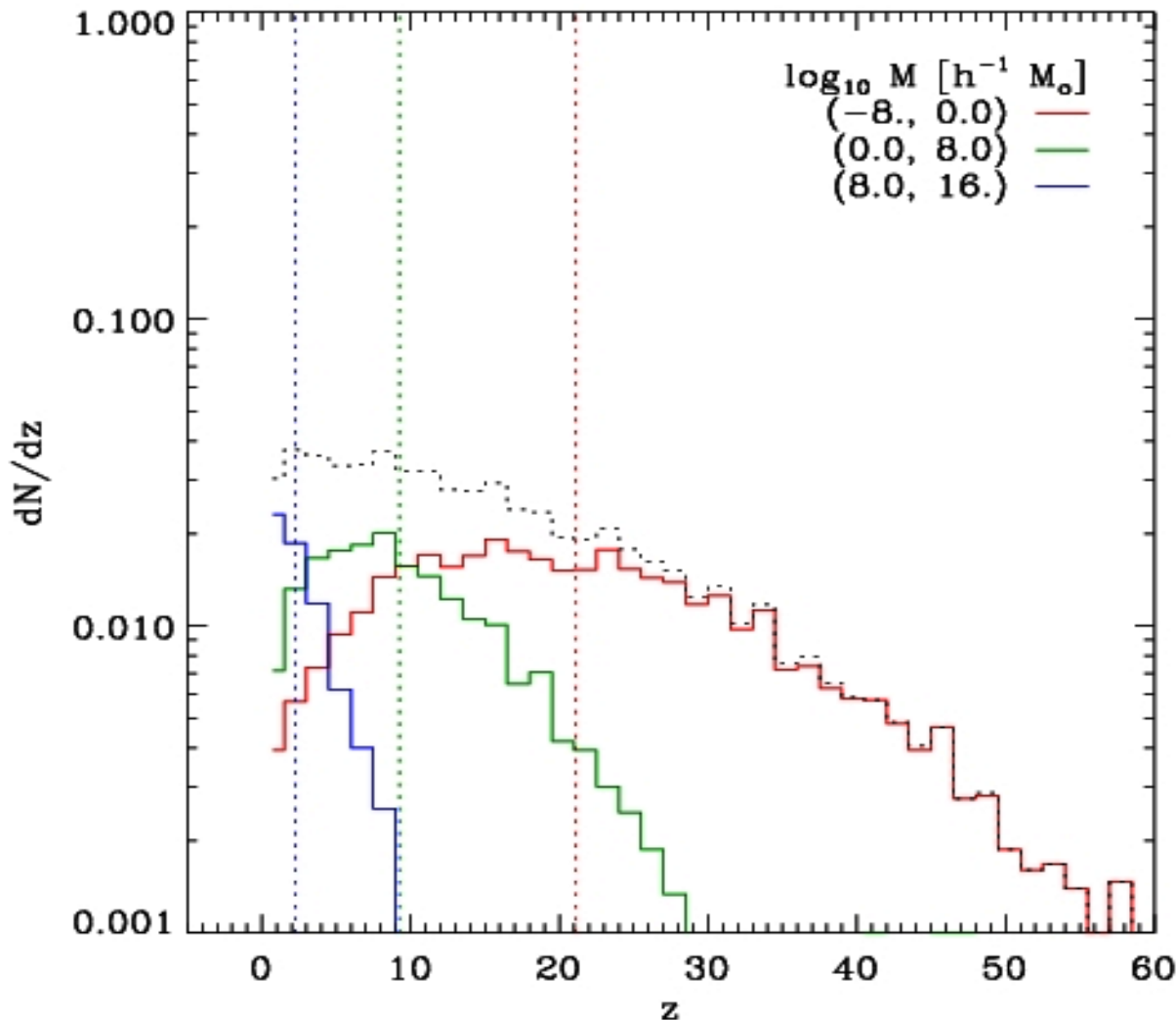
For 10% of the mass the first halo collapses at  $z > 34$

For 1% at  $z > 55$

# EPS statistics for the standard $\Lambda$ CDM cosmology

Millennium Simulation cosmology:  $\Omega_m = 0.25$ ,  $\Omega_\Lambda = 0.75$ ,  $n=1$ ,  $\sigma_8 = 0.9$

Angulo et al 2009



Distribution of the collapse redshifts of the first halos for dark matter particles split by the mass of the first object

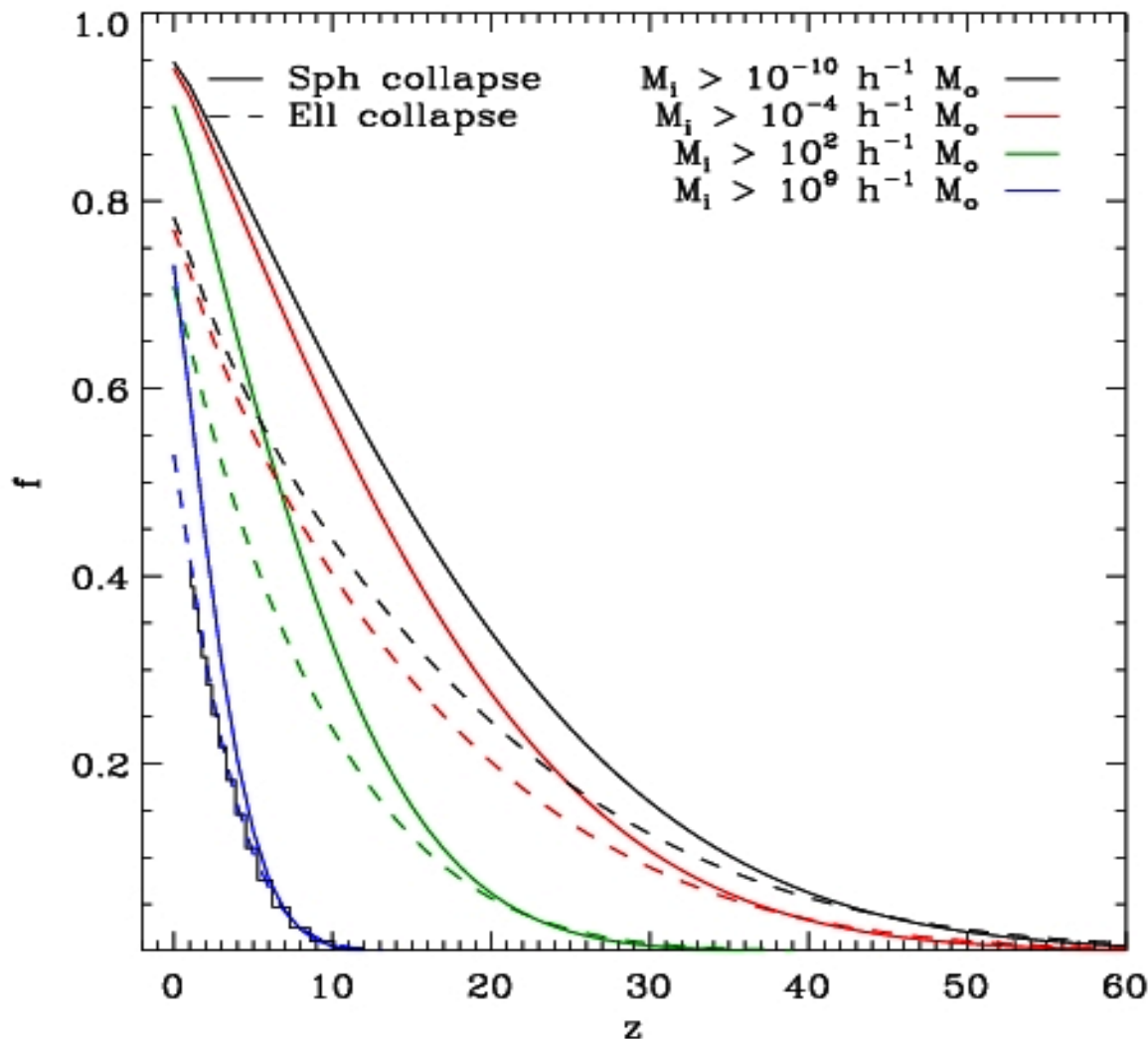
The high redshift tail is entirely due to matter in small first halos

For first halo masses below a solar mass, the median collapse redshift is  $z = 21$

# EPS statistics for the standard $\Lambda$ CDM cosmology

Millennium Simulation cosmology:  $\Omega_m = 0.25$ ,  $\Omega_\Lambda = 0.75$ ,  $n=1$ ,  $\sigma_8 = 0.9$

Angulo et al 2009



Total mass fraction in halos

At  $z = 0$  about 5% (Sph) or 20% (Ell) of the mass is still diffuse

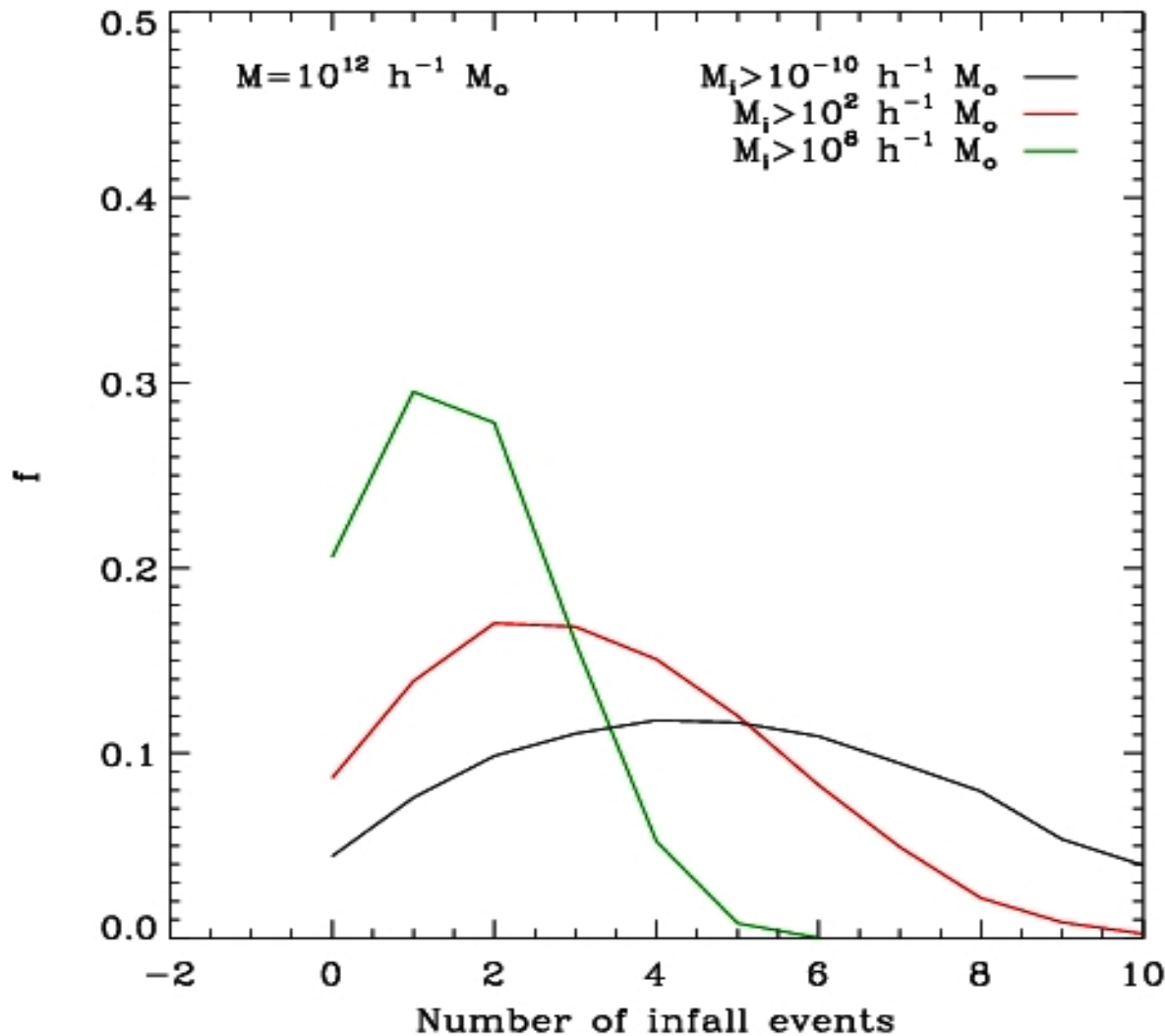
Beyond  $z = 50$  almost all the mass is diffuse

Only at  $z < 2$  (Sph) or  $z < 0.5$  (Ell) is most mass in halos with  $M > 10^8 M_\odot$ . The “Ell” curve agrees with simulations

# EPS statistics for the standard $\Lambda$ CDM cosmology

Millennium Simulation cosmology:  $\Omega_m = 0.25$ ,  $\Omega_\Lambda = 0.75$ ,  $n=1$ ,  $\sigma_8 = 0.9$

Angulo et al 2009



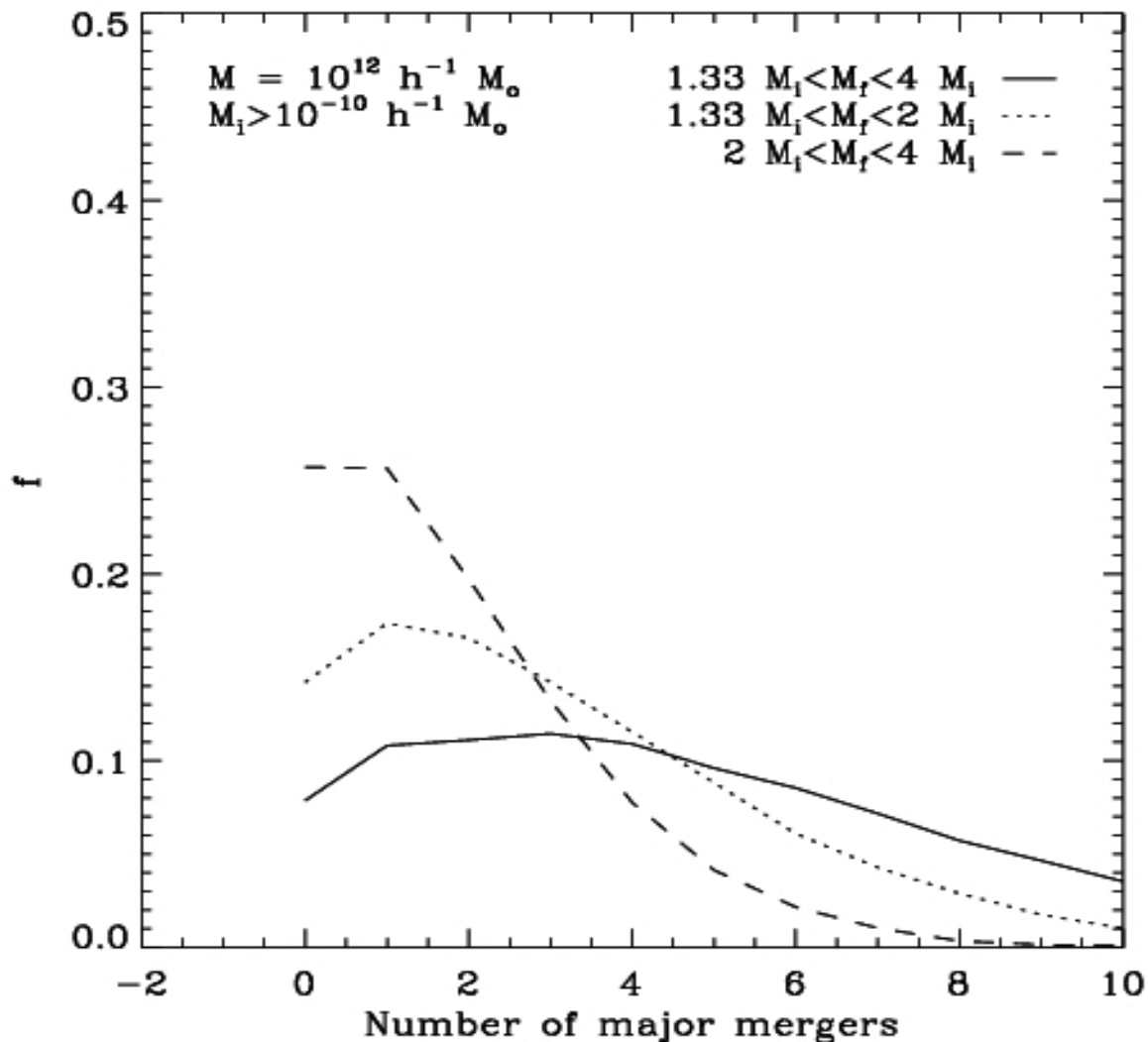
The typical mass element in a “Milky Way” halo goes through  $\sim 5$  “infall events” where its halo falls into a halo bigger than itself.

Typically only one of these is as part of a halo with  $M > 10^8 M_\odot$ .

# EPS statistics for the standard $\Lambda$ CDM cosmology

Millennium Simulation cosmology:  $\Omega_m = 0.25$ ,  $\Omega_\Lambda = 0.75$ ,  $n=1$ ,  $\sigma_8 = 0.9$

Angulo et al 2009



The typical mass element in a “Milky Way” halo goes through  $\sim 3$  “major mergers” where the two halos are within a factor of 3 in mass

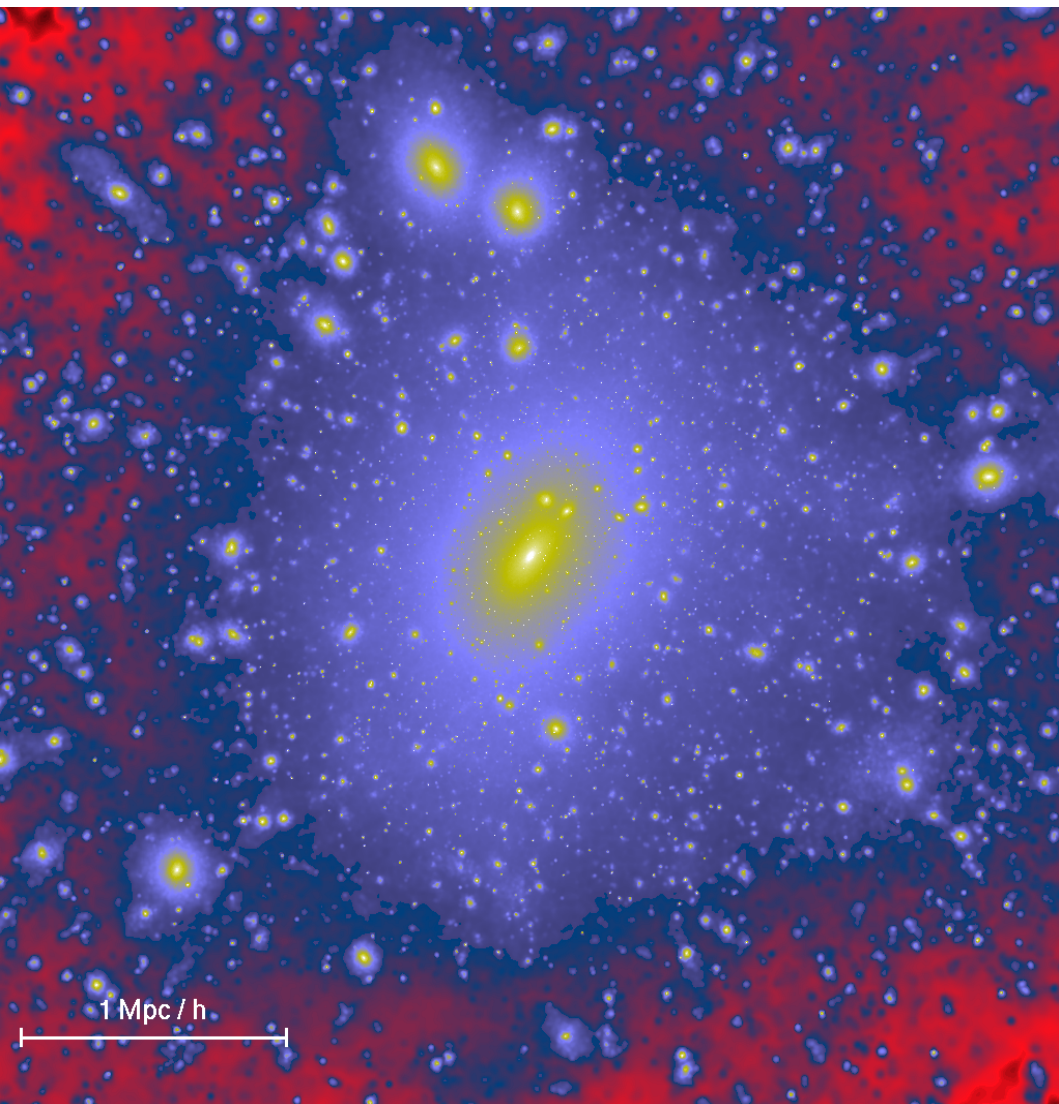
The majority of these occur when the element is part of the larger halo

# EPS halo assembly: conclusions

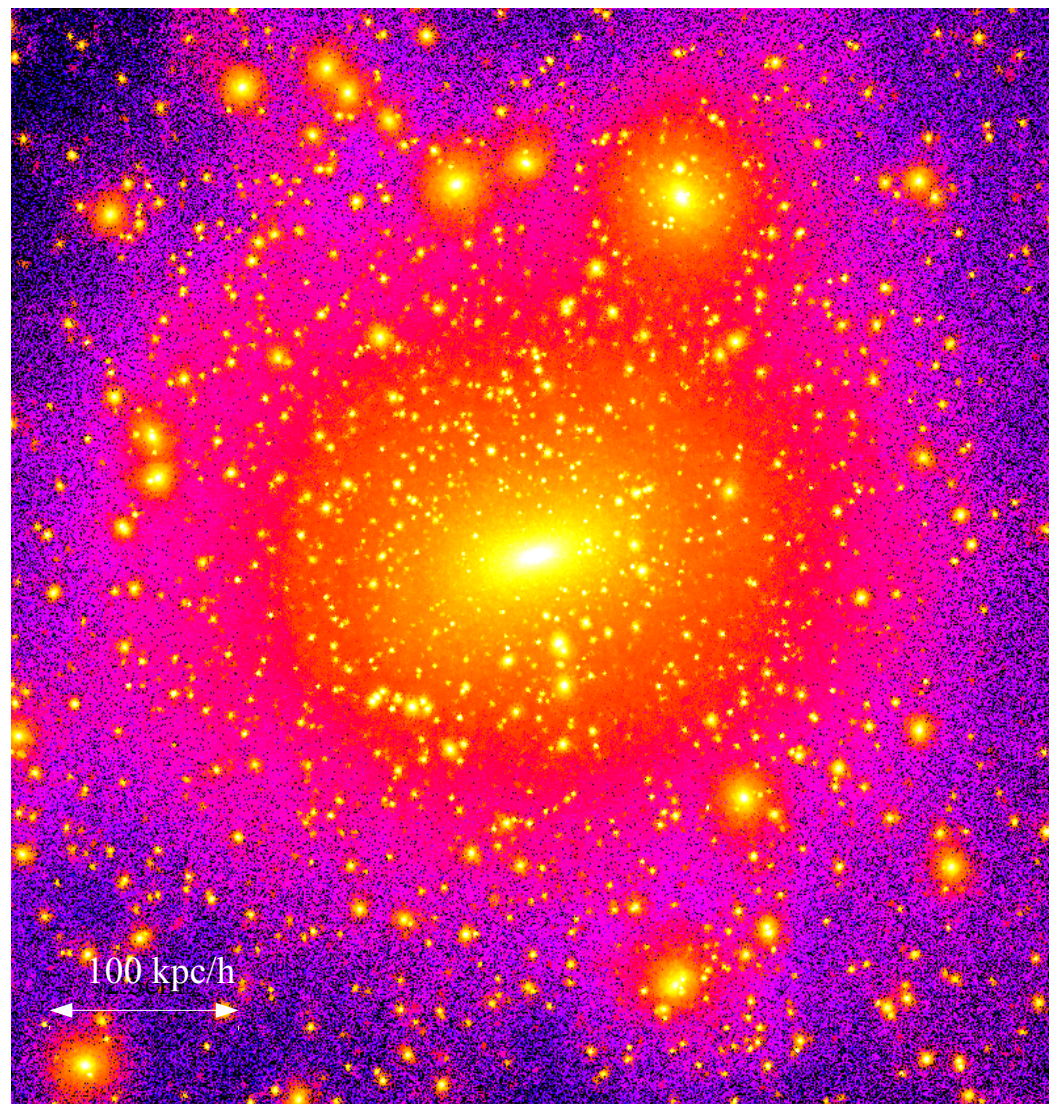
- The typical first halo is much more massive than the free streaming mass
- First halos typically collapse quite late  $z \sim 13$
- Halo growth occurs mainly by accretion of much smaller halos
- There are rather few “generations” of accretion/merger events
- Major mergers are not a major part of the growth of many halos

# The dark matter structure of $\Lambda$ CDM halos

A rich galaxy cluster halo  
Springel et al 2001



A 'Milky Way' halo  
Power et al 2002

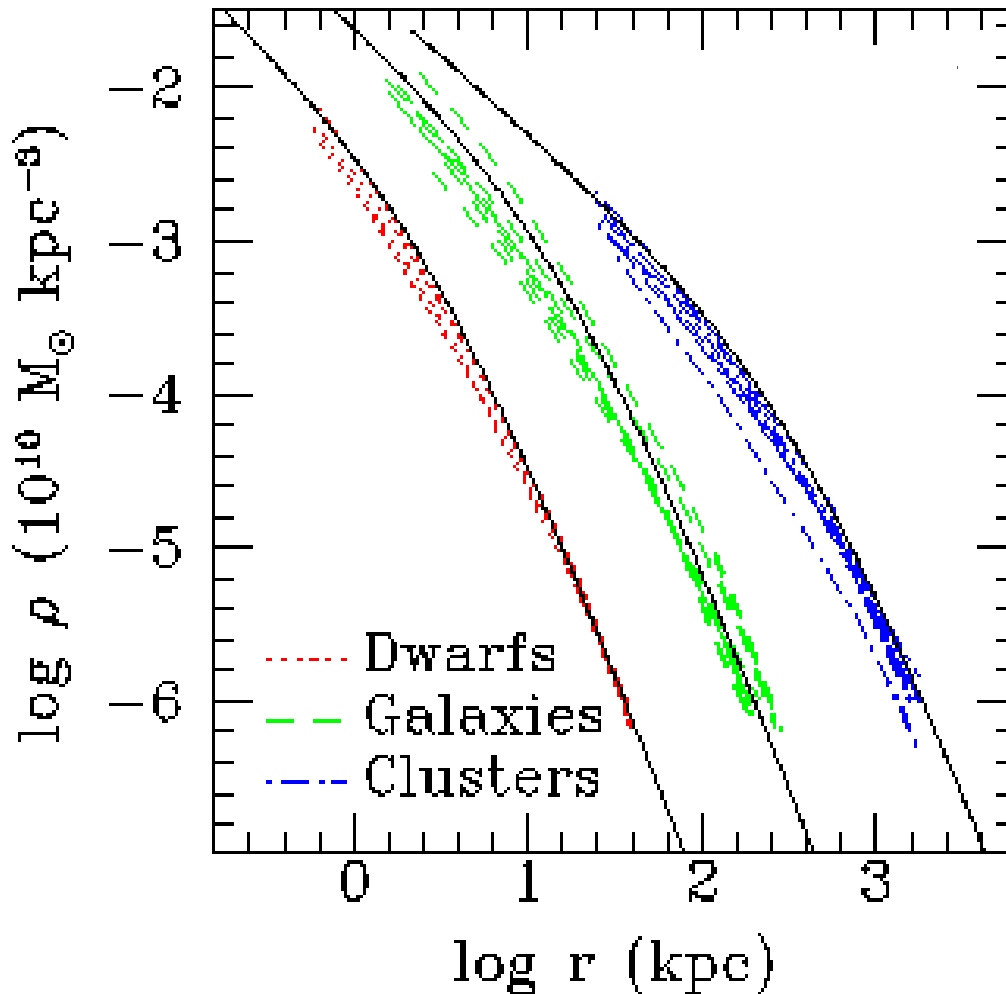


# $\Lambda$ CDM galaxy halos (without galaxies!)

- Halos extend to  $\sim 10$  times the 'visible' radius of galaxies and contain  $\sim 10$  times the mass in the visible regions
  - Halos are not spherical but approximate triaxial ellipsoids
    - more prolate than oblate
    - axial ratios greater than two are common
  - "Cuspy" density profiles with outwardly increasing slopes
    - $d \ln \rho / d \ln r = \gamma$  with  $\gamma < -2.5$  at large  $r$
    - $\gamma > -1.2$  at small  $r$
  - Substantial numbers of self-bound subhalos contain  $\sim 10\%$  of the halo's mass and have  $dN/dM \sim M^{-1.8}$
-  Most substructure mass is in most massive subhalos

# Density profiles of dark matter halos

Navarro, Frenk & White 1996



The average dark matter density of a dark halo depends on distance from halo centre in a very similar way in halos of all masses at all times

-- a universal profile shape --

$$\rho(r)/\rho_{crit} \approx \delta r_s / r(1 + r/r_s)^2$$

More massive halos and halos that form earlier have higher densities (bigger  $\delta$ )

Concentration  $c = r_{200} / r_s$  is an alternative density measure  
Beware variety of definitions!

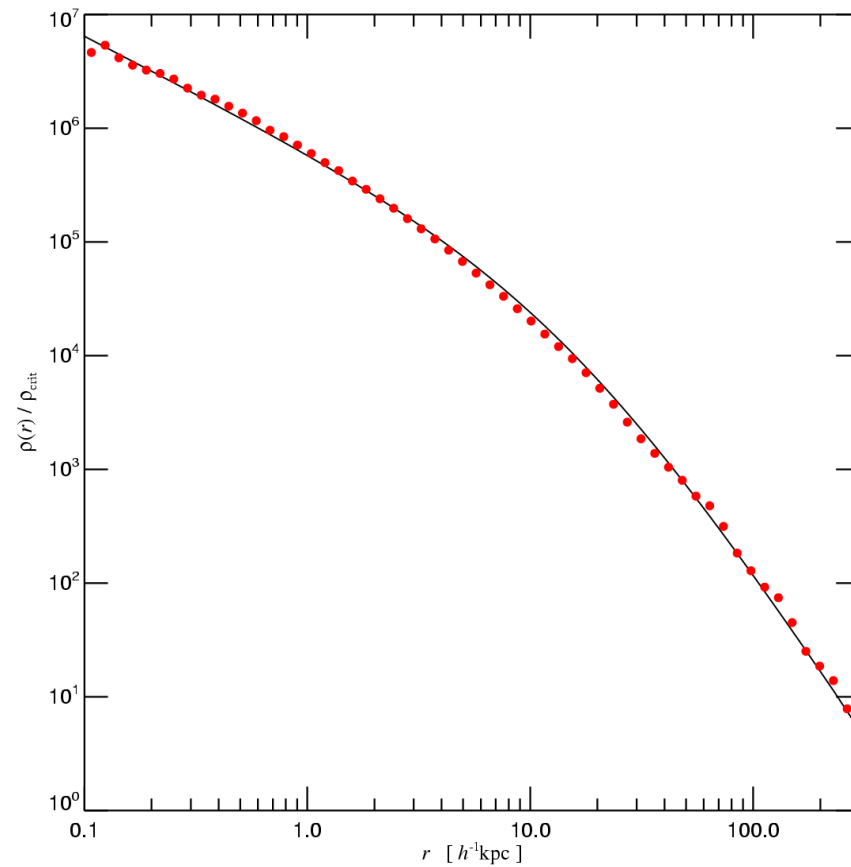
**NFW profiles may not be pretty....**



...but they work surprisingly well



600 kpc



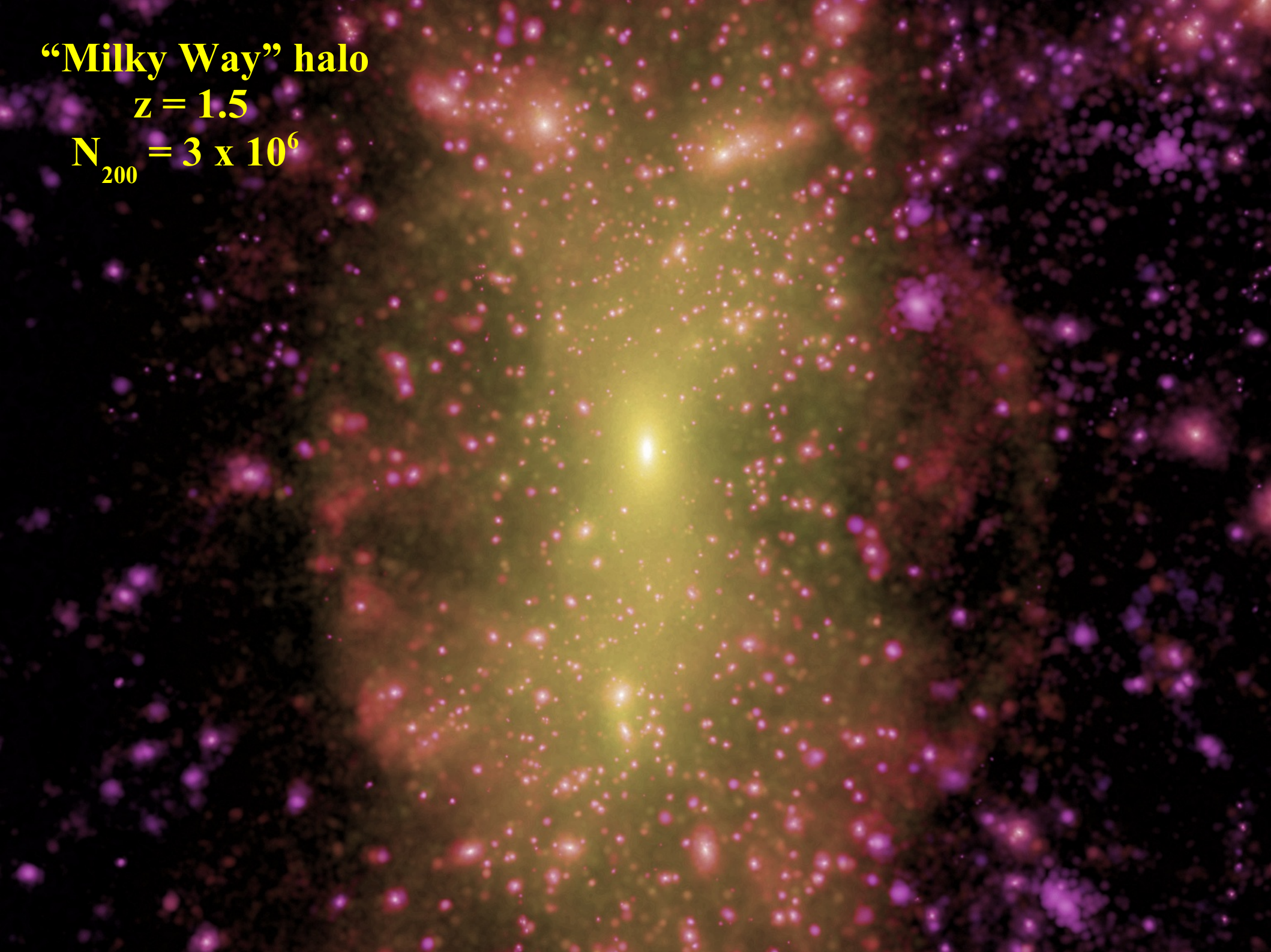
$$N_{200} \sim 3 \times 10^7$$

Navarro et al 2006

**“Milky Way” halo**

**$z = 1.5$**

**$N_{200} = 3 \times 10^6$**



**“Milky Way” halo**

$$z = 1.5$$

$$N_{200} = 94 \times 10^6$$



**“Milky Way” halo**

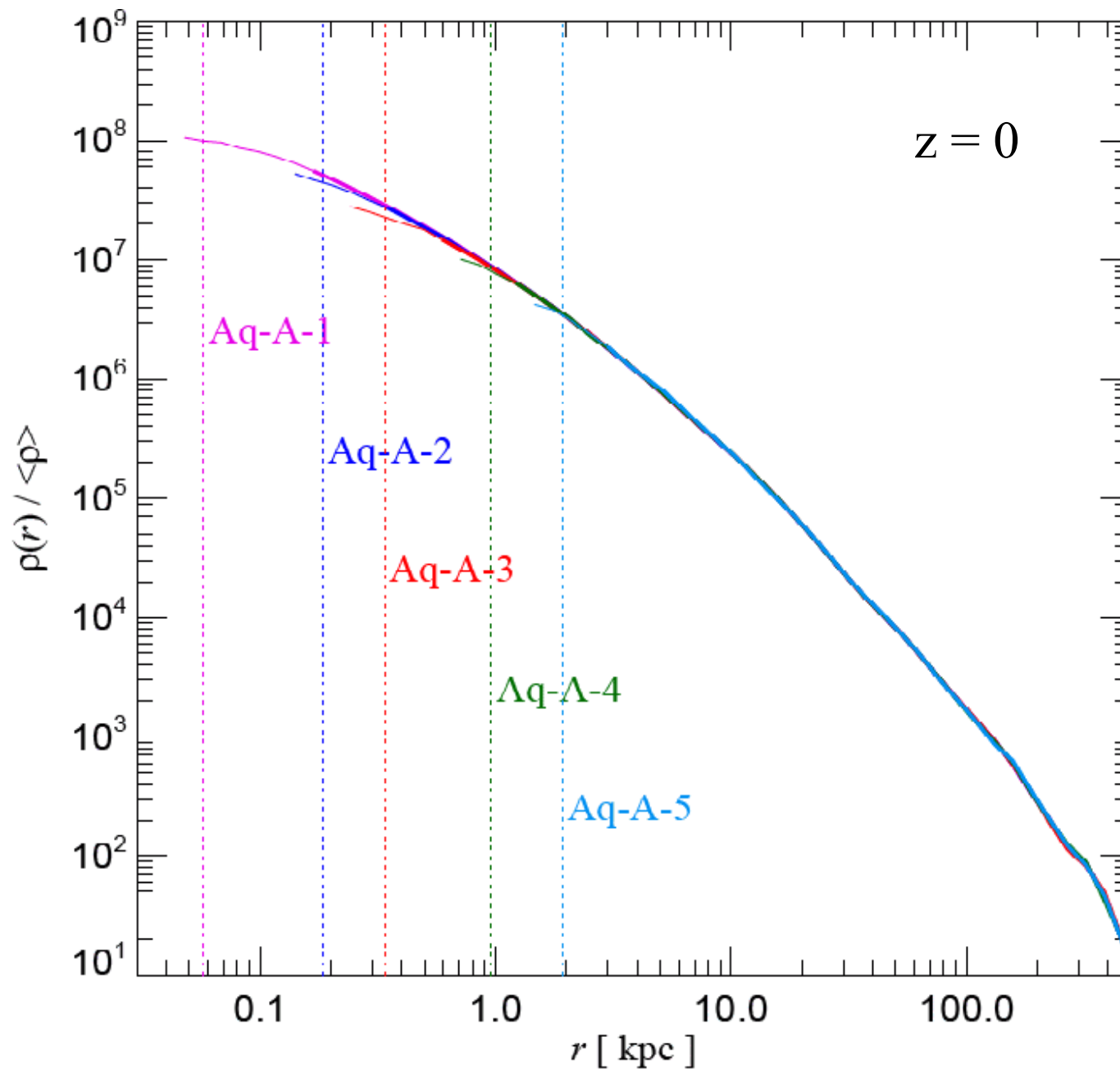
$$z = 1.5$$

$$N_{200} = 750 \times 10^6$$



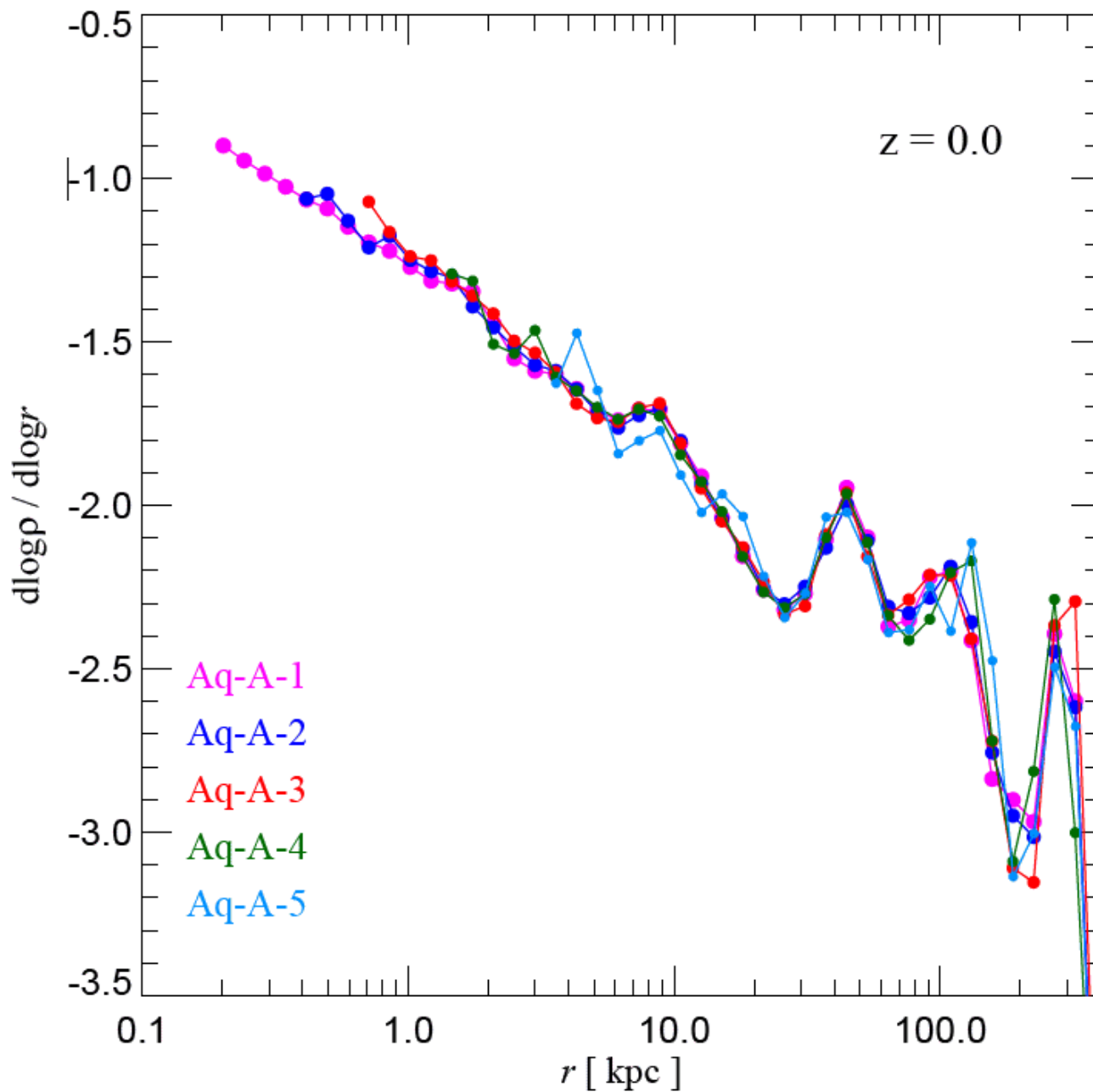
# How well do density profiles converge?

Aquarius Project: Springel et al 2008



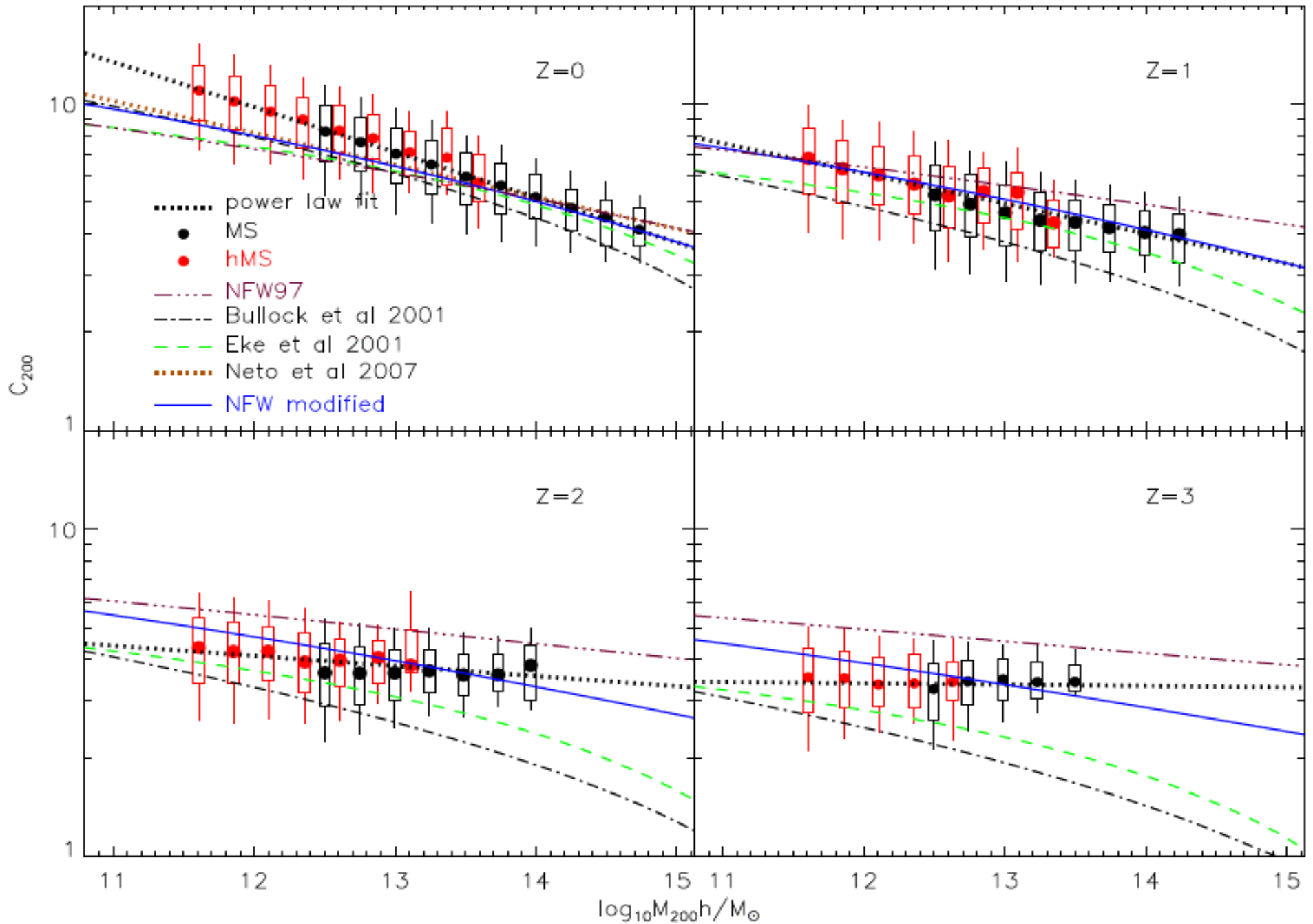
# How well do density profiles converge?

Aquarius Project: Springel et al 2008



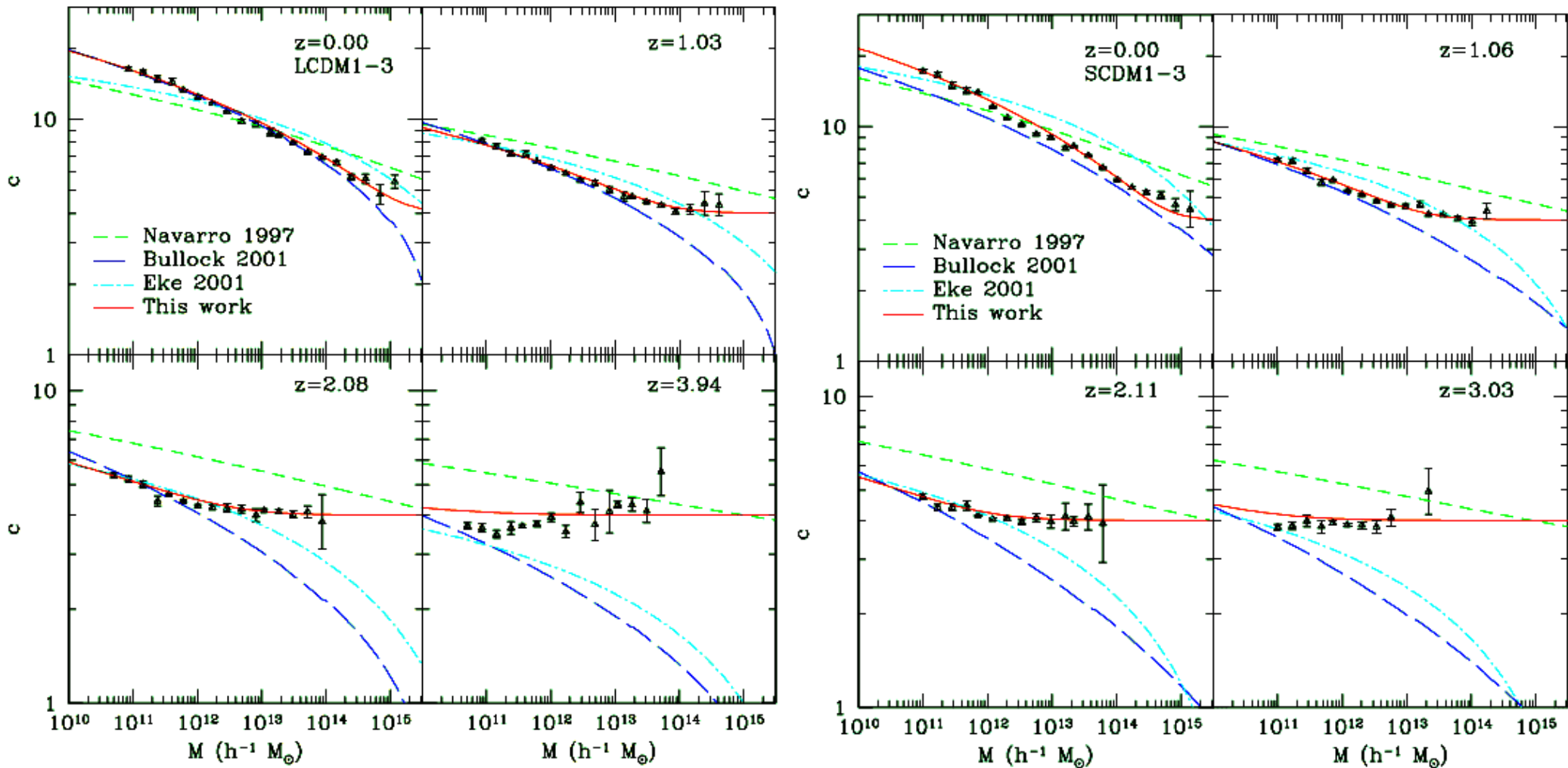
# Concentration scatter and trend with M and z

Gao et al 2008



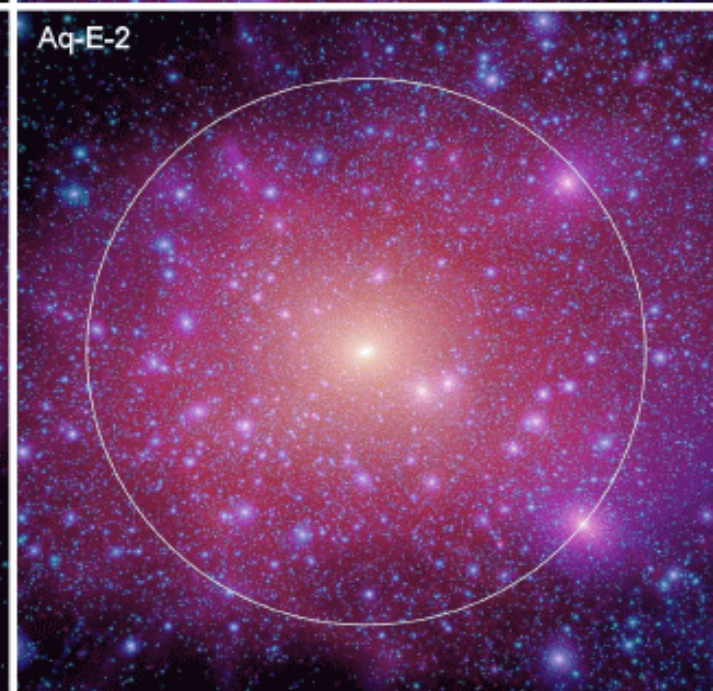
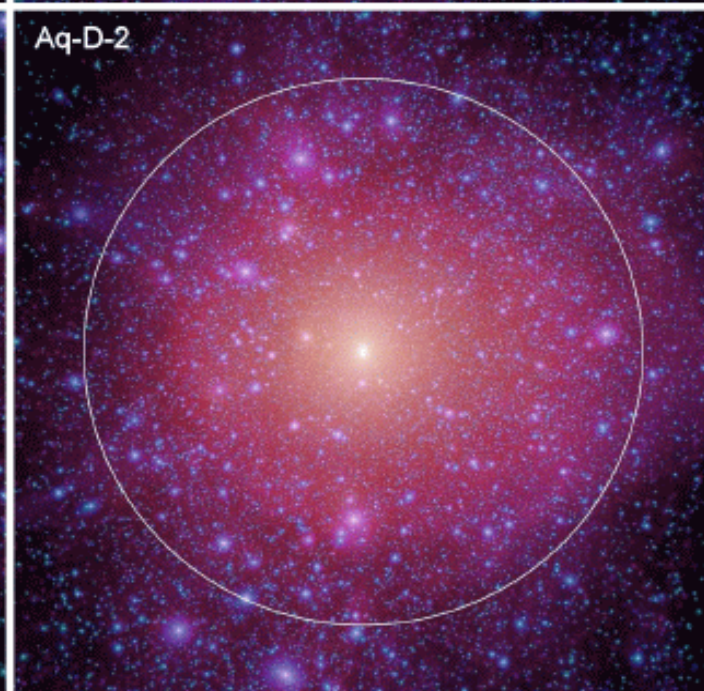
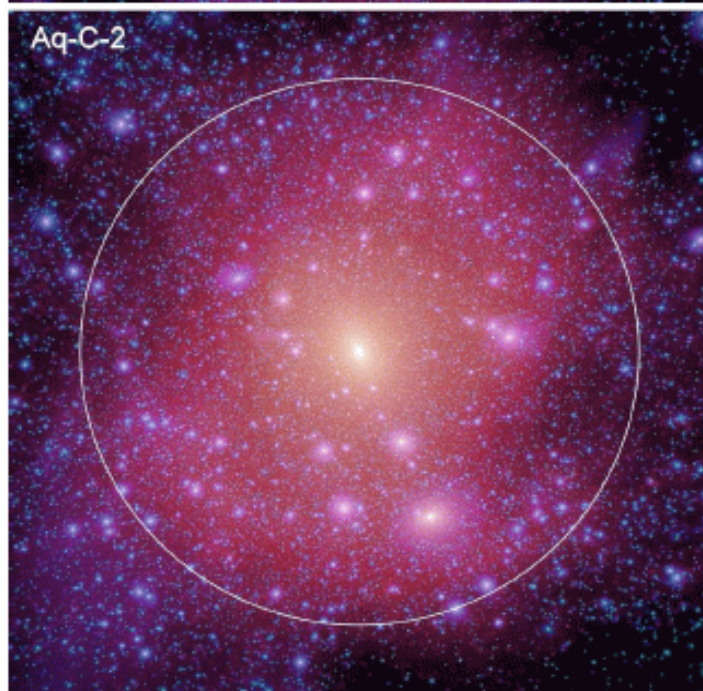
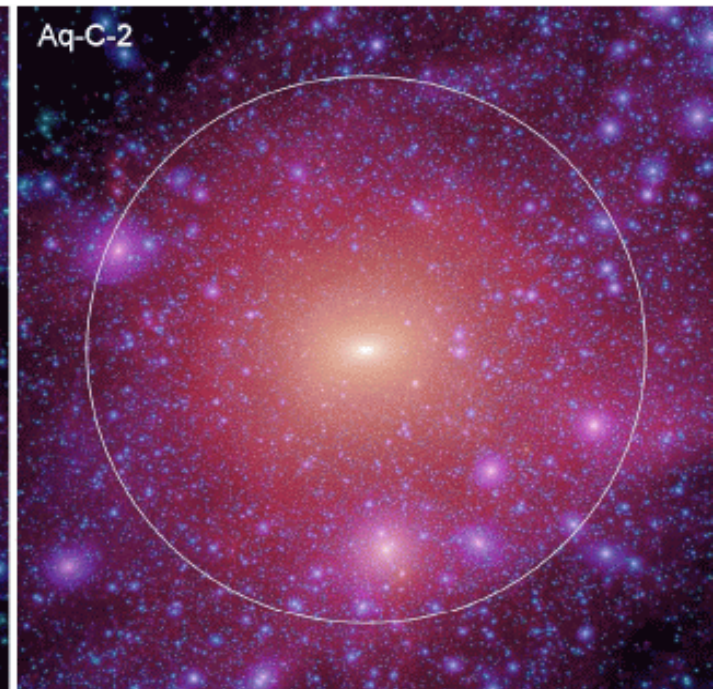
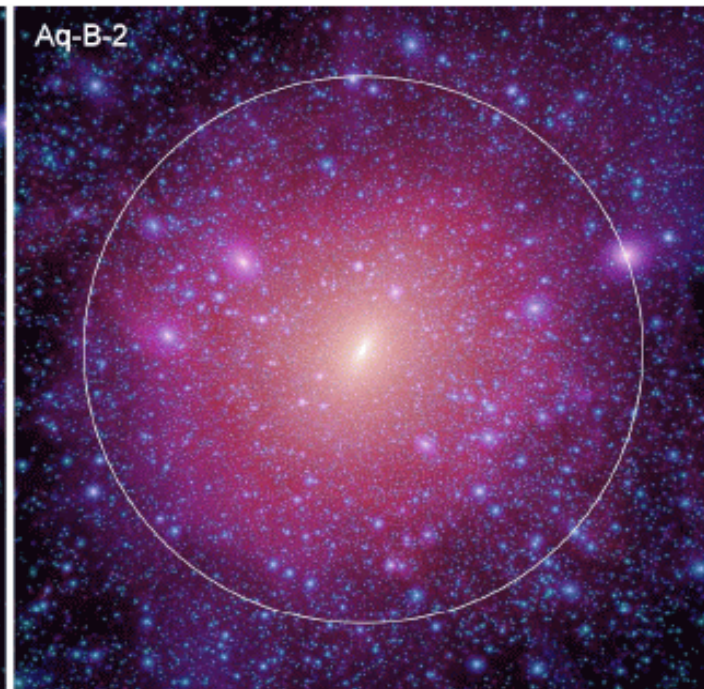
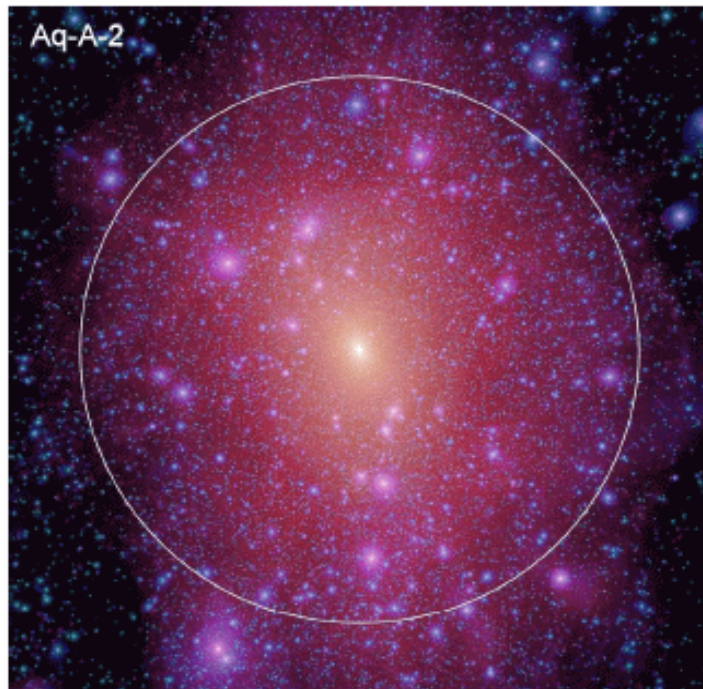
# Concentration trends with $M$ , $z$ and cosmology

Zhao et al 2008



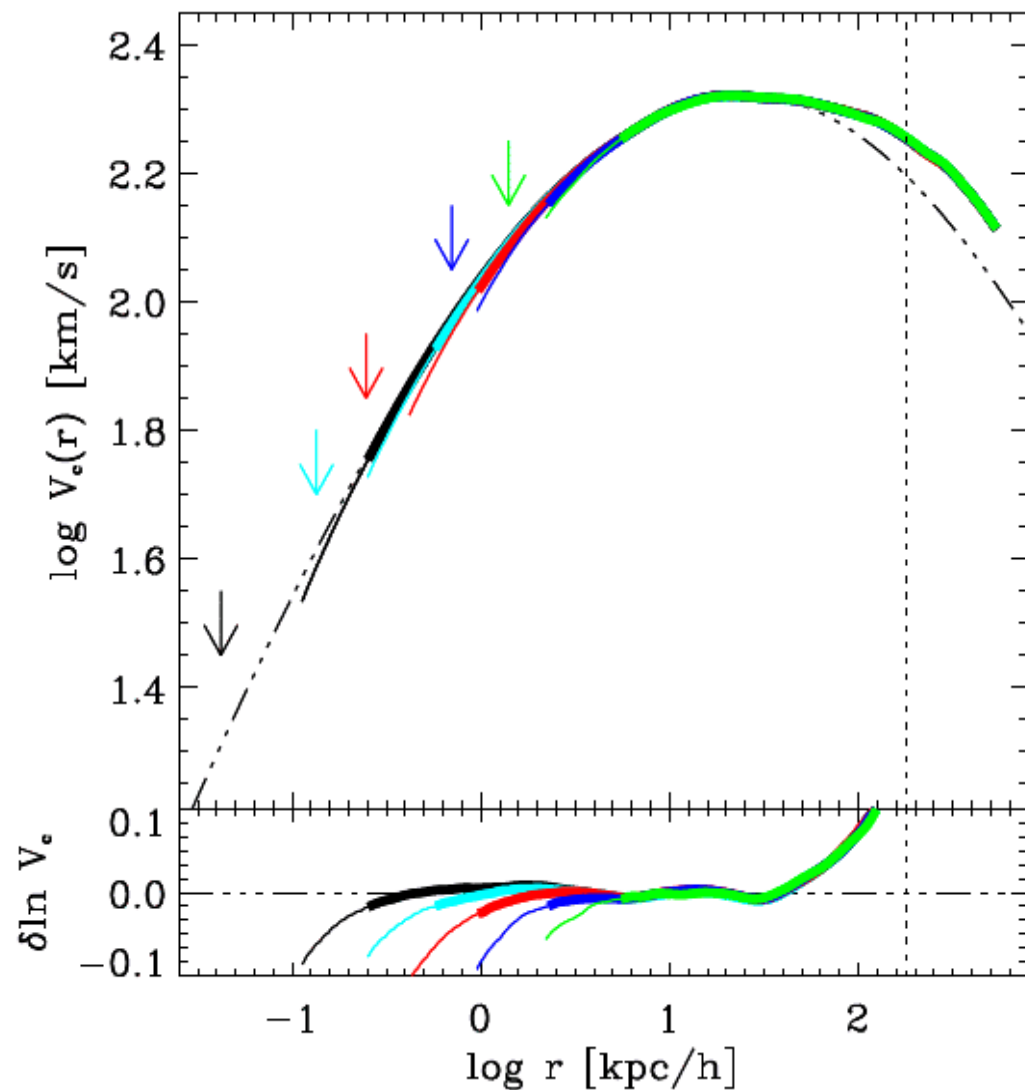
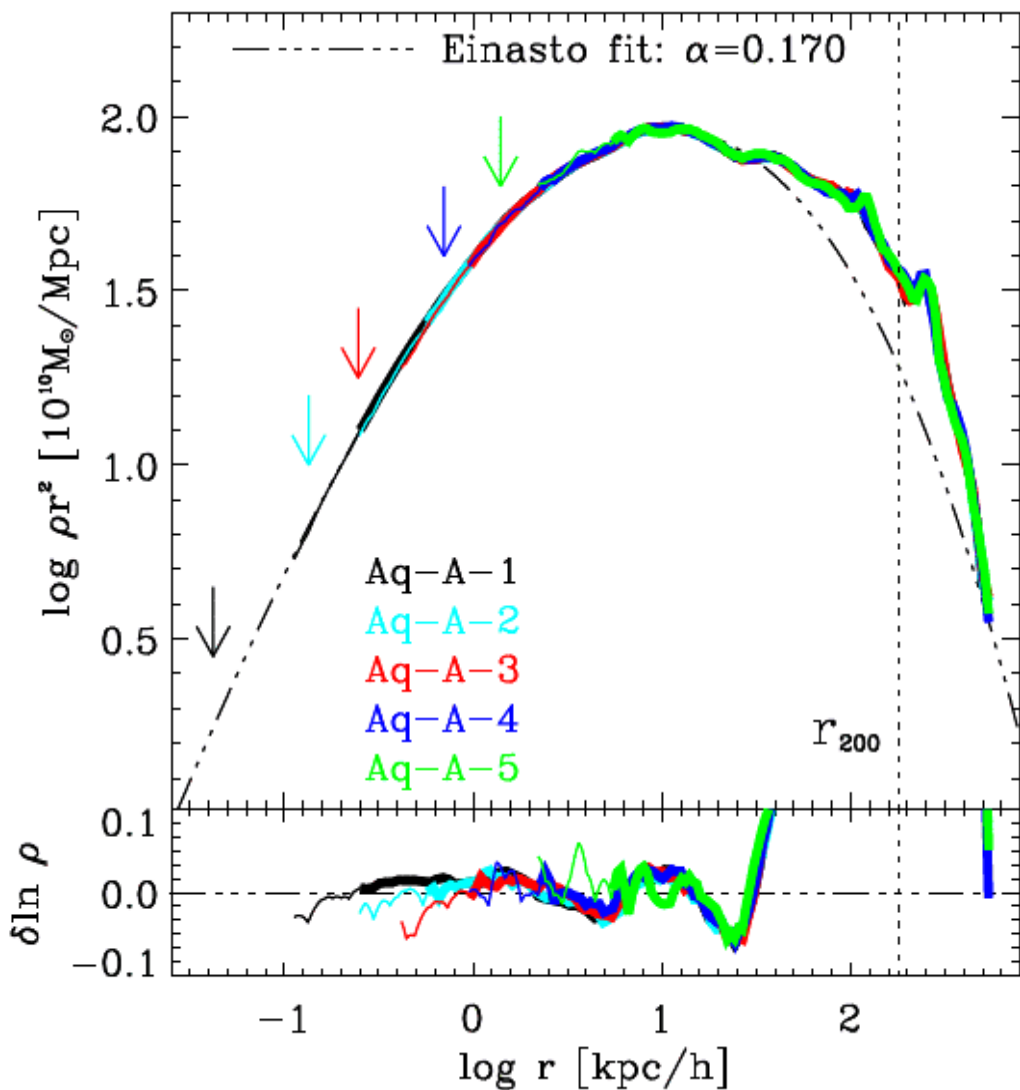
# The Aquarius halos

Springel et al 2008



# The Einasto profile fits the inner cusps

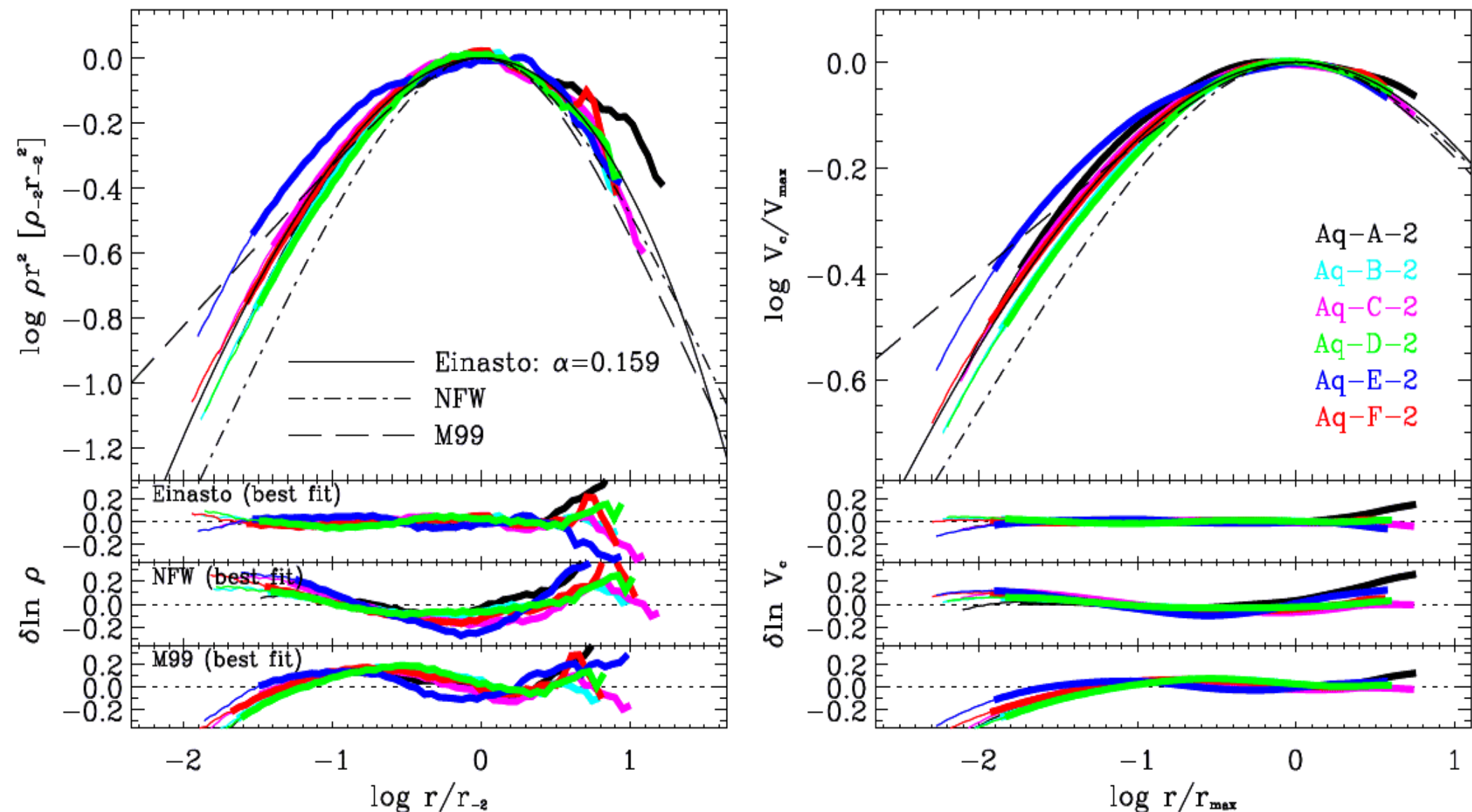
Navarro et al 2009



Einasto's (1965) profile:  $\ln \rho(r) / \rho_{-2} = -2 / \alpha [(r / r_{-2})^\alpha - 1]$

# The Einasto profile fits the inner cusps

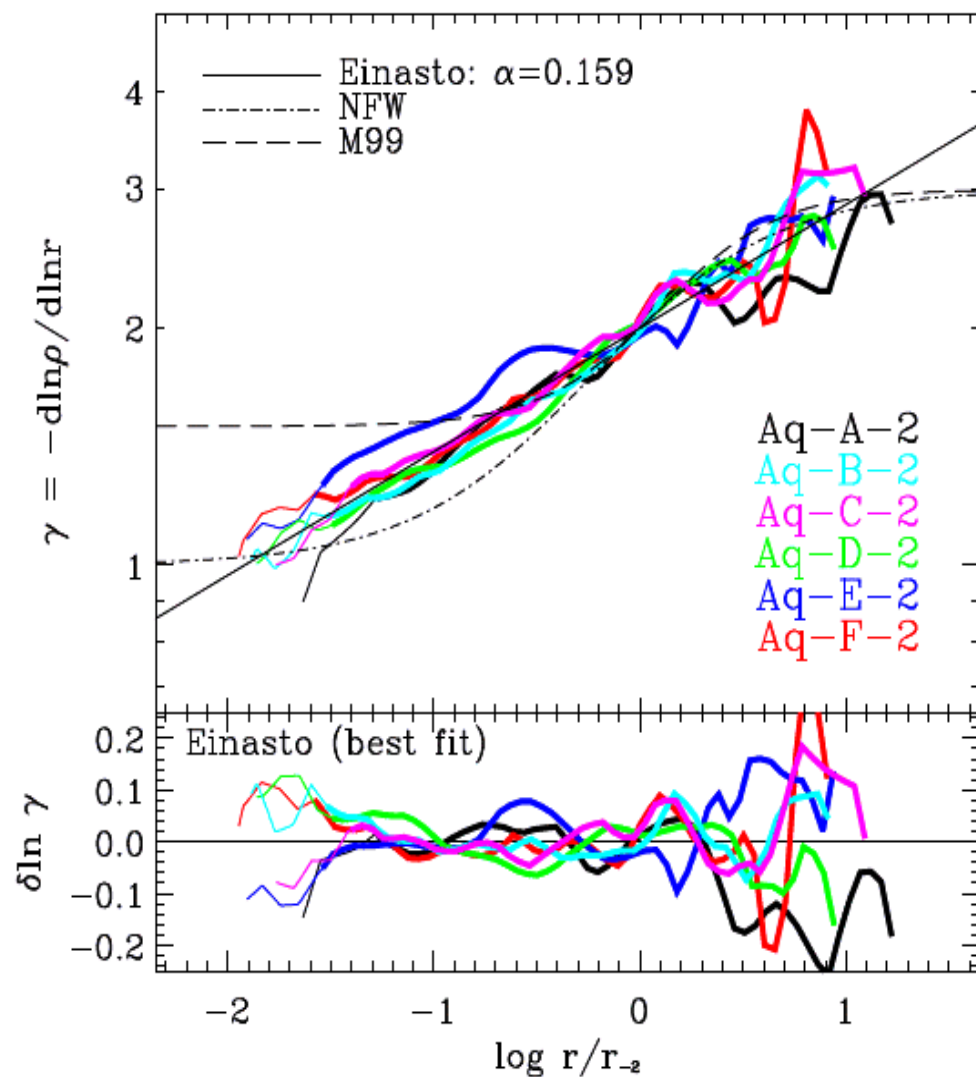
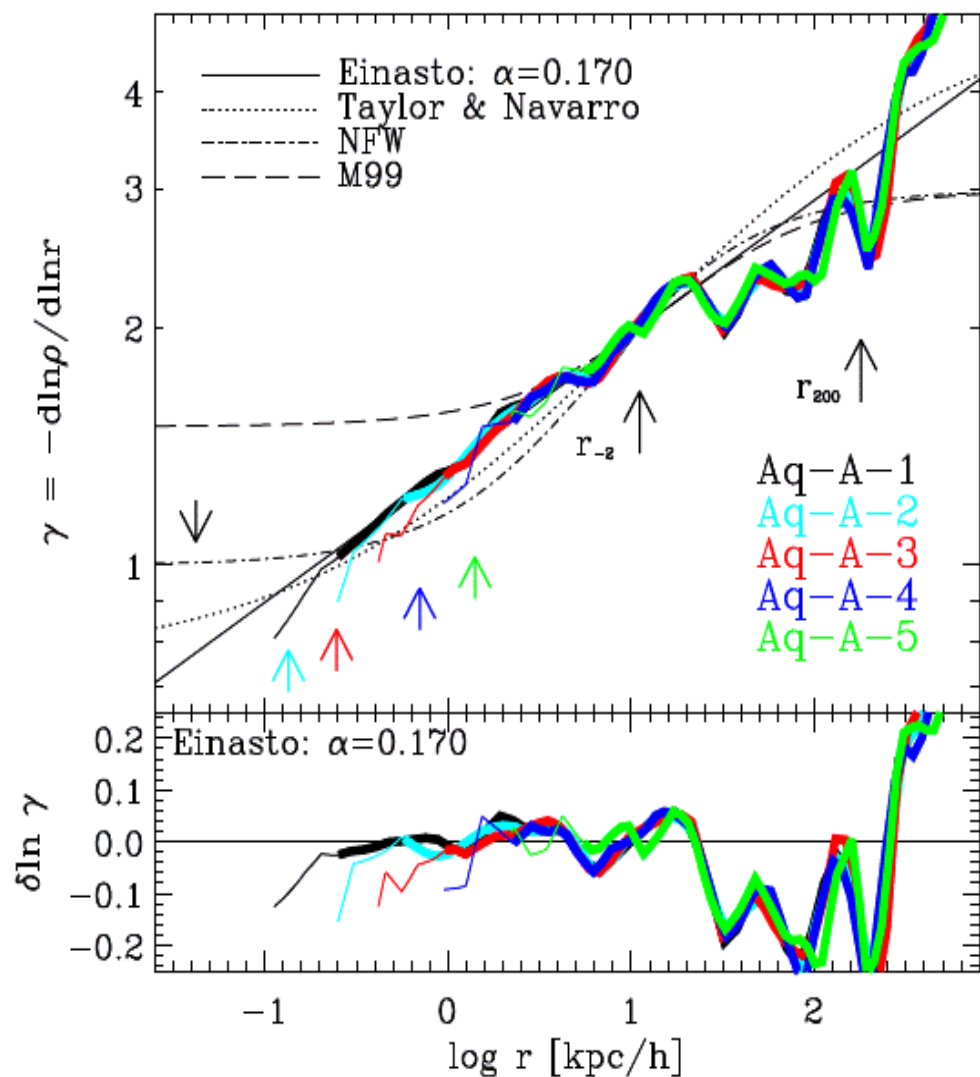
Navarro et al 2009



Einasto's (1965) profile:  $\ln \rho(r) / \rho_{-2} = -2 / \alpha \left[ (r / r_{-2})^\alpha - 1 \right]$

# The Einasto profile fits the inner cusps

Navarro et al 2009

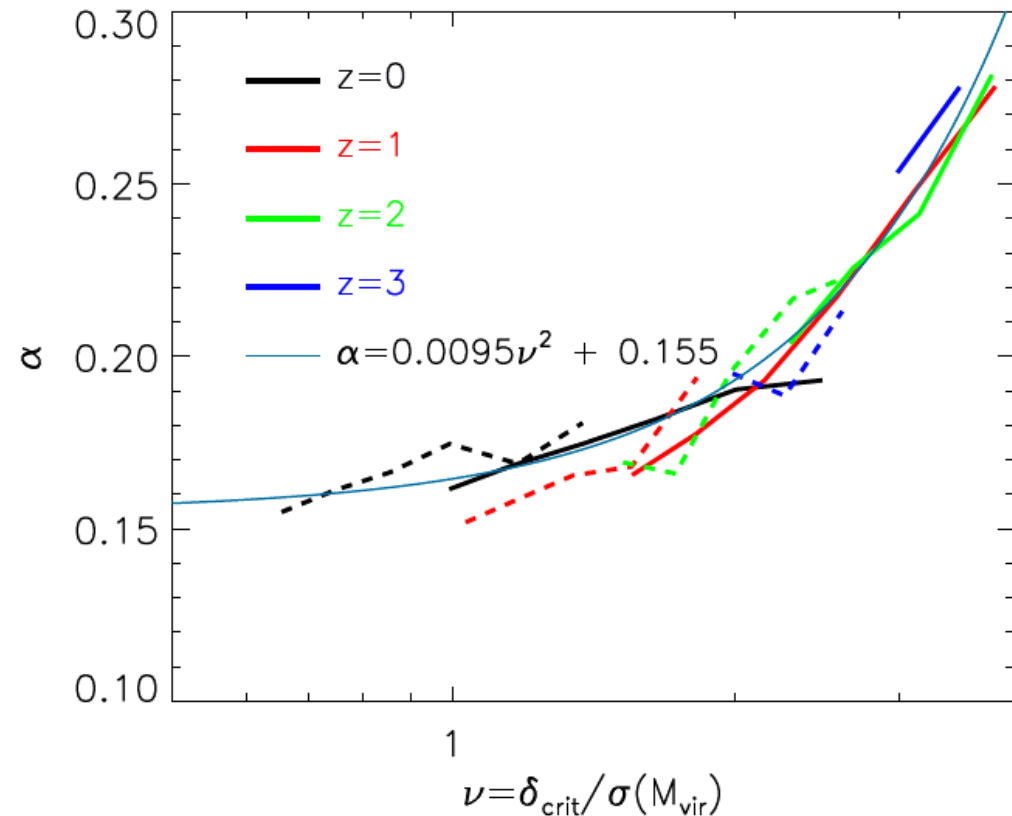
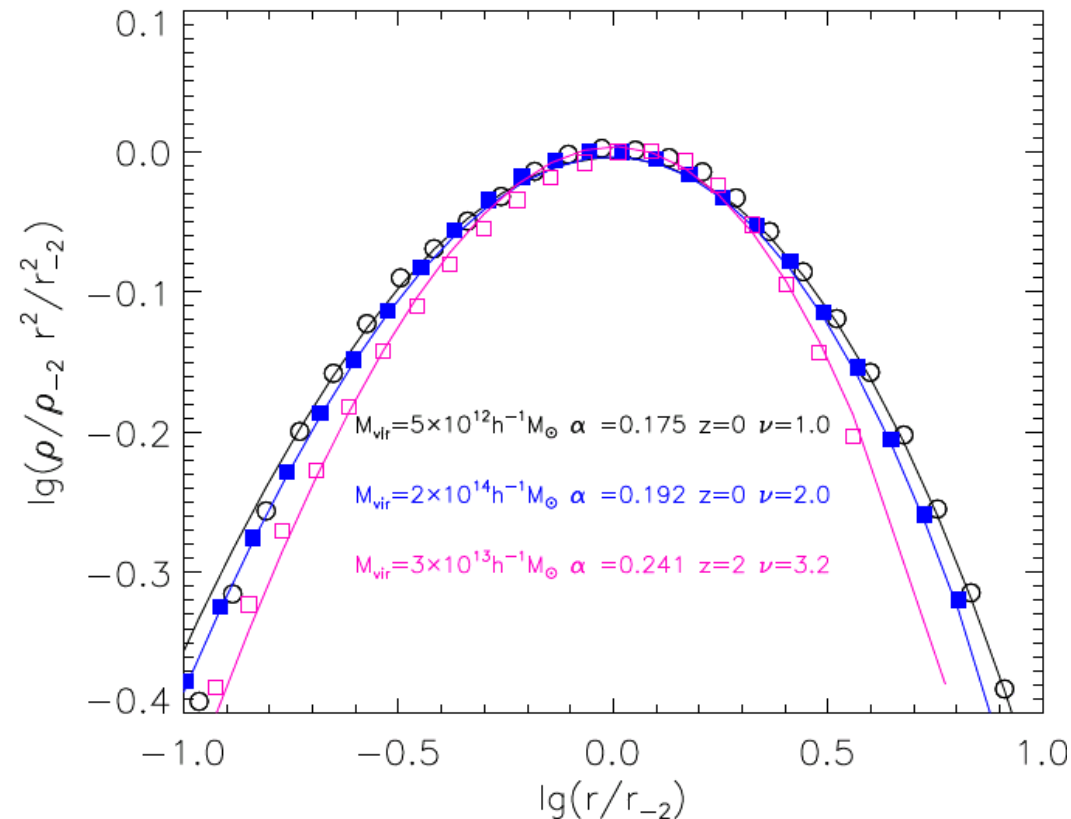


Einasto's (1965) profile:  $\ln \rho(r) / \rho_{-2} = -2 / \alpha [(r / r_{-2})^\alpha - 1]$

# The Einasto $\alpha$ varies with mass

Gao et al 2008

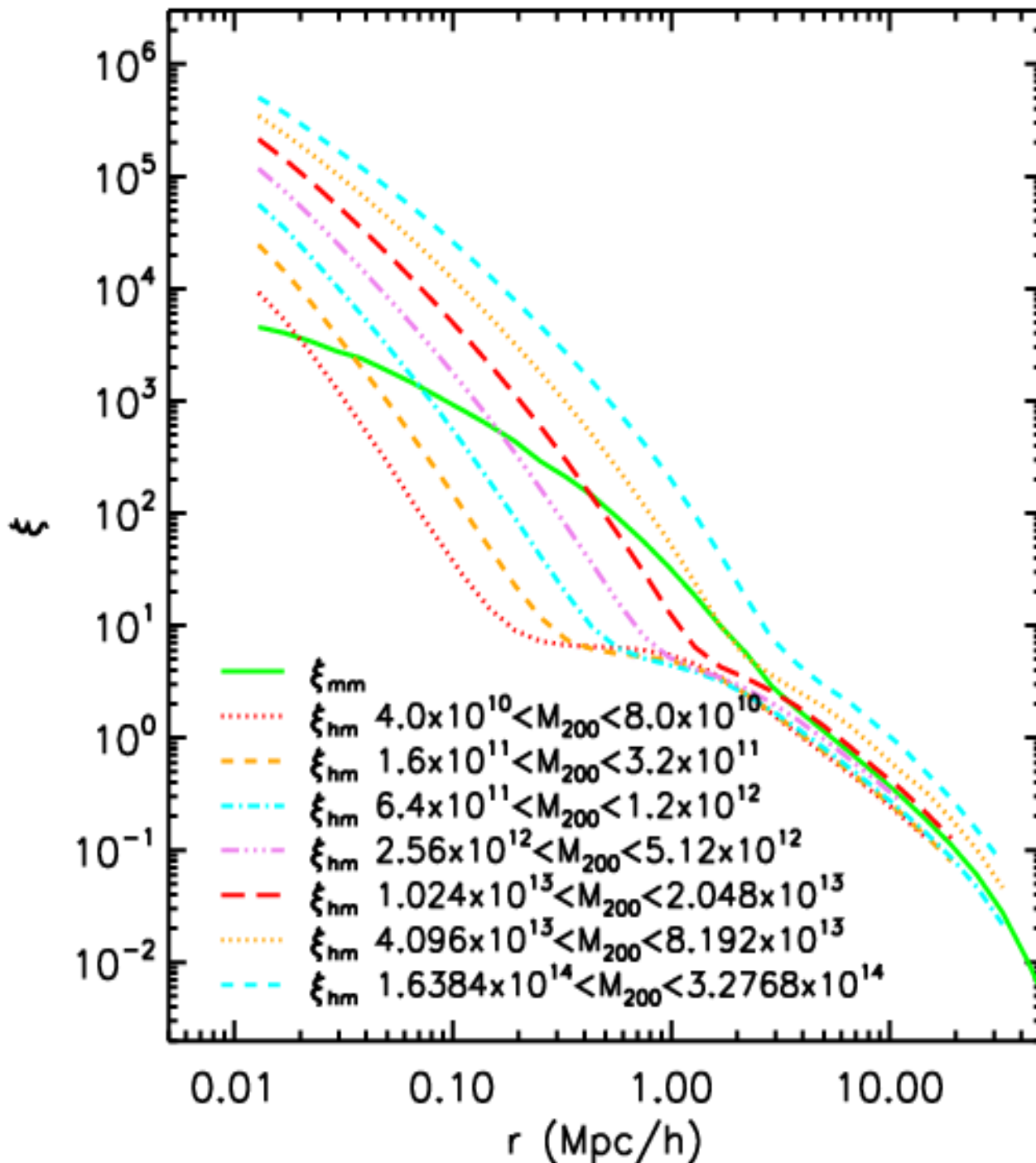
Results for stacked halos in the Millennium run



Einasto's (1965) profile:  $\ln \rho(r)/\rho_{-2} = -2/\alpha [(r/r_{-2})^\alpha - 1]$

# Mean profiles to much larger radii

Hayashi & White 2008



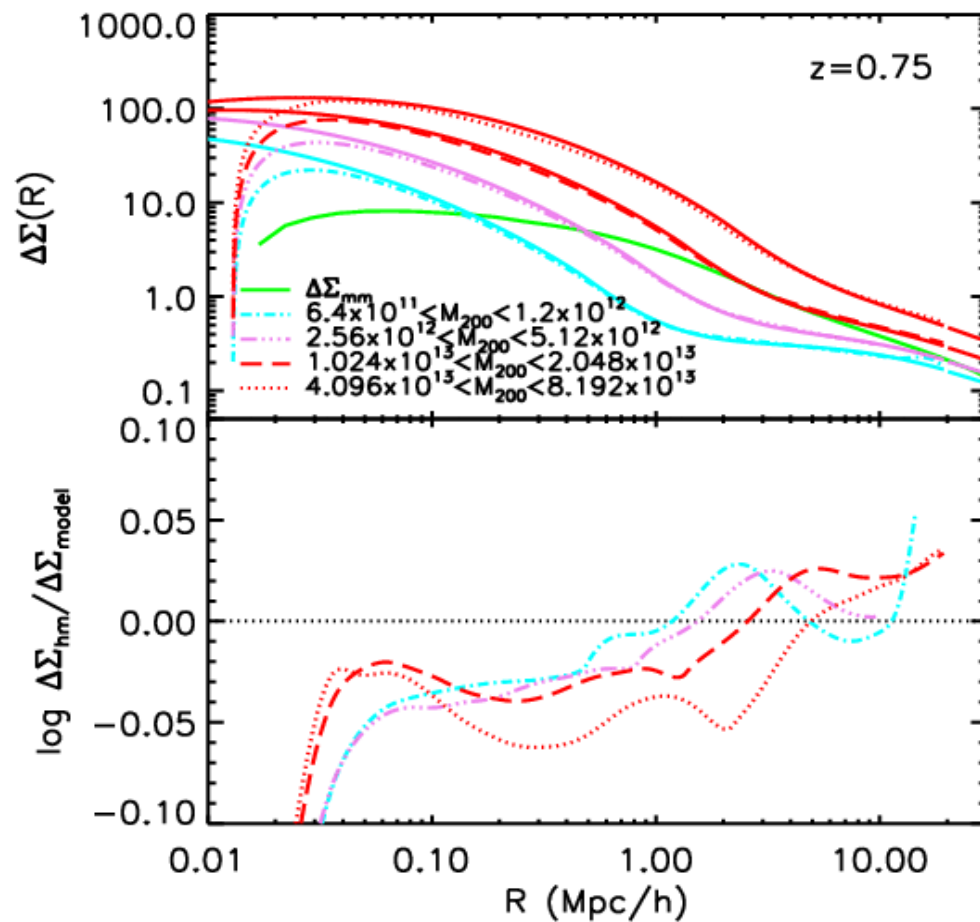
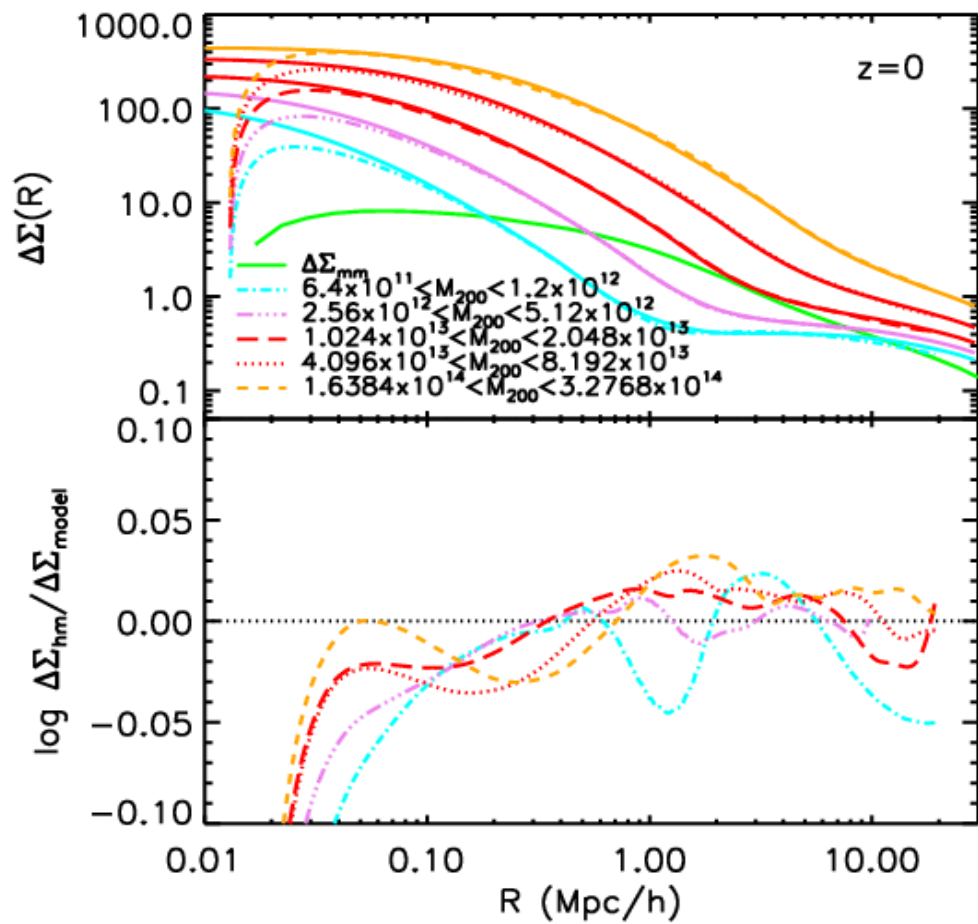
At large radii, the mean density profile  $\bar{\rho}(r) \propto \xi_{lin}(r)$ , the *linear* mass correlation function

To a good approximation

$$\bar{\rho}(r) = \max[ \rho_{Ein}(r), b \xi_{lin}(r) ]$$

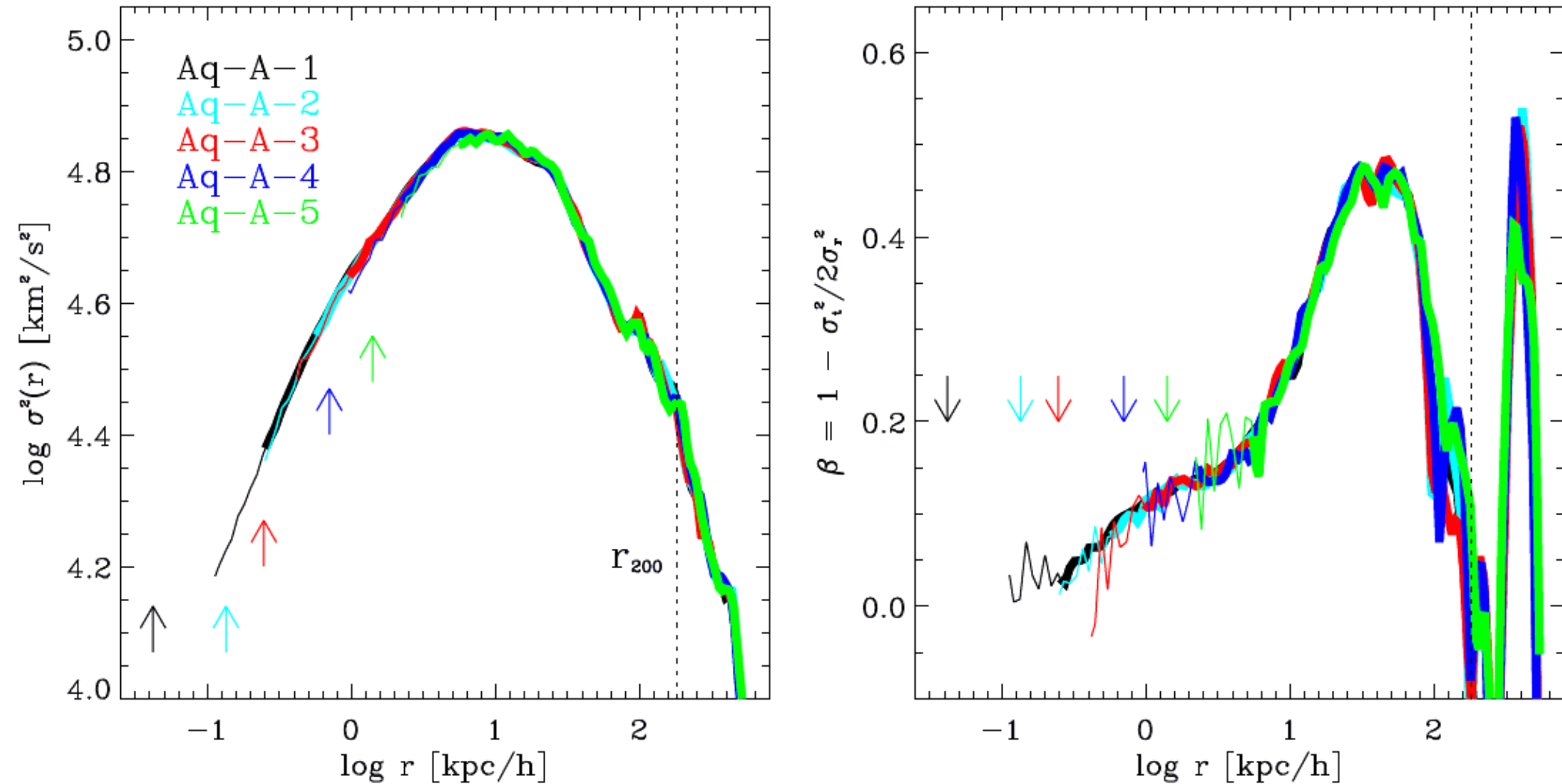
# A lensing test of the DM paradigm?

Hayashi & White 2008



# Velocity dispersion profiles

Navarro et al 2009

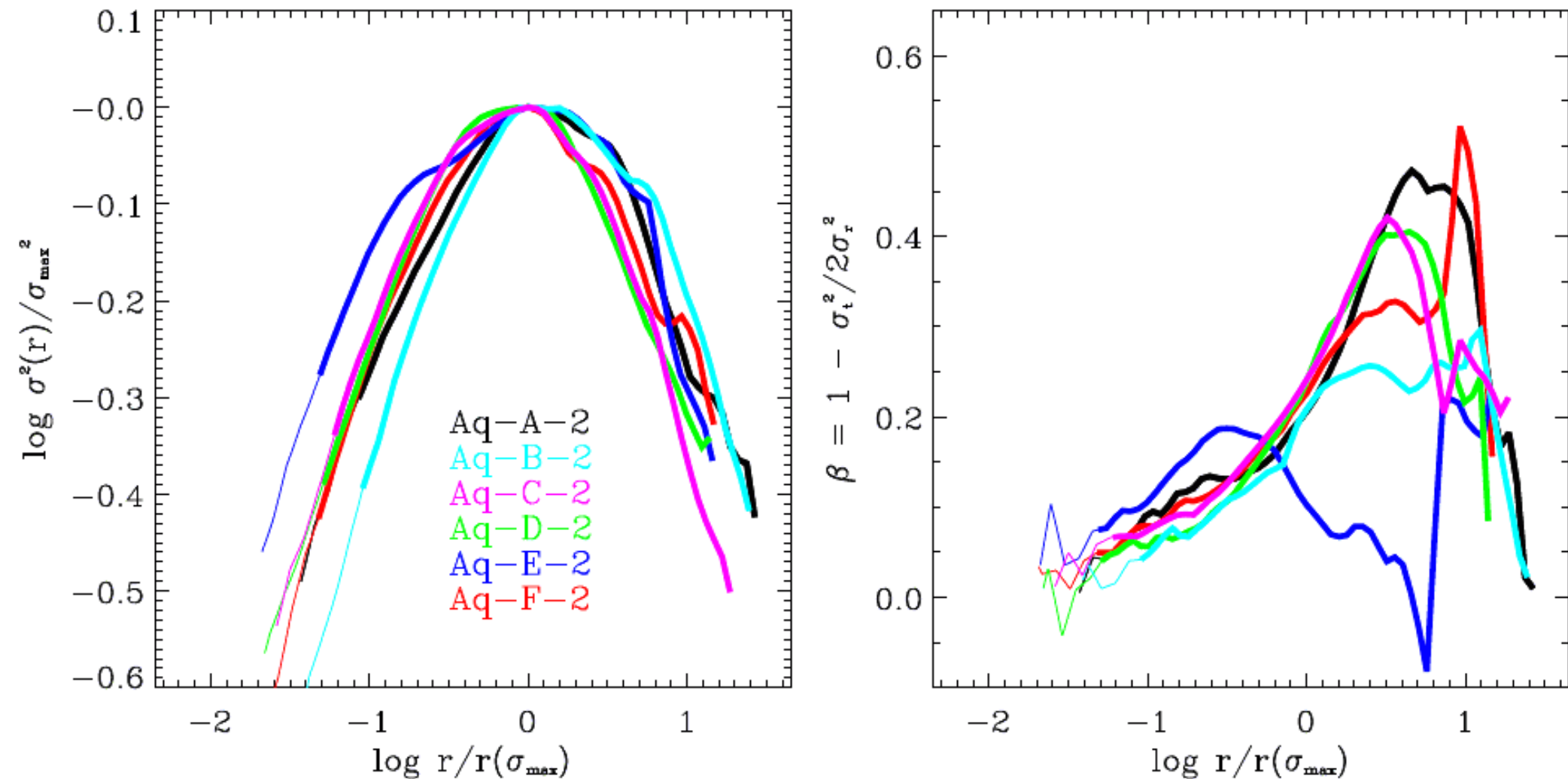


Results are well converged

Velocity dispersion and anisotropy peak at intermediate radii

# Velocity dispersion profiles

Navarro et al 2009



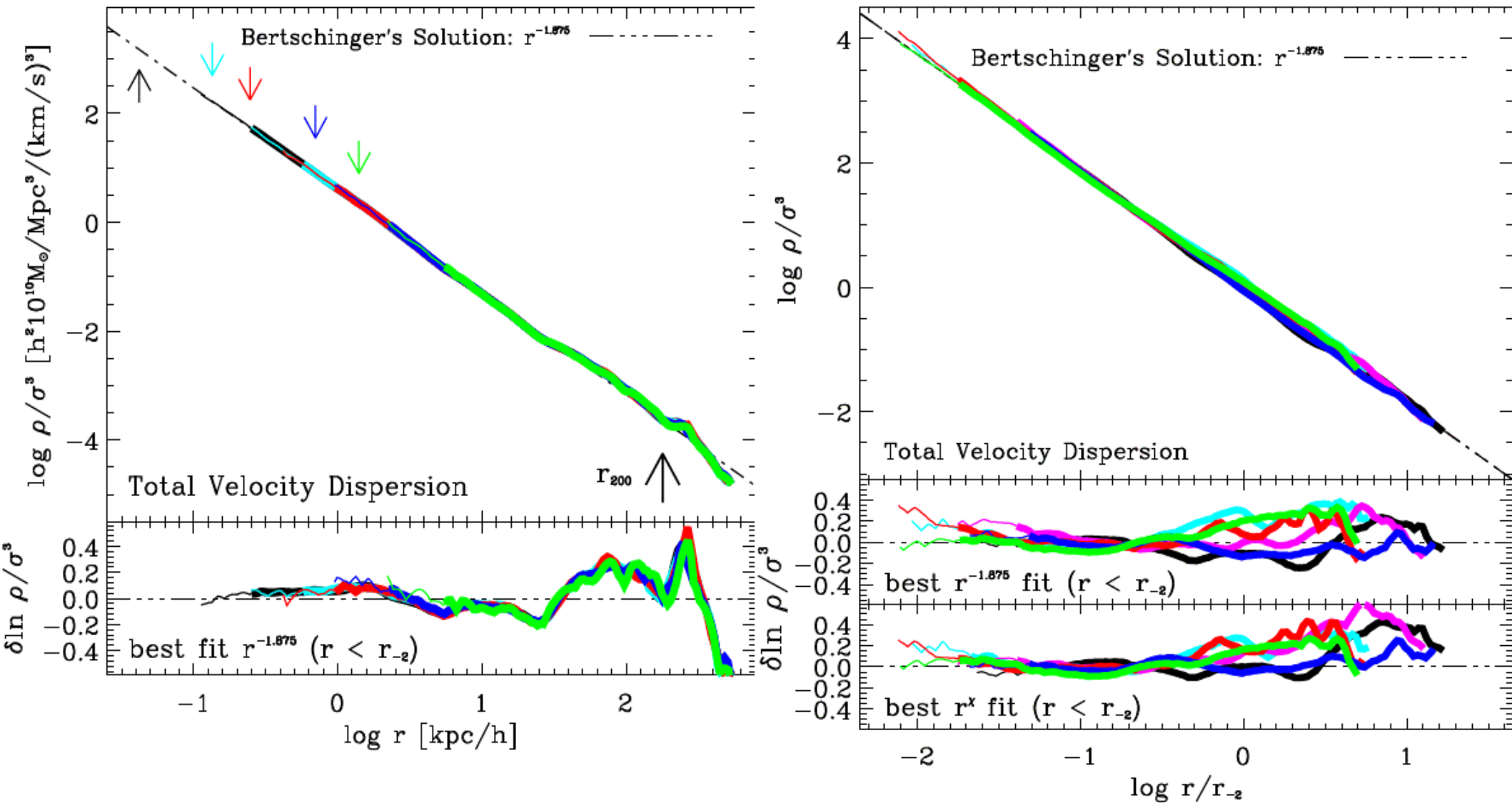
Results are well converged

Velocity dispersion and anisotropy peak at intermediate radii

Profiles vary significantly between halos

# Pseudo-phase-space density profiles

Navarro et al 2009



Shape variations in the density and velocity dispersion profiles compensate to make  $\rho(r) / \sigma(r)^3$  an almost universal power law

# Halo profiles: conclusions

- The NFW formula fits spherically averaged profiles of most objects to within 10% out to at least  $2 r_s$
- The characteristic density (or concentration) varies with mass, redshift and cosmology
- The Einasto formula fits better – its additional shape parameter varies systematically with mass
- There is no indication of *any* “asymptotic inner power law”
- The scatter among halos is larger than the Einasto-NFW difference
- Mean profiles change shape dramatically for  $\delta < 10$
- Velocity dispersion profiles show considerable variation
- Variations in  $\rho(r)$  and  $\sigma(r)$  compensate to give power law  $\rho/\sigma^3$

January 2009

# The Los Cabos Lectures

## Dark Matter Halos: 3

*Simon White*

*Max Planck Institute for Astrophysics*

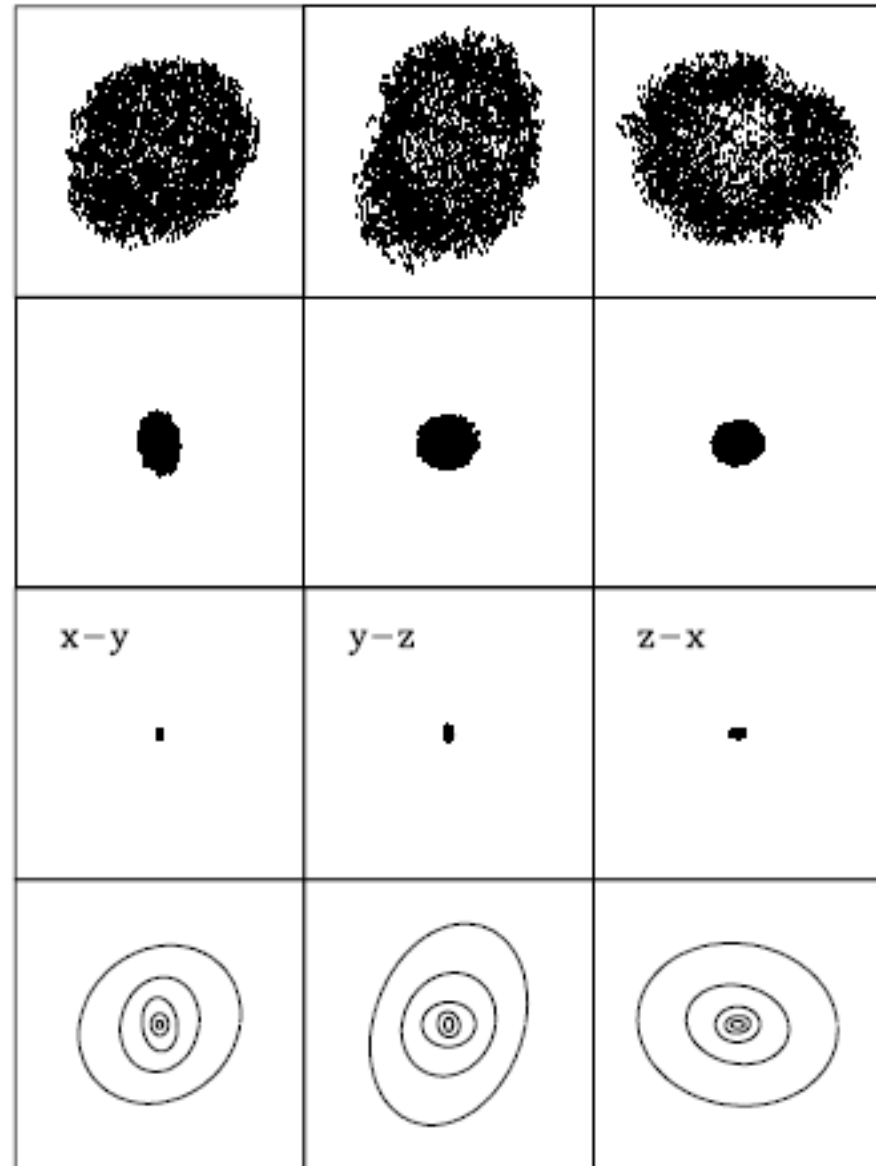
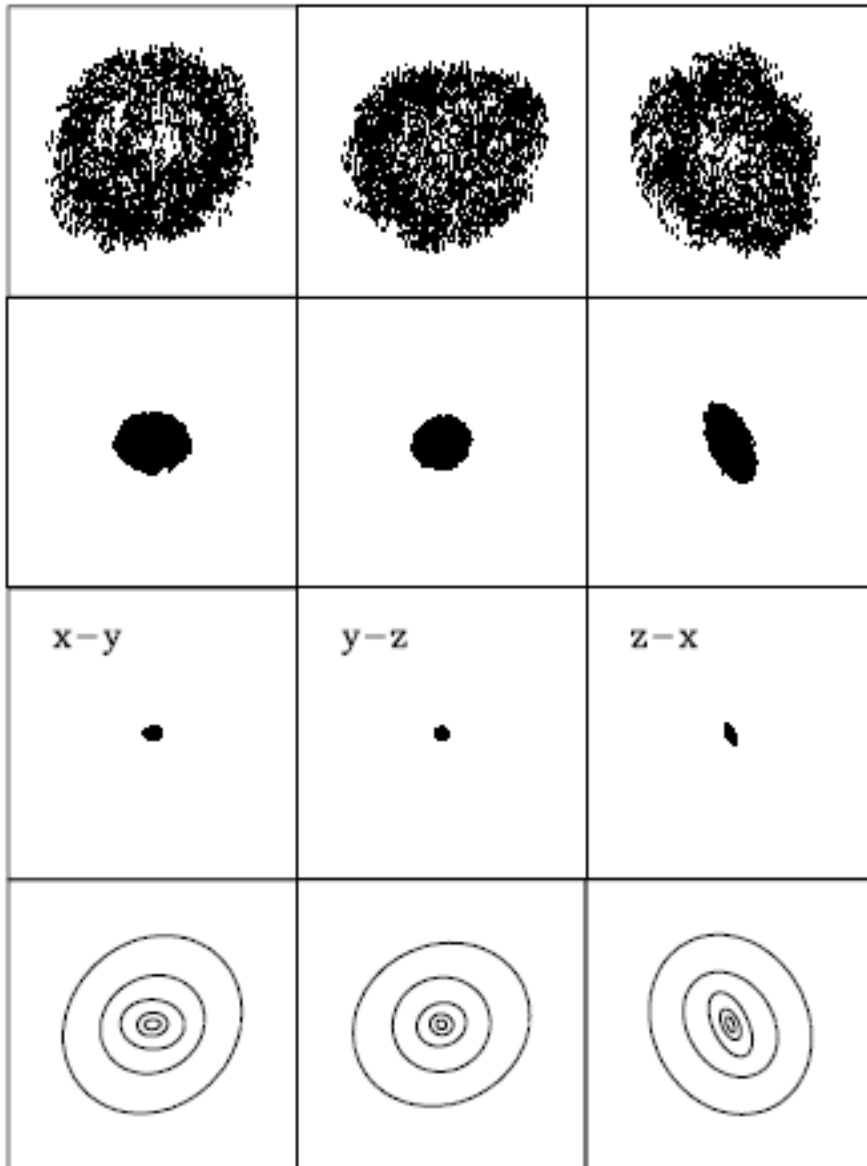
# Shapes of halo equidensity surfaces

Group

Jing & Suto 2002

Galaxy

$\delta$

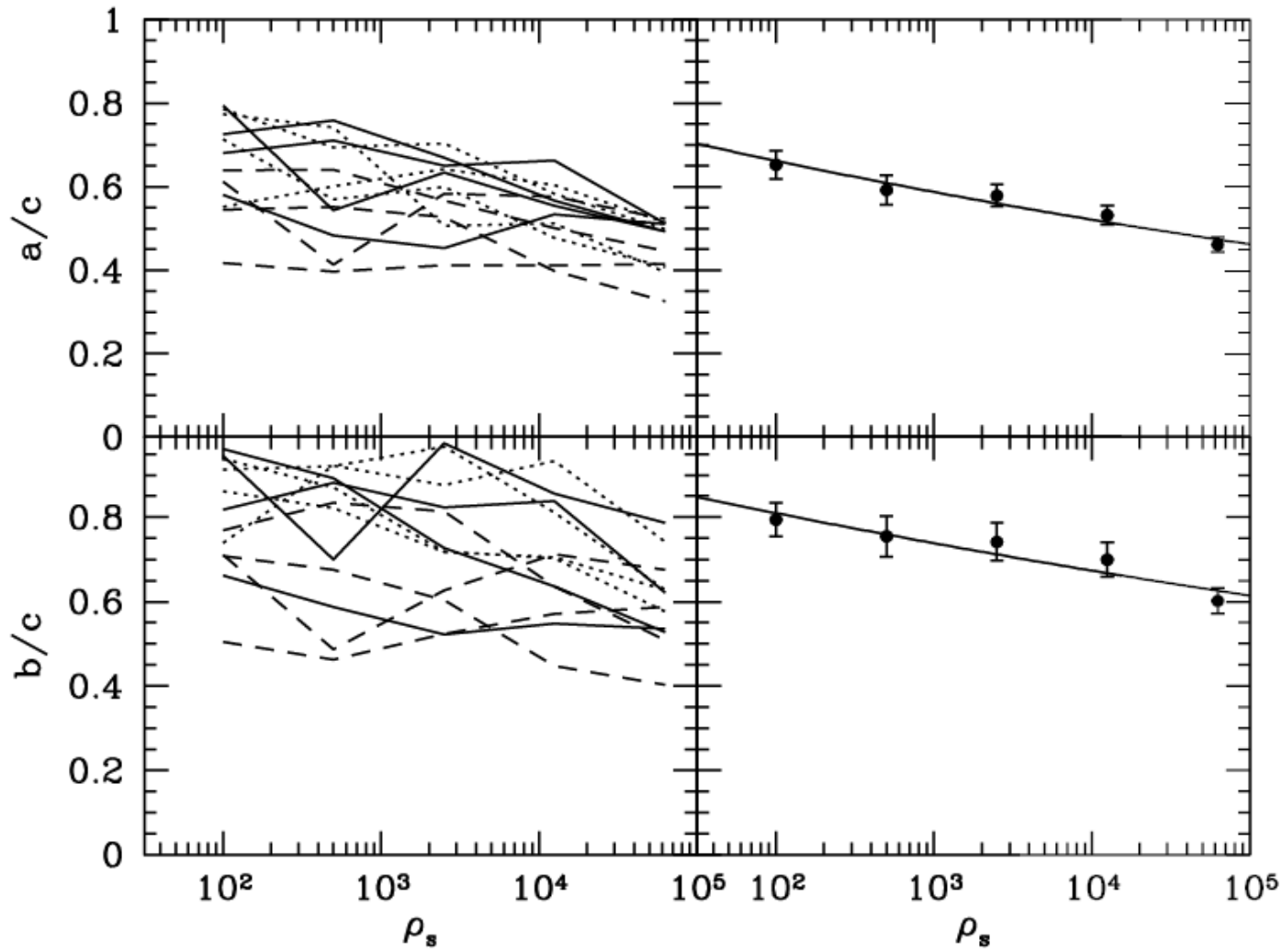


100

2500

6250

# Shapes of halo equidensity surfaces

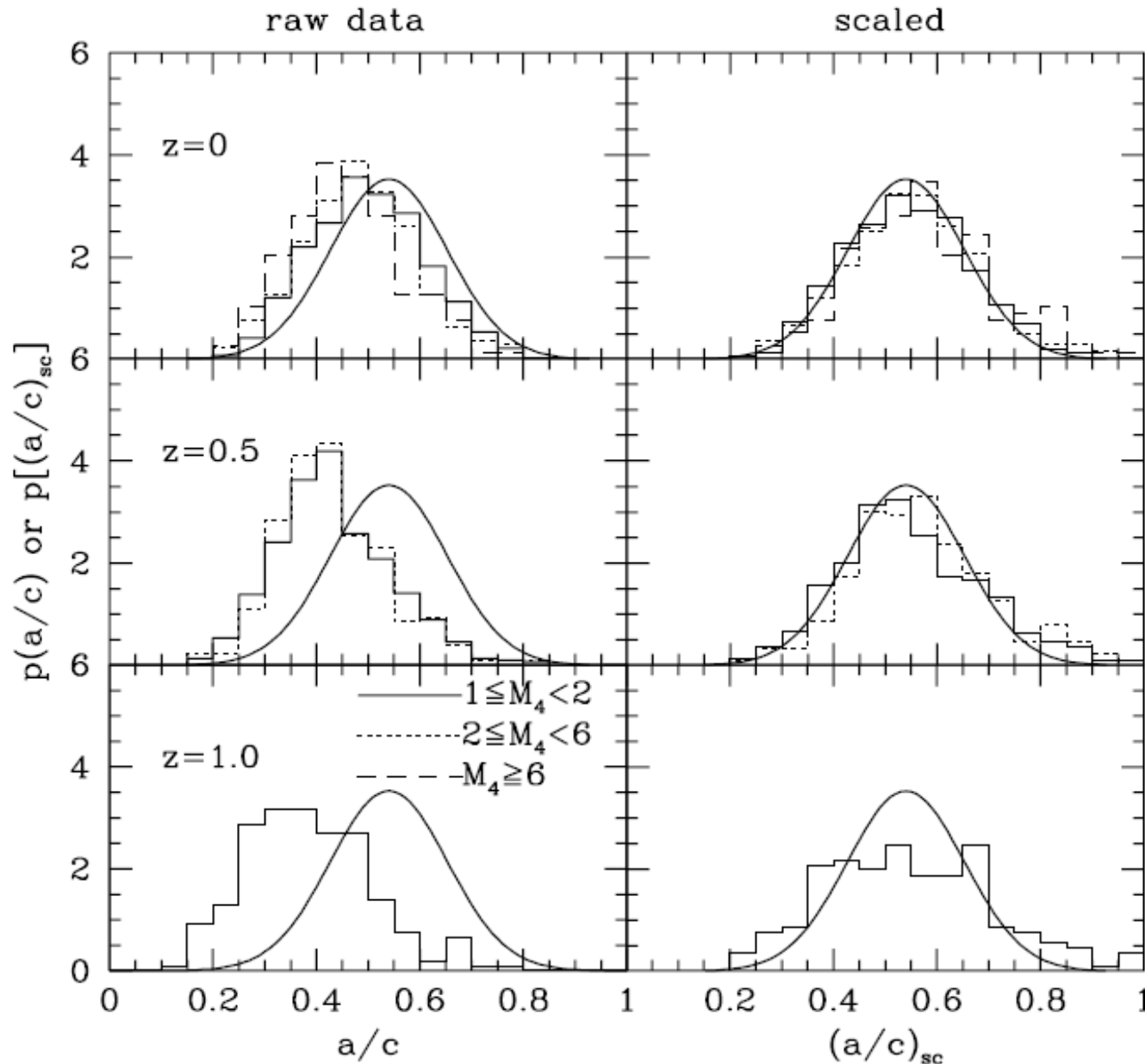


Jing & Suto 2002

Shapes become systematically less spherical with decreasing radius

# Shapes of halo equidensity surfaces

$$\Omega_0=1.0, \Lambda_0=0.0, \sigma_8=0.55$$



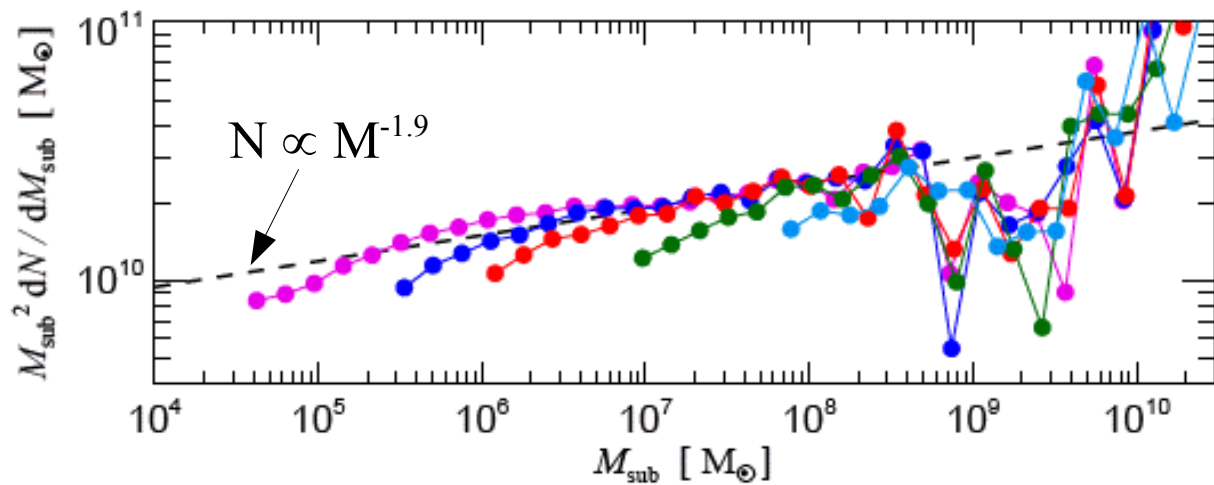
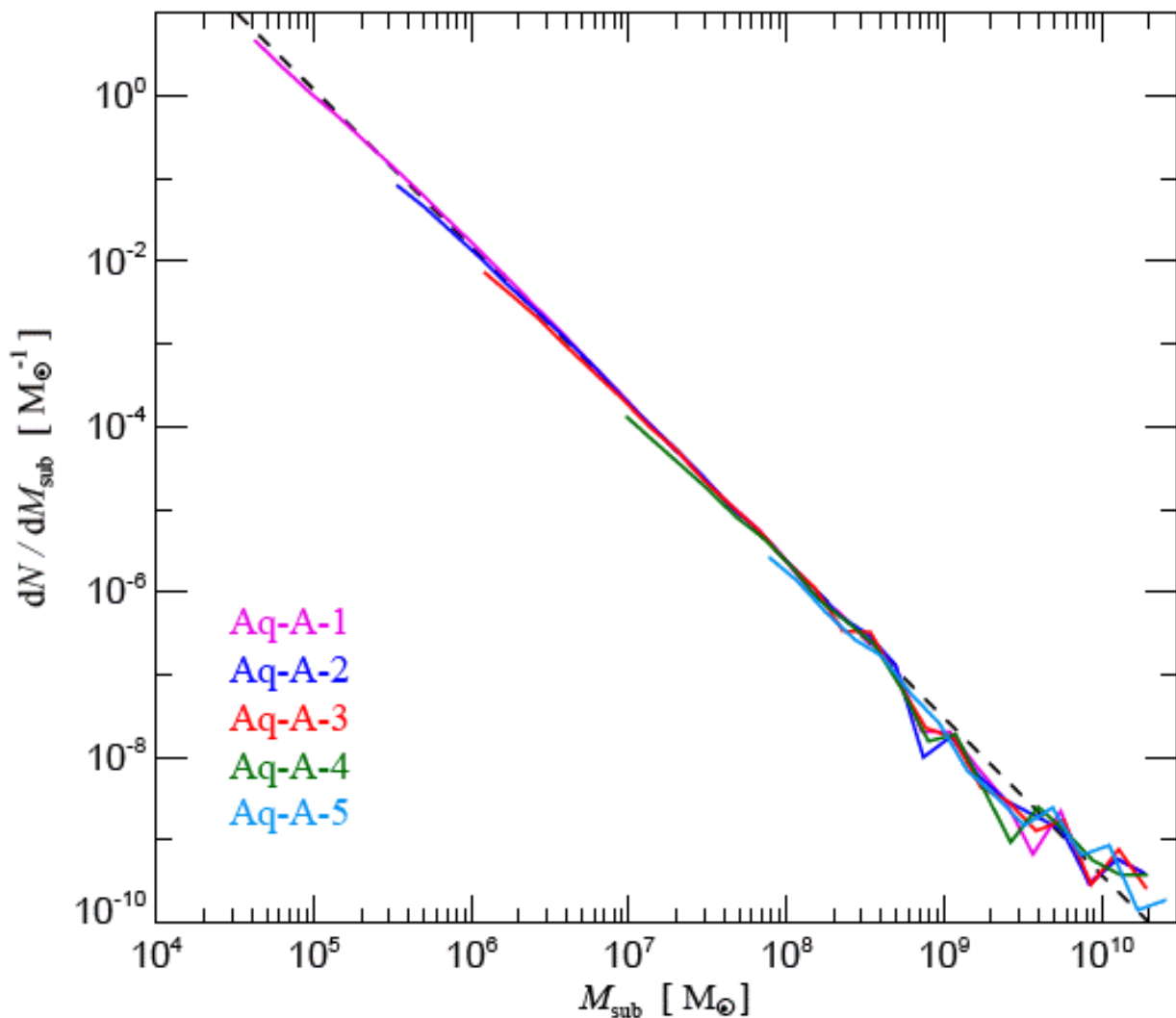
Jing & Suto 2002

Shapes become systematically less spherical with increasing mass

A simple scaling leaves a "universal" result for the axis ratio distributions

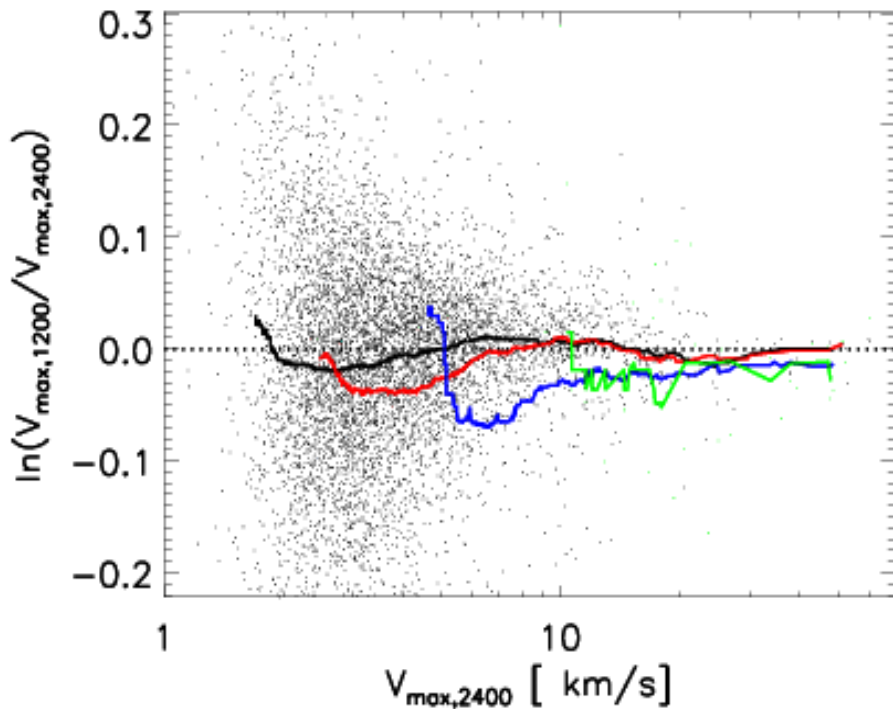
# How well does substructure converge?

Springel et al 2008

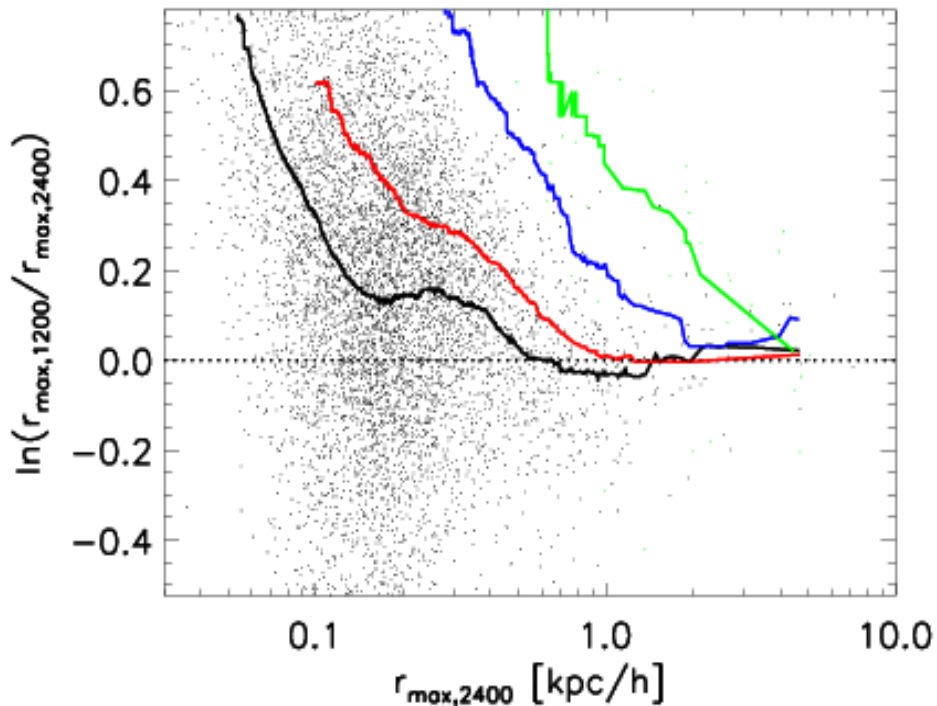


# How well does substructure converge?

Aquarius Project: Springel et al 2008



Convergence in the size and maximum circular velocity for individual subhalos cross-matched between simulation pairs.



Biggest simulation gives convergent results for

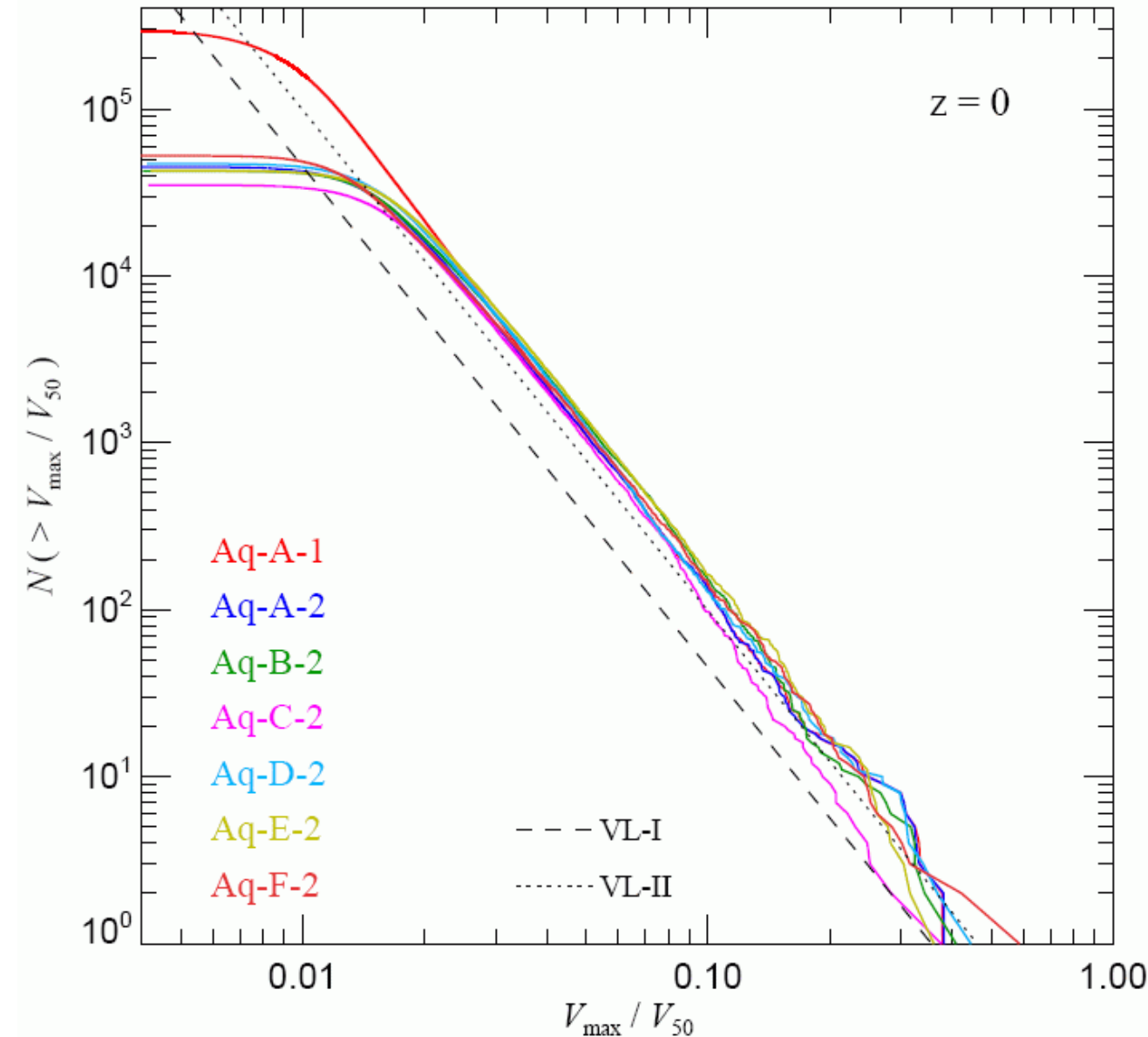
$$V_{\max} > 1.5 \text{ km/s}$$

$$r_{\max} > 165 \text{ pc}$$

Much smaller than the halos inferred for even the faintest dwarf galaxies

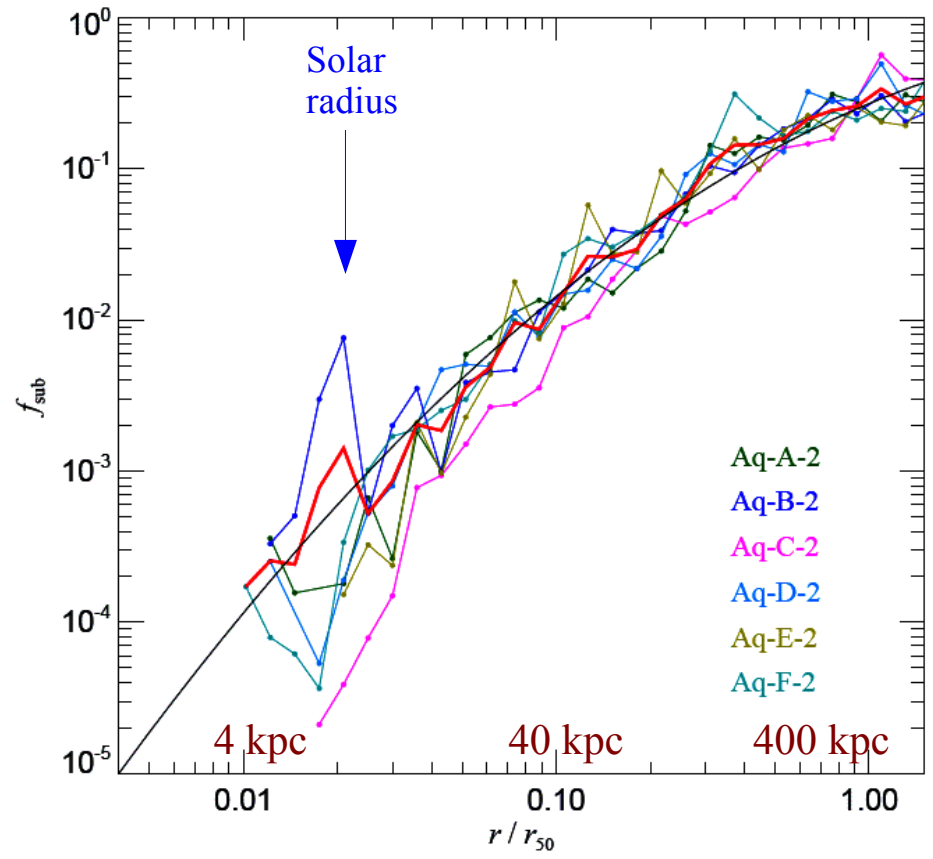
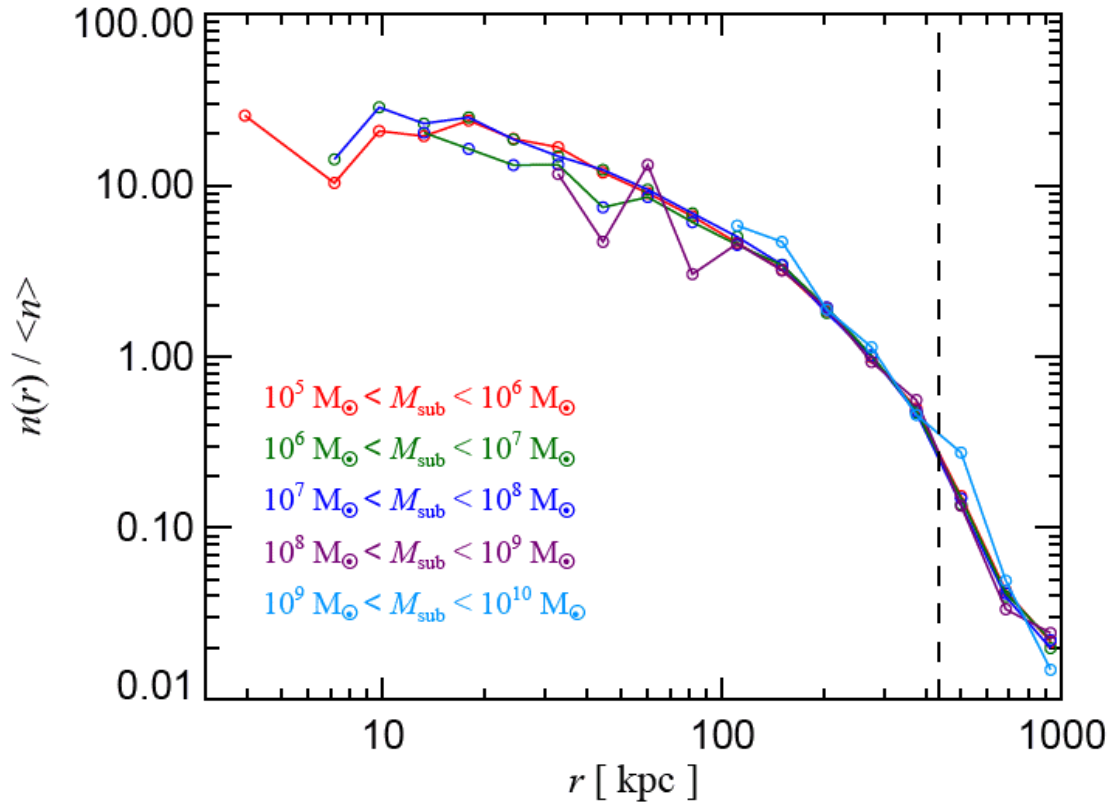
# How uniform are subhalo populations?

Springel et al 2008

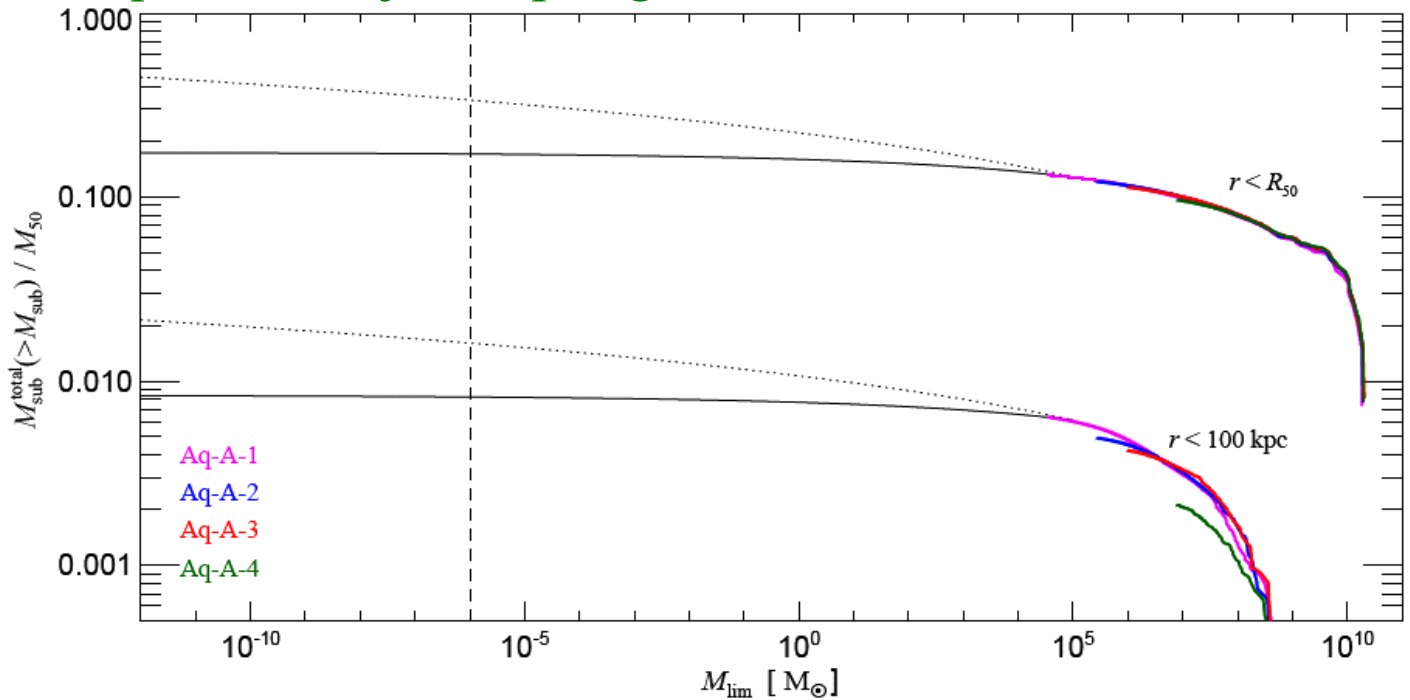


For the six Aquarius halos, the scatter in subhalo abundance is Poisson at high mass and  $\sim 20\%$  at low mass

The Via Lactea simulations differ significantly



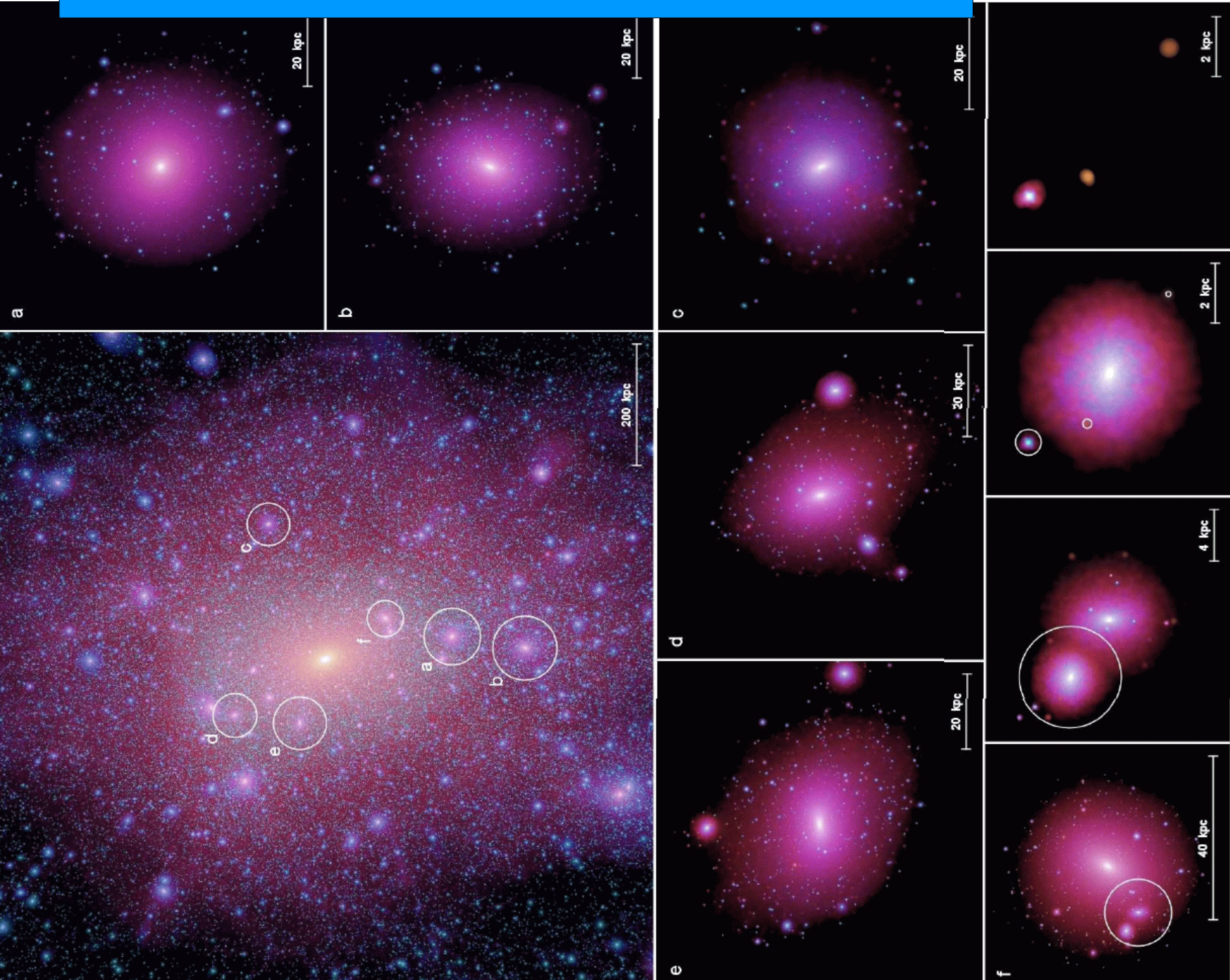
### Aquarius Project: Springel et al 2008



- All mass subhalos are similarly distributed
- A small fraction of the inner mass in subhalos
- $\ll 1\%$  of the mass near the Sun is in subhalos

# Subhalos have subhalos have subhalos...

Springel et al 2008



# Substructure: conclusions

- Substructure is primarily in the outermost parts of halos
- The radial distribution of subhalos is almost mass-independent
- Subhalo populations scale (almost) with the mass of the host
- The subhalo mass distribution converges only weakly at small  $m$
- Subhalos contain a small fraction of the mass in the inner halo

# Small-scale structure of the CDM distribution

- Direct detection involves bolometers/cavities of meter scale which are sensitive to particle momentum
  - what is the density structure between m and kpc scales?
  - how many streams intersect the detector at any time?
- Intensity of annihilation radiation depends on
$$\int \rho^2(\mathbf{x}) \langle \sigma v \rangle dV$$
  - what is the density distribution around individual CDM particles on the annihilation interaction scale?

Predictions for detection experiments depend on the CDM distribution on scales far below those accessible to simulation

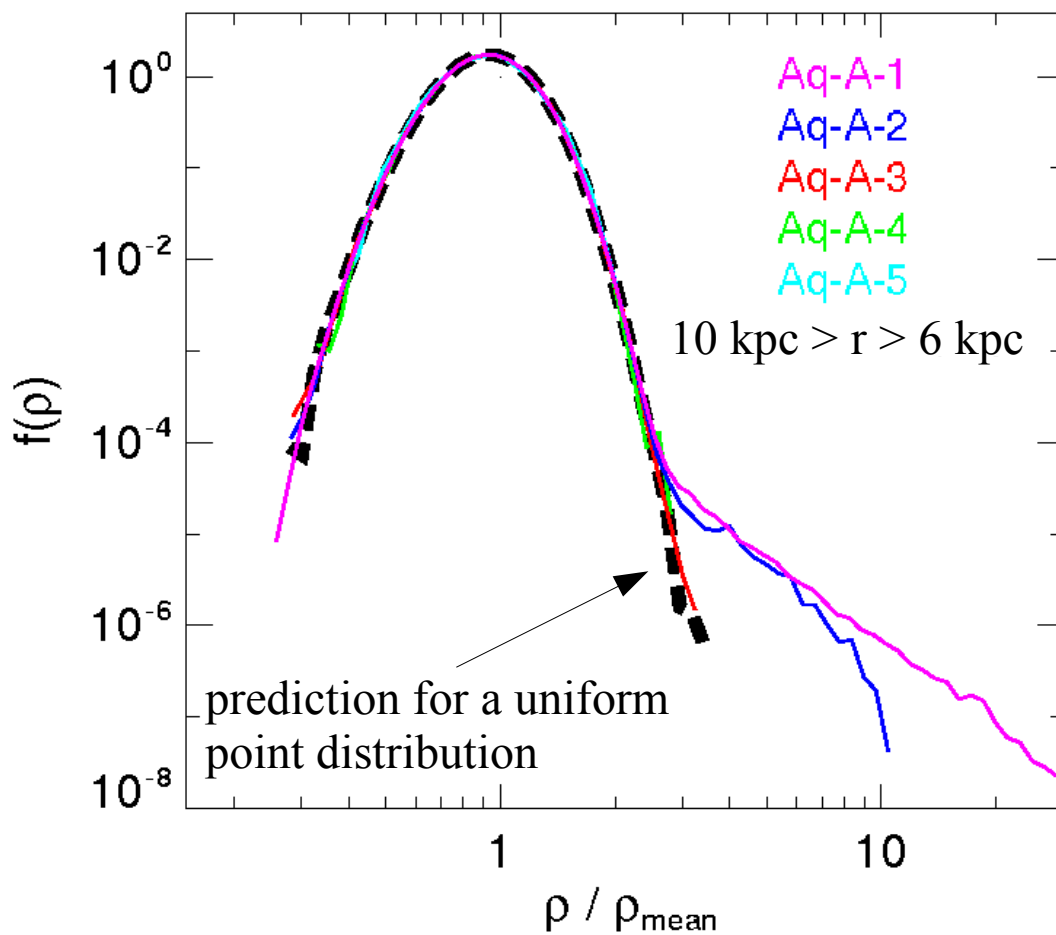
→ We require a good theoretical understanding of mixing and small-scale structure

# Detectability issues for the CDM distribution

- Laboratory experiments
  - What is the expected CDM distribution in space and in velocity on the scale of the apparatus?
- Small-scale clumping
  - How much  $\gamma$ -emission comes from small clumps?
  - Which structures should be most easily detected?
- Unbound phase-space structure
  - How much  $\gamma$ -emission comes from caustics?
- Galactic Centre
  - How much  $\gamma$ -emission comes from the black hole's cusp?

# Density relative to a smooth ellipsoidal model

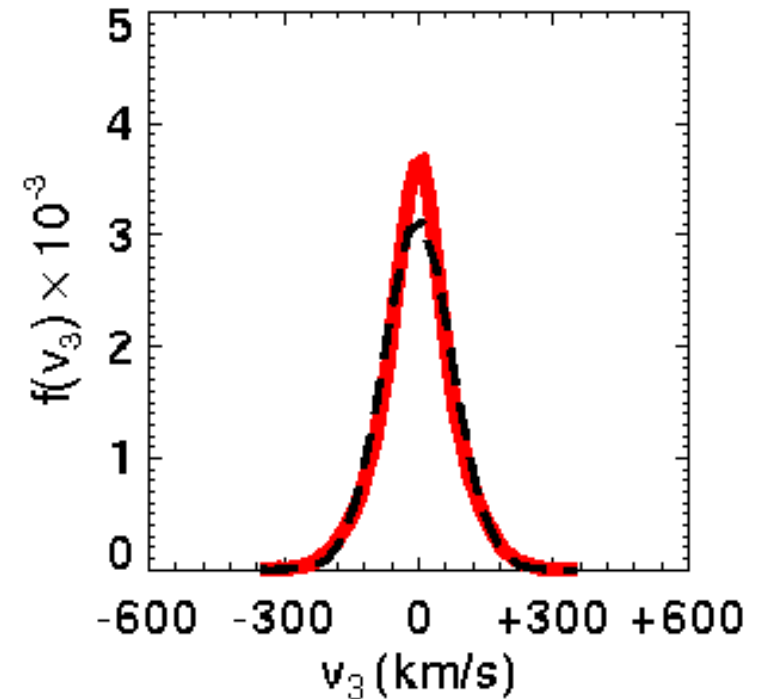
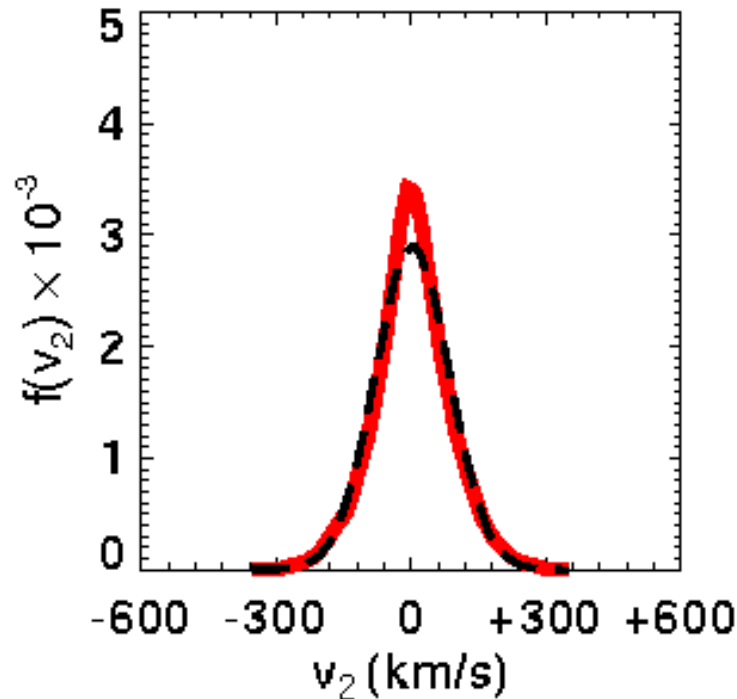
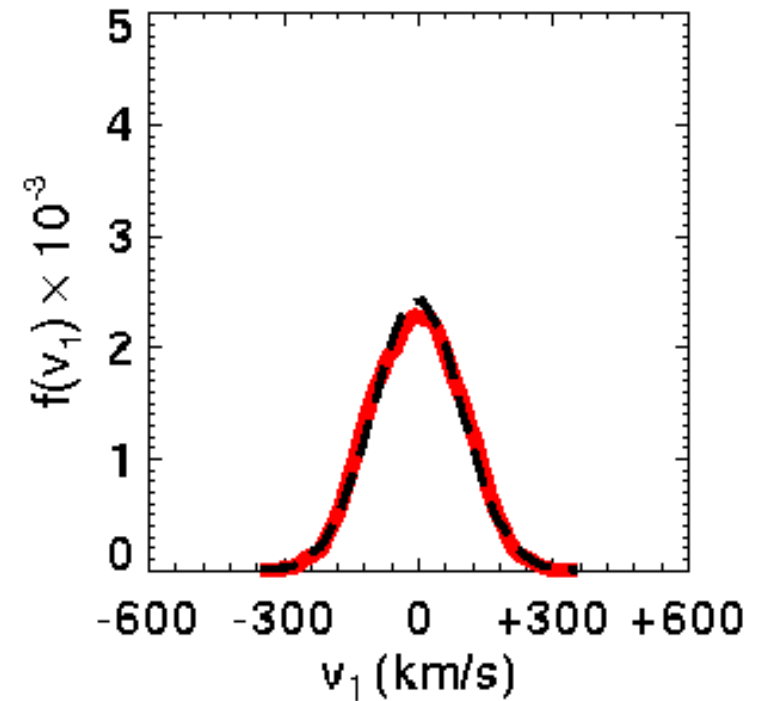
Vogelsberger et al 2008



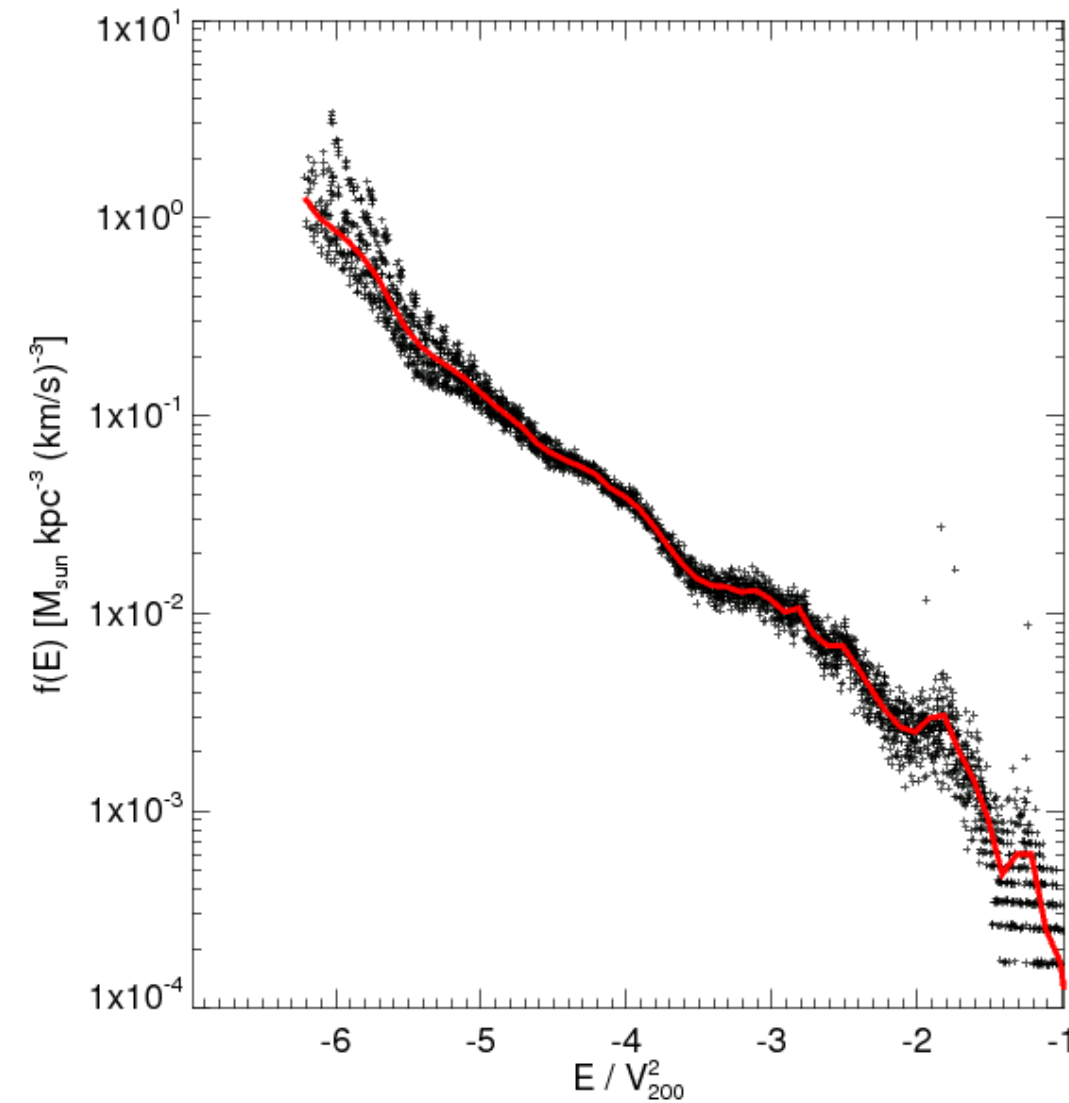
- Estimate a density  $\rho$  at each point by adaptively smoothing using the 64 nearest particles
- Fit to a smooth density profile stratified on similar ellipsoids
- The chance of a random point lying in a substructure is  $< 10^{-4}$
- The *rms* scatter about the smooth model for the remaining points is only about 4%

# Local velocity distribution

- Velocity histograms for particles in a typical  $(2\text{kpc})^3$  box at  $R = 8$  kpc
- Distributions are smooth, near-Gaussian and different in different directions
- No individual streams are visible



# Energy space features – fossils of formation



The energy distribution within  $(2 \text{ kpc})^3$  boxes shows bumps which

- repeat from box to box
- are stable over Gyr timescales
- repeat in simulations of the same object at varying resolution
- are different in simulations of different objects

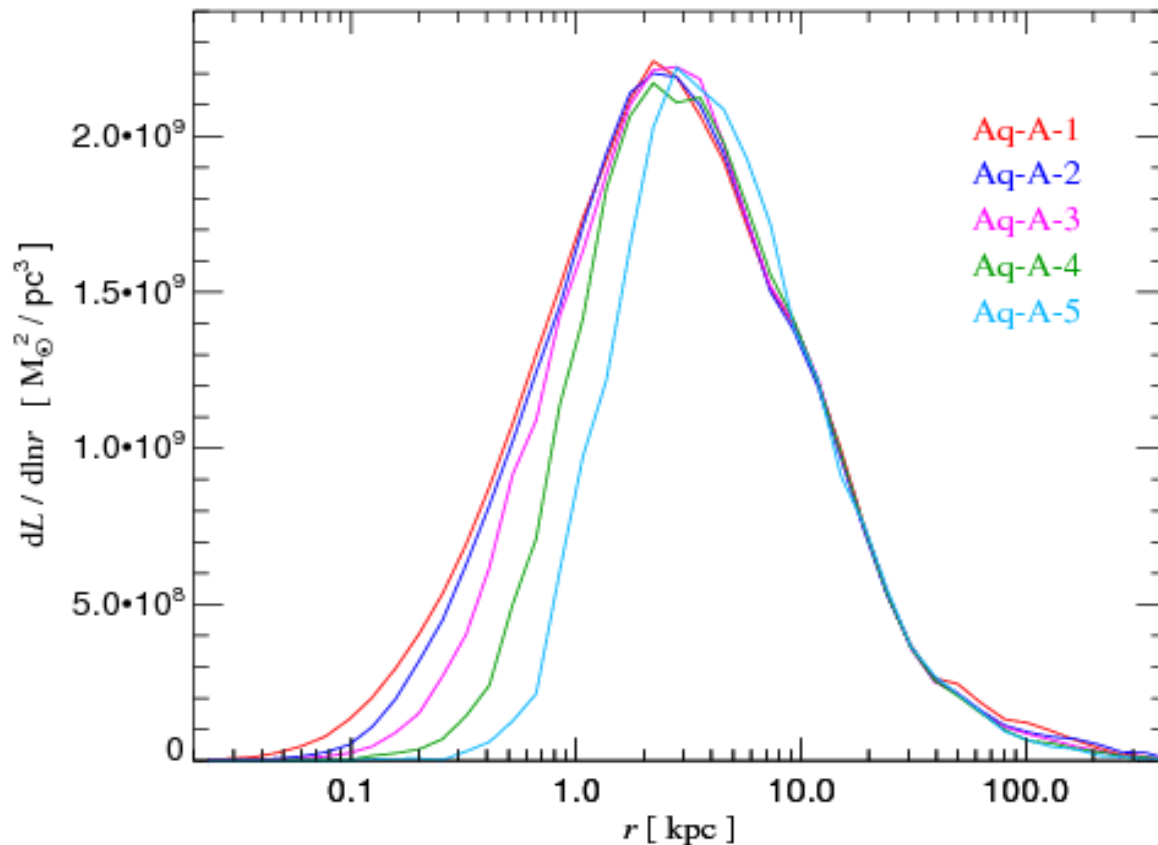
These are potentially observable fossils of the formation process

# Conclusions for direct detection experiments

- With more than 99.9% confidence the Sun lies in a region where the DM density differs from the smooth mean value by  $< 20\%$
- The local velocity distribution of DM particles is similar to a trivariate Gaussian with no measurable “lumpiness” due to individual DM streams
- The energy distribution of DM particles should contain broad features with  $\sim 20\%$  amplitude which are the fossils of the detailed assembly history of the Milky Way's dark halo

# Convergence of annihilation luminosity of main halo

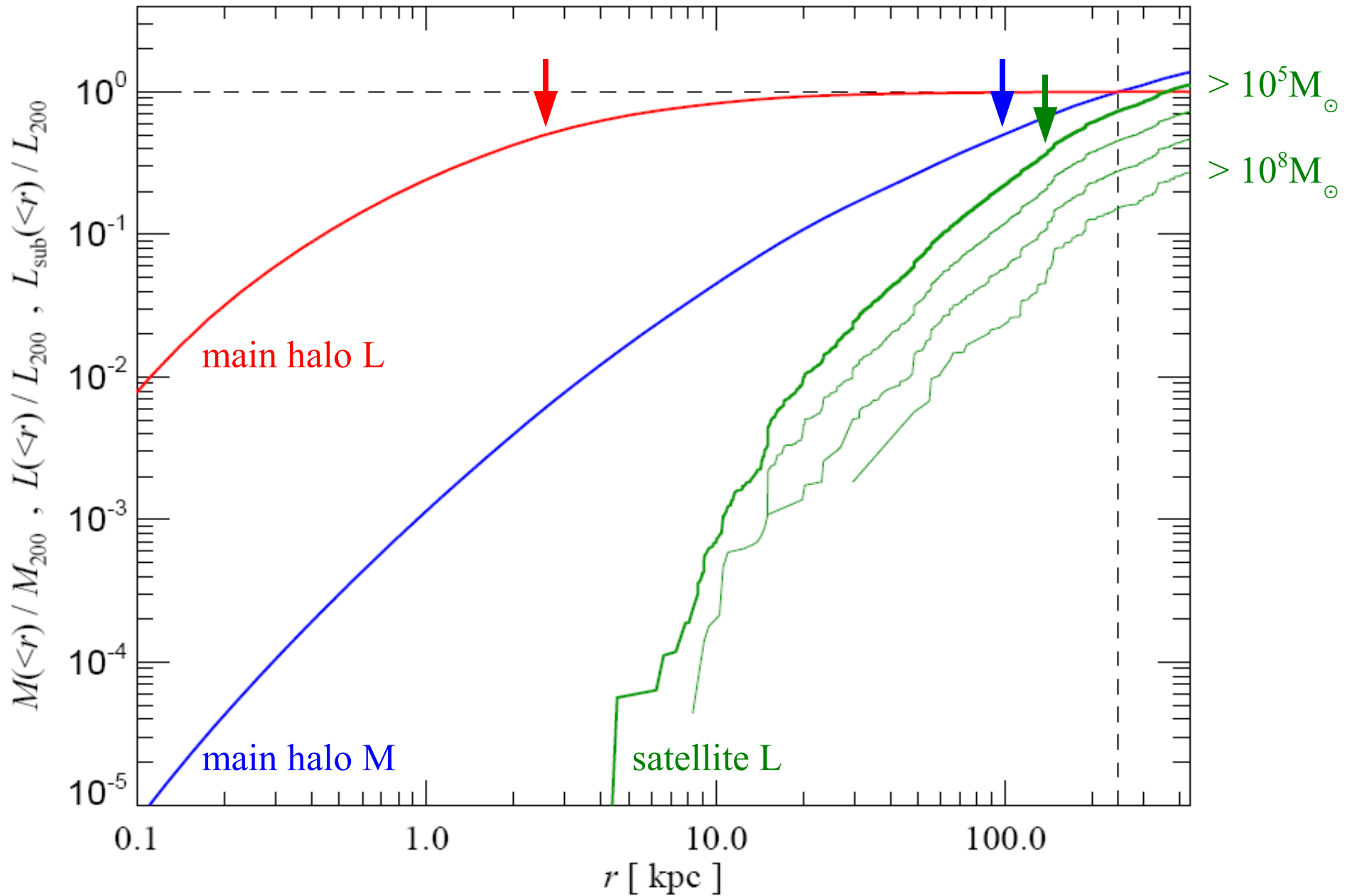
Springel et al 2008



- Distribution has converged at the percent level for the main halo
- Most emission comes from  $0.5 \text{ kpc} < r < 20 \text{ kpc}$
- Emission is not converged for most subhalos but should scale as  $V_{\text{max}}^4 / r_{\text{max}}$
- This estimate is converged for  $V_{\text{max}} > 1.5 \text{ km/s}$   
 $r_{\text{max}} > 165 \text{ pc}$

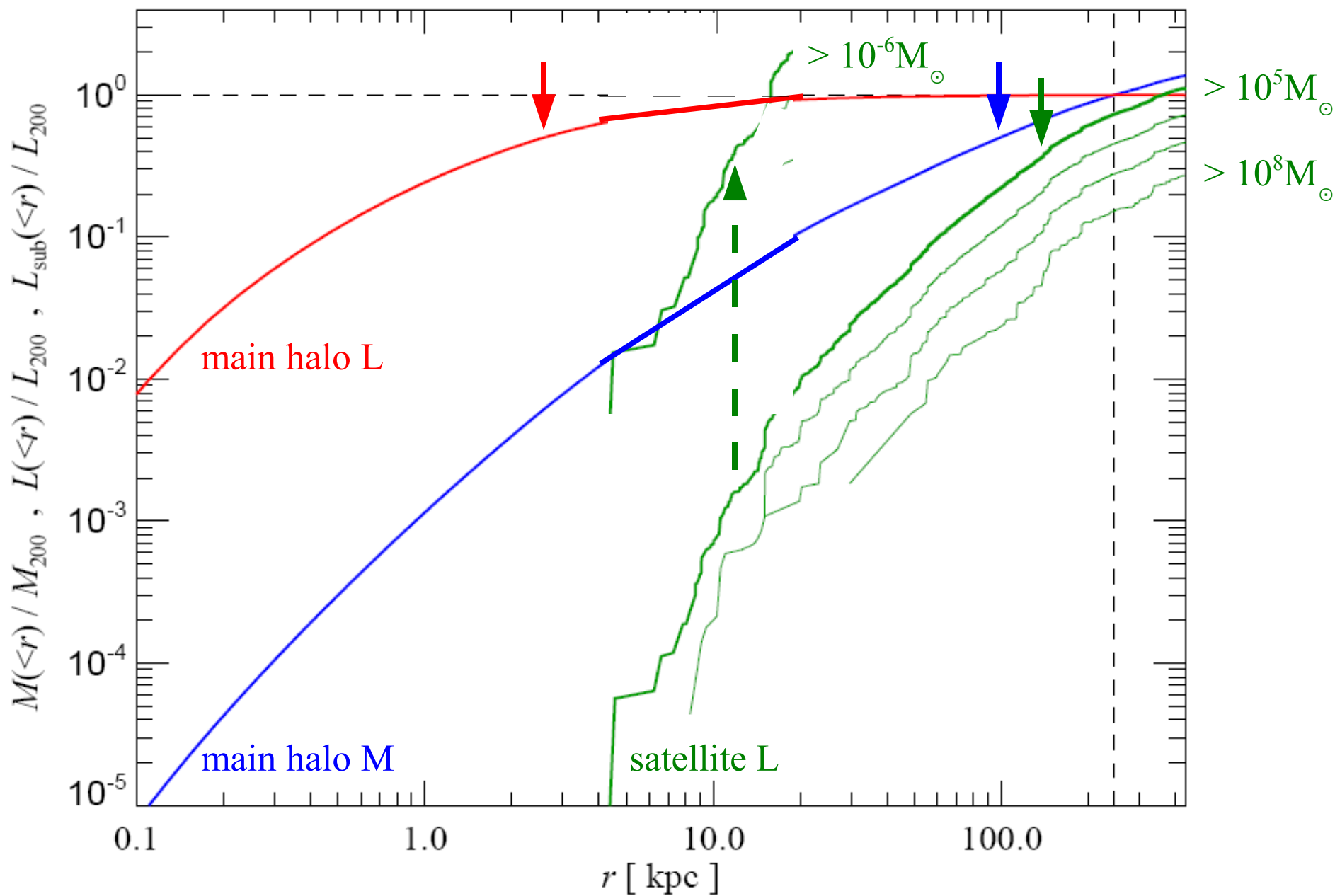
# Mass and annihilation radiation profiles of a MW halo

Springel et al 2008



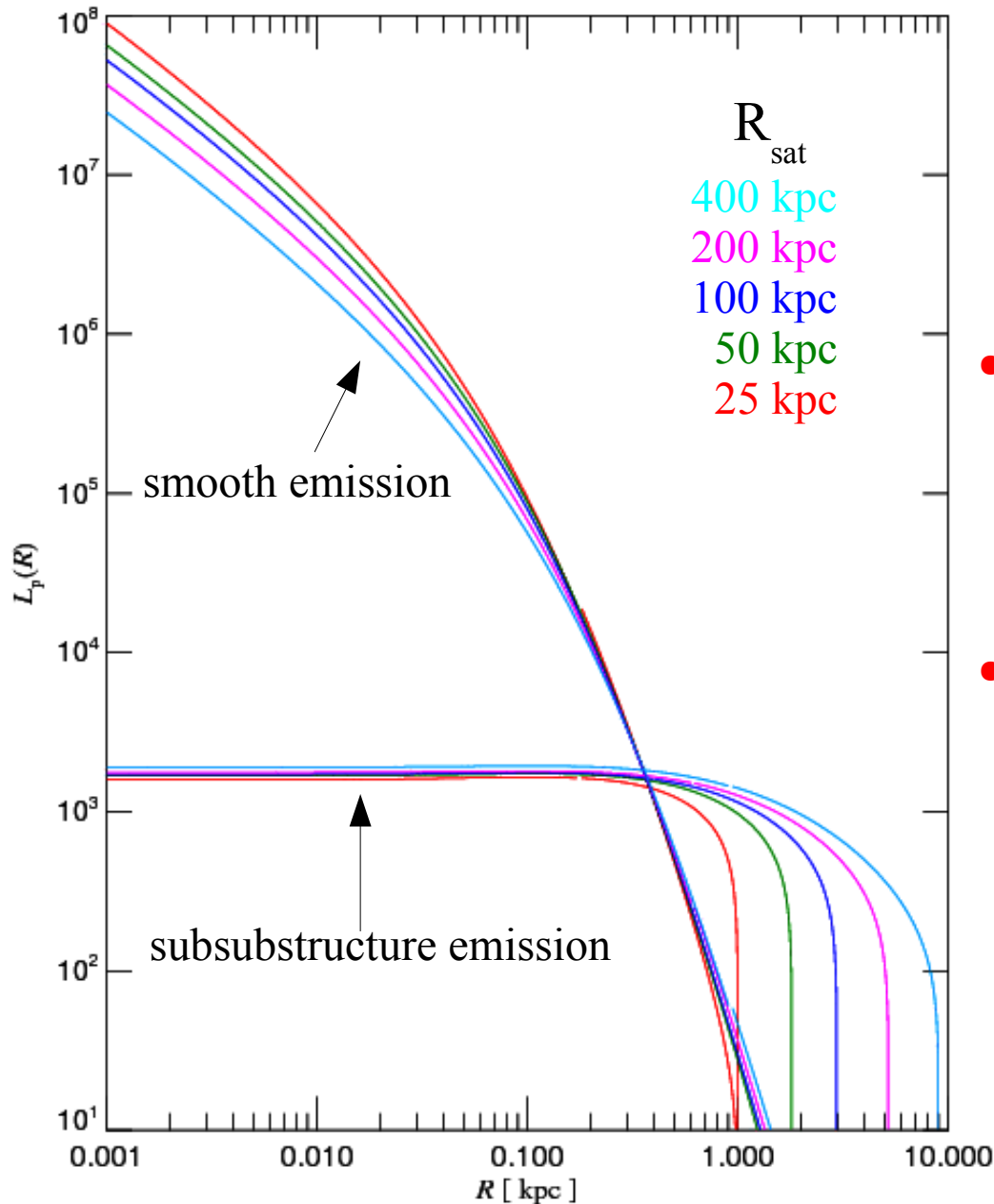
# Mass and annihilation radiation profiles of a MW halo

Springel et al 2008



# Subhalo annihilation luminosity profiles: $V_{\text{max}} = 10 \text{ km/s}$

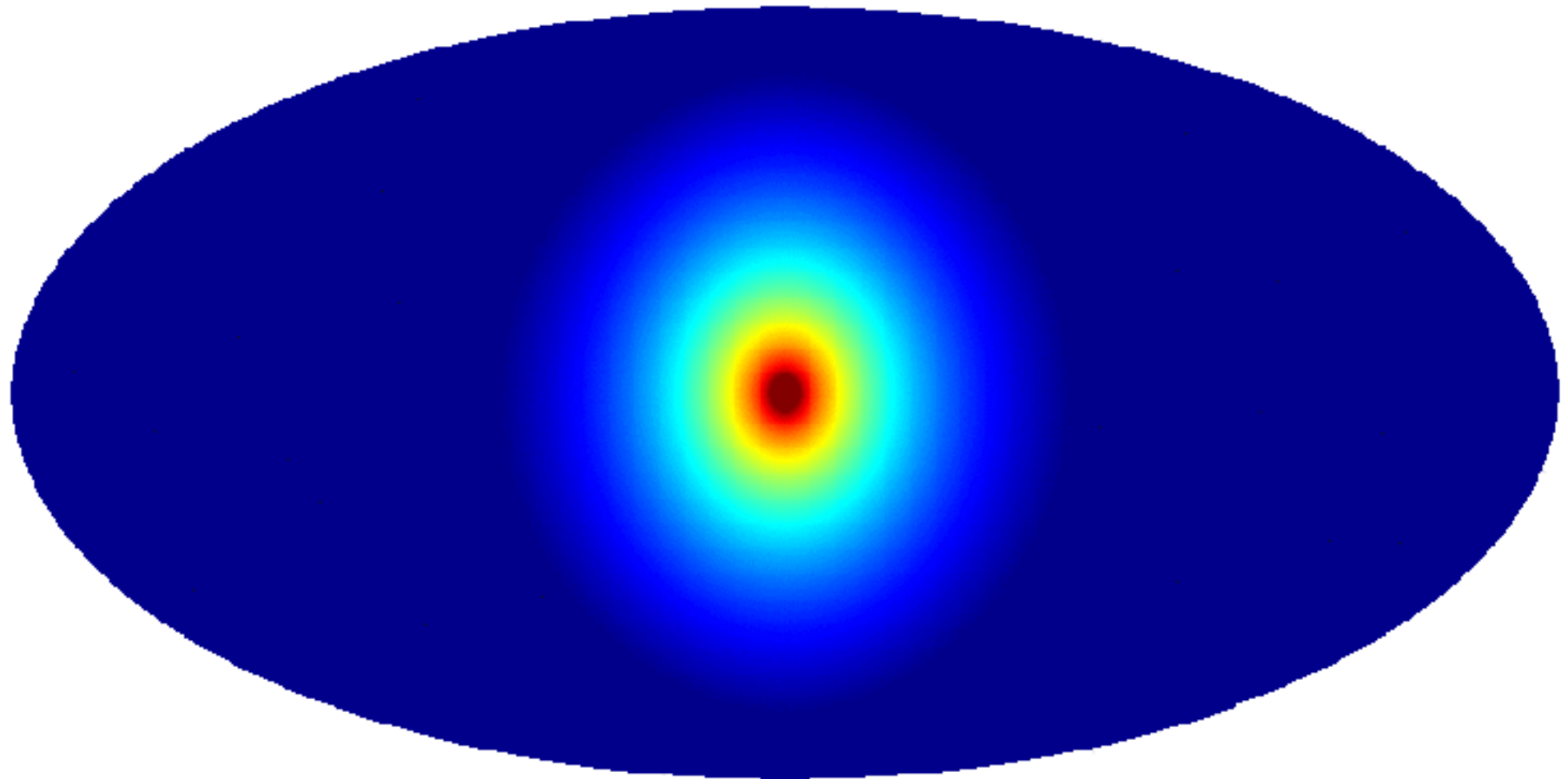
Springel et al 2008



- MW subhalos above Earth mass contribute 230 times as much luminosity within 250 kpc as the smooth halo mass distribution
  - The projected surface brightness of the subhalo population is almost uniform
  - When a small object falls into the MW, tides remove its subhalos but don't affect its smooth emission
- substructure does not much boost subhalo luminosities in the inner Galaxy ( $r < 30 \text{ kpc}$ )

# Milky Way halo seen in DM annihilation radiation

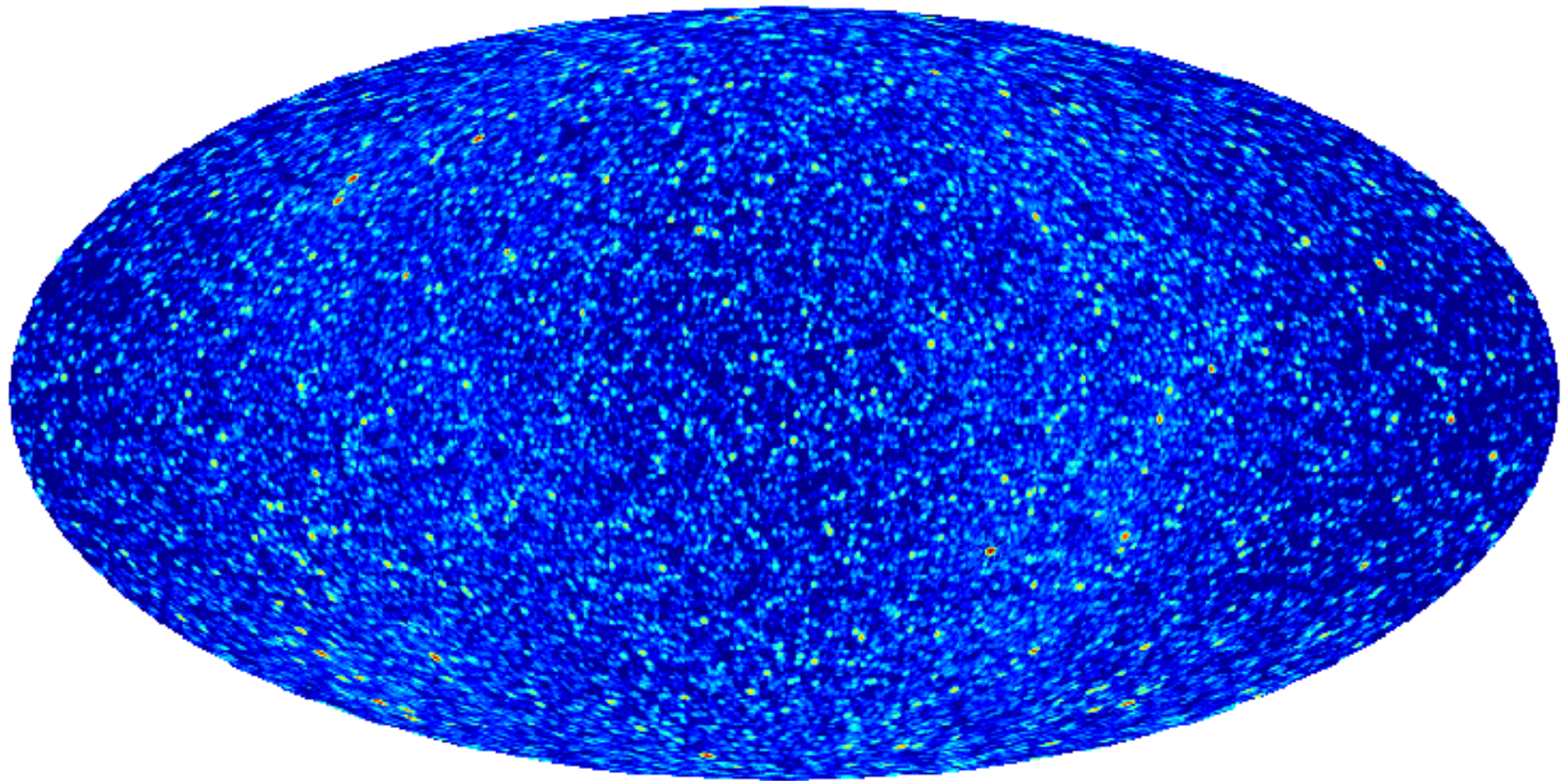
*smooth main halo emission (MainSm)*



-0.50  2.0 Log(Intensity)

# Milky Way halo seen in DM annihilation radiation

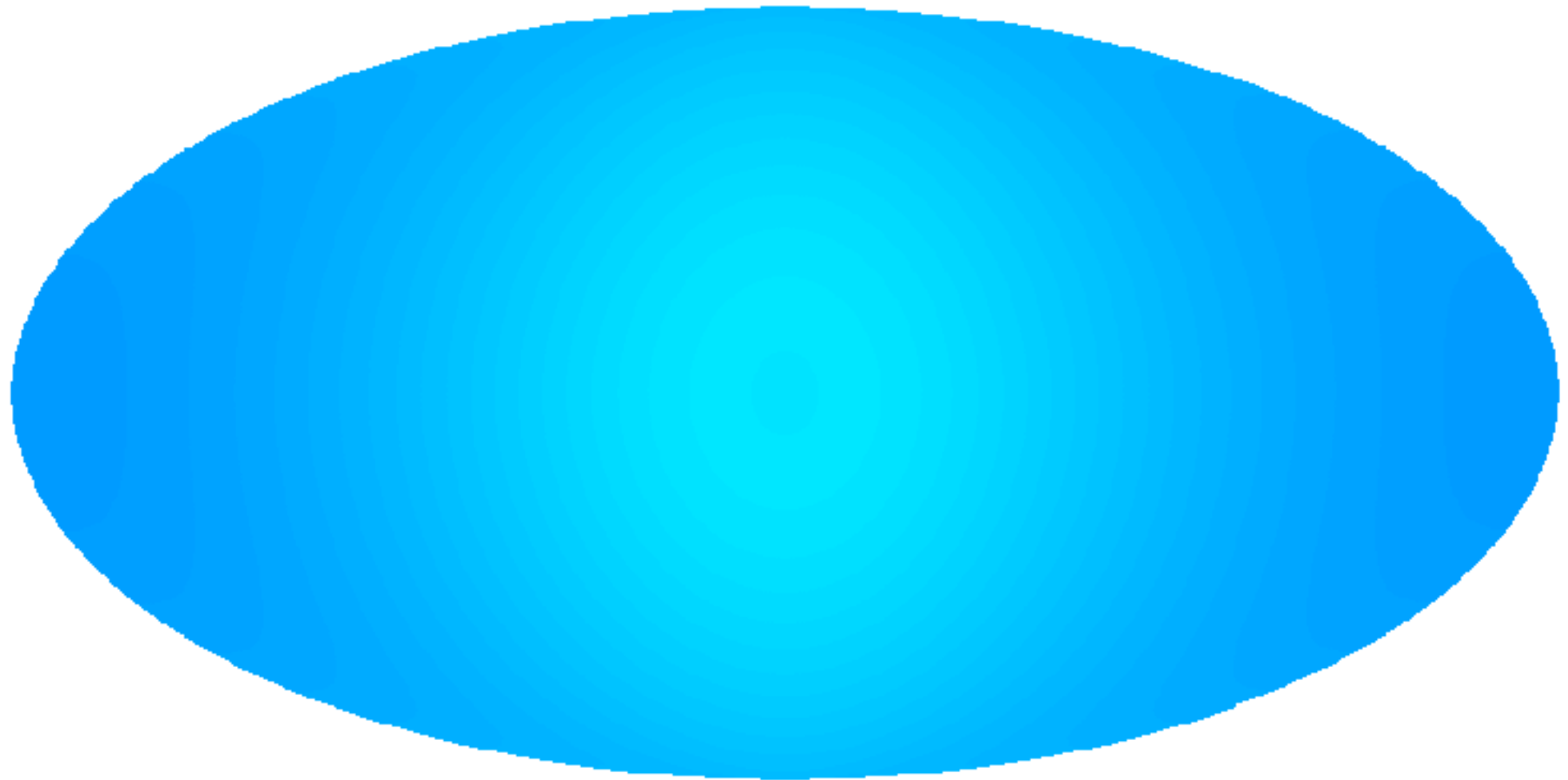
*emission from resolved subhalos (SubSm+SubSub)*



-3.0  2.0 Log(Intensity)

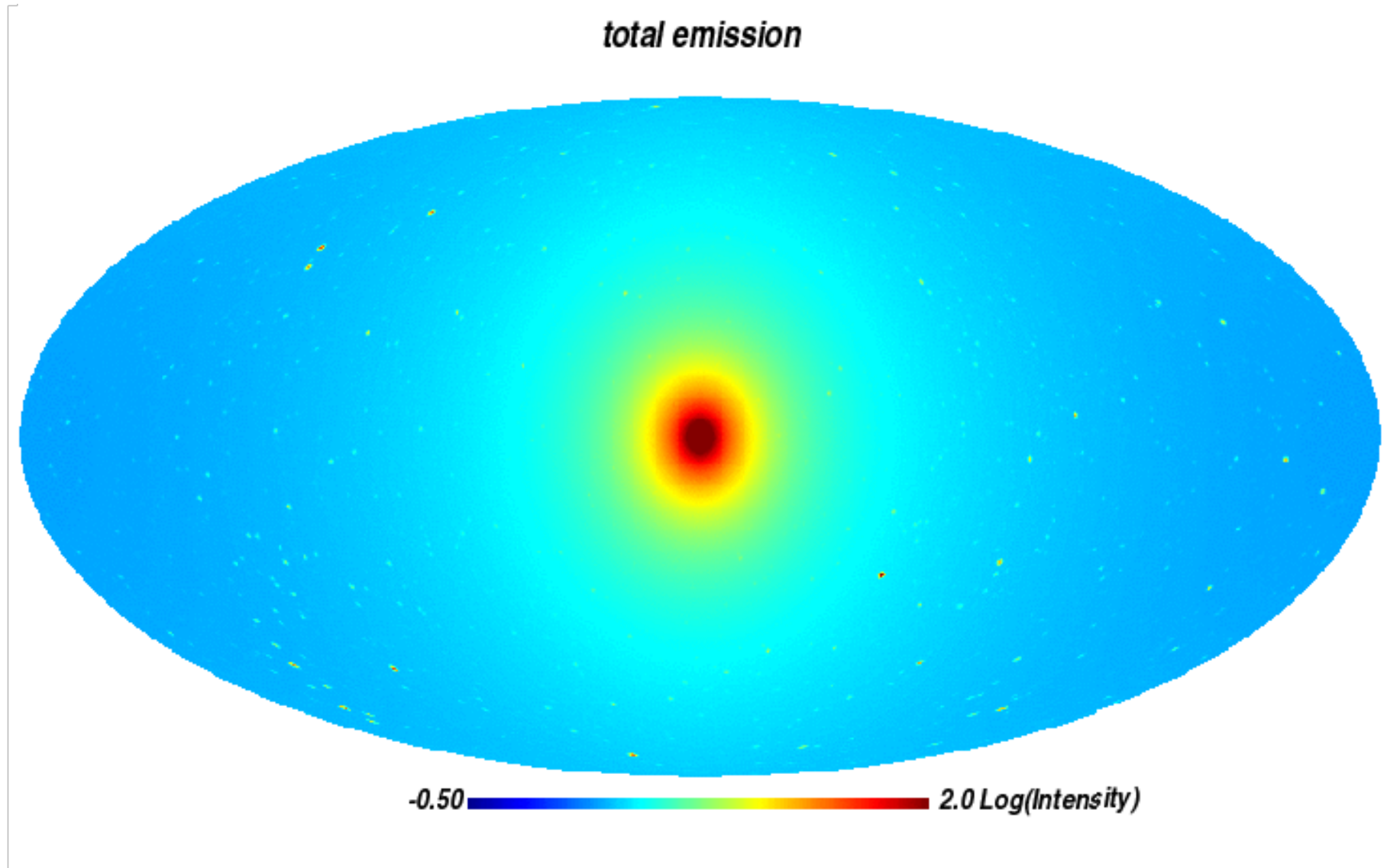
# Milky Way halo seen in DM annihilation radiation

*unresolved subhalo emission (MainUn)*

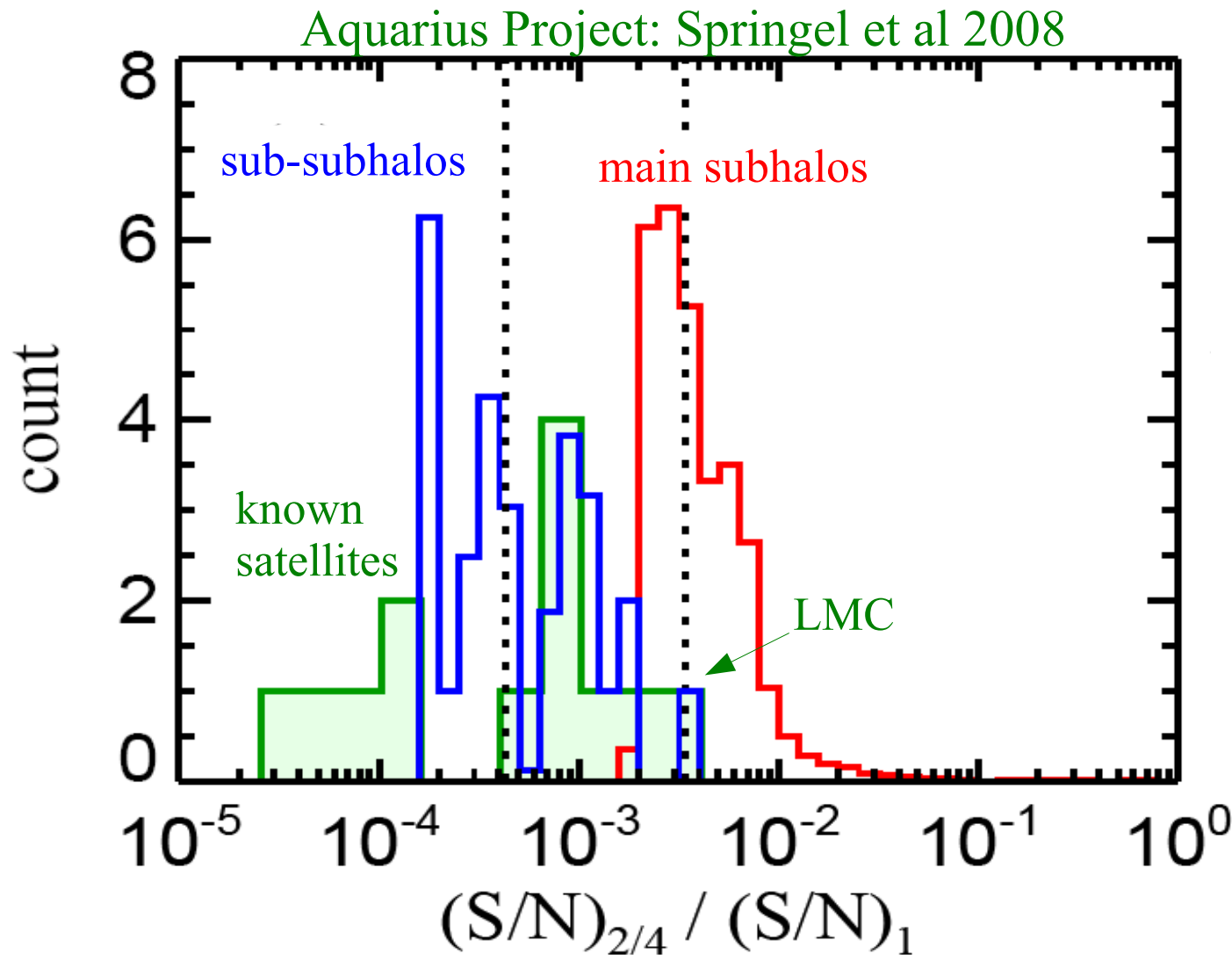


-0.50  2.0 Log(Intensity)

# Milky Way halo seen in DM annihilation radiation

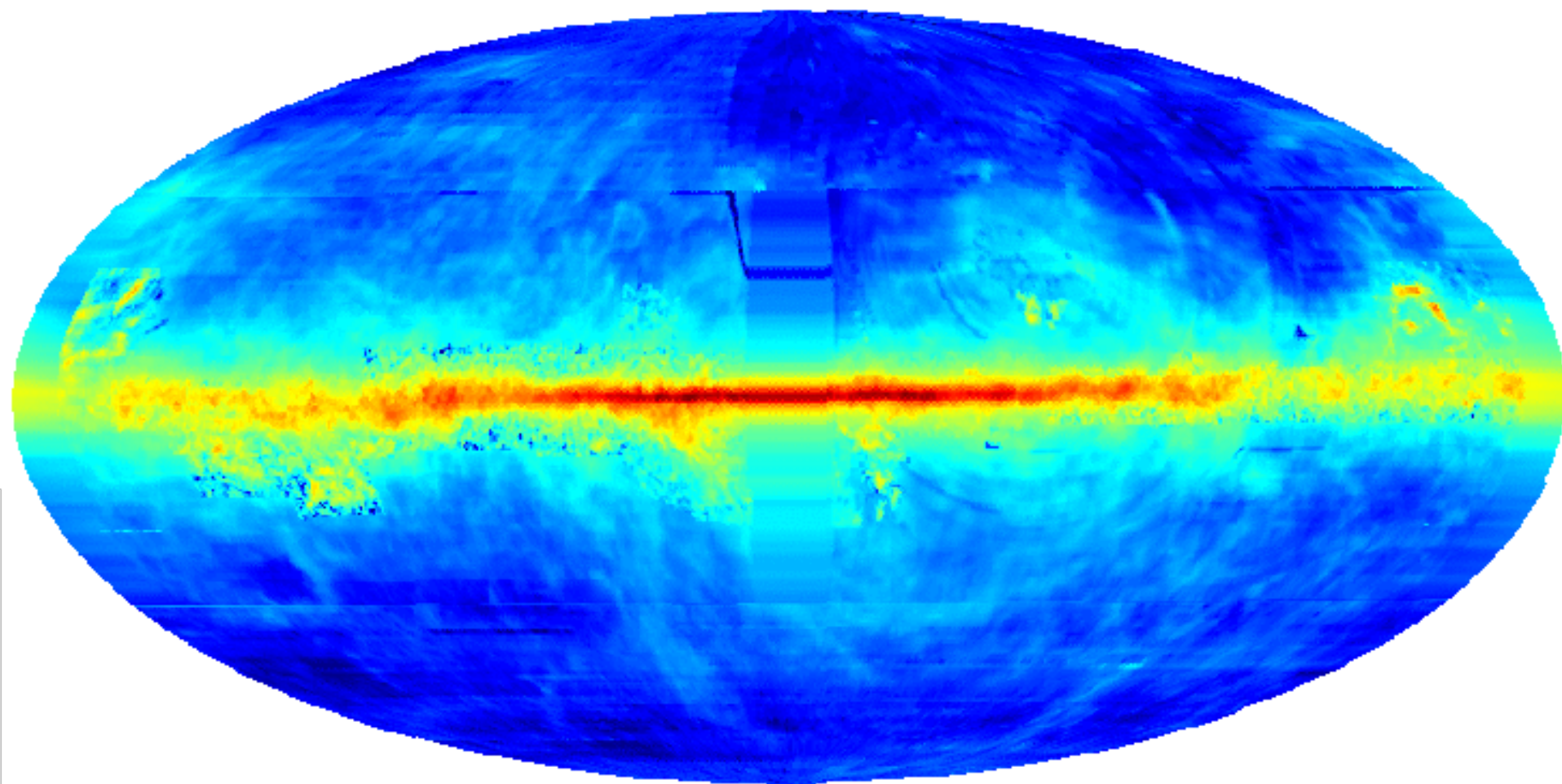


S/N for detecting subhalos in units of that for detecting the main halo  
30 highest S/N objects, assuming use of optimal filters



- Highest S/N subhalos have 1% of S/N of main halo
- Highest S/N subhalos have 10 times S/N of known satellites
- Substructure of subhalos has no influence on detectability

***GALPROP, optimized***



**-1.0**  **2.0 Log(Intensity)**

# Conclusions about clumping and annihilation

- Subhalos increase the MW's total flux within 250 kpc by a factor of 230 as seen by a distant observer, but its flux on the sky by a factor of only 2.9 as seen from the Sun
- The luminosity from subhalos is dominated by small objects and is nearly uniform across the sky (contrast is a factor of  $\sim 1.5$ )
- Individual subhalos have lower S/N for detection than the main halo
- The highest S/N *known* subhalo should be the LMC, but smaller subhalos without stars are likely to have higher S/N

# Cold Dark Matter at high redshift (e.g. $z \sim 10^5$ )

Well *after* CDM particles become nonrelativistic, but *before* they dominate the cosmic density, their distribution function is

$$f(\mathbf{x}, \mathbf{v}, t) = \rho(t) [1 + \delta(\mathbf{x})] N[\{\mathbf{v} - \mathbf{V}(\mathbf{x})\}/\sigma]$$

where  $\rho(t)$  is the mean mass density of CDM,

$\delta(\mathbf{x})$  is a Gaussian random field with finite variance  $\ll 1$ ,

$\mathbf{V}(\mathbf{x}) = \nabla \psi(\mathbf{x})$  where  $\nabla^2 \psi(\mathbf{x}) \propto \delta(\mathbf{x})$

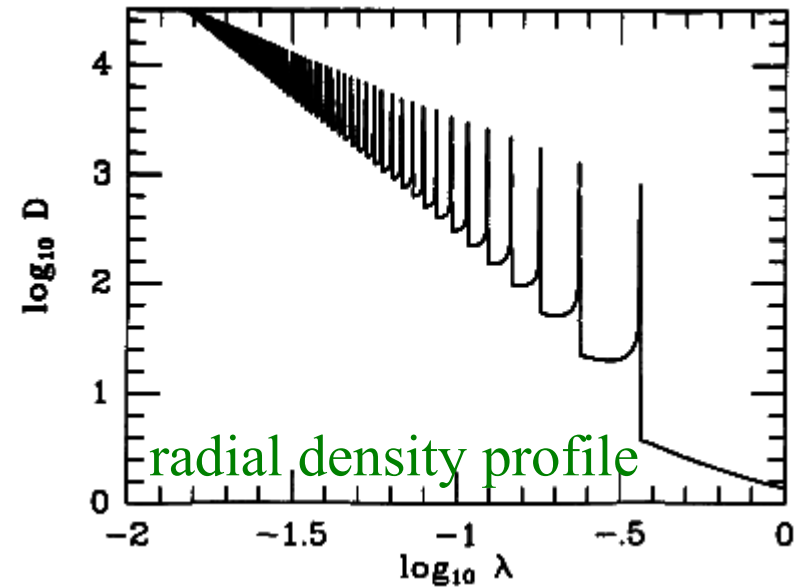
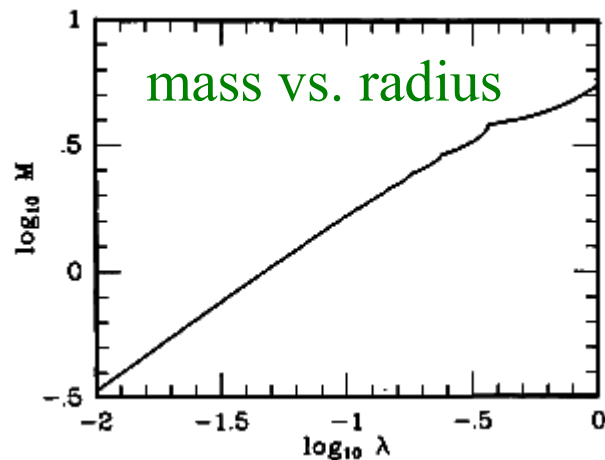
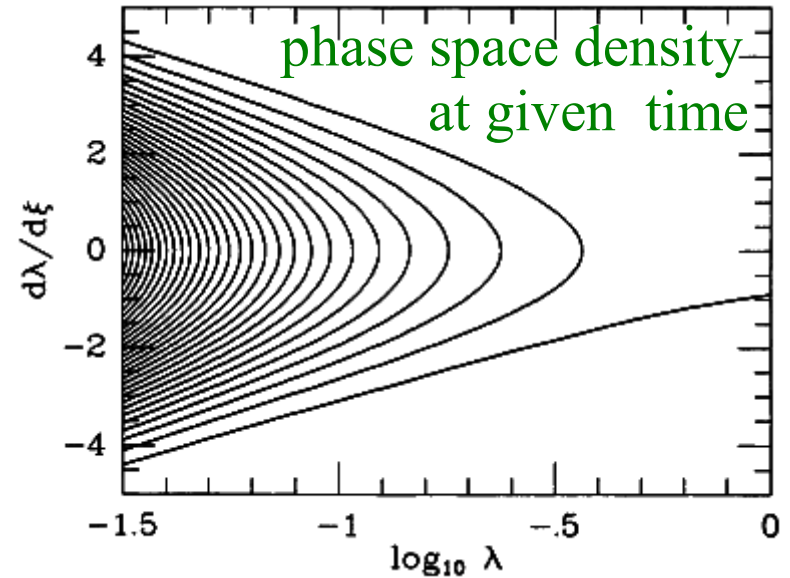
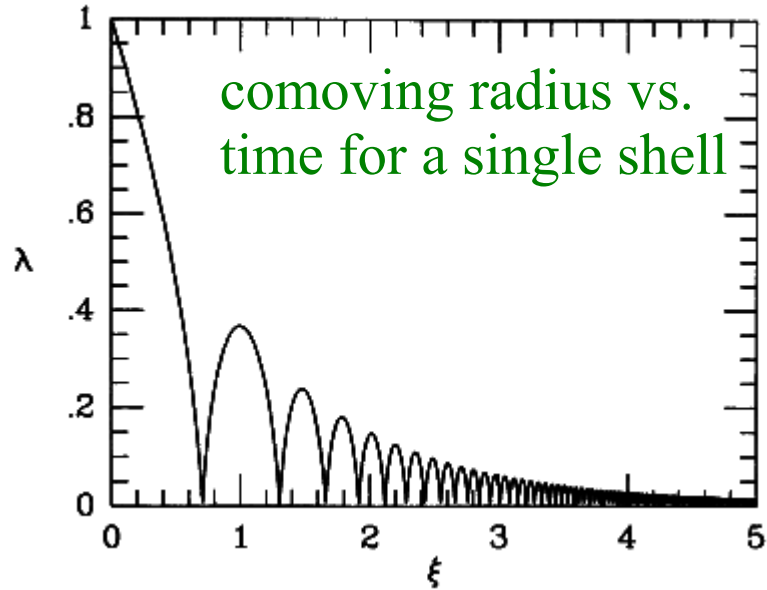
and  $N$  is standard normal with  $\sigma^2 \ll \langle |\mathbf{V}|^2 \rangle$

CDM occupies a thin 3-D 'sheet' within the full 6-D phase-space and its projection onto  $\mathbf{x}$ -space is near-uniform.

$Df/Dt = 0$   $\longrightarrow$  only a 3-D subspace is occupied at later times.  
Nonlinear evolution leads to a complex, multi-stream structure.

# Similarity solution for spherical collapse in CDM

Bertschinger 1985



# Evolution of CDM structure

## Consequences of $Df / Dt = 0$

- The 3-D phase sheet can be stretched and folded but not torn
- At least 1 sheet must pass through every point  $\mathbf{x}$
- In nonlinear objects there are typically many sheets at each  $\mathbf{x}$
- Stretching which reduces a sheet's density must also reduce its velocity dispersions to maintain  $f = \text{const.}$
- At a caustic, at least one velocity dispersion must  $\longrightarrow \infty$
- All these processes can be followed in fully general simulations by tracking the phase-sheet local to each simulation particle

# The geodesic deviation equation

Particle equation of motion:  $\dot{X} = \begin{bmatrix} \dot{\mathbf{x}} \\ \dot{\mathbf{v}} \end{bmatrix} = \begin{bmatrix} \mathbf{v} \\ -\nabla\phi \end{bmatrix}$

Offset to a neighbor:  $\delta\dot{X} = \begin{bmatrix} \delta\mathbf{v} \\ \mathbf{T} \cdot \delta\mathbf{x} \end{bmatrix} = \begin{bmatrix} 0 & \mathbf{I} \\ \mathbf{T} & 0 \end{bmatrix} \cdot \delta X$ ;  $\mathbf{T} = -\nabla(\nabla\phi)$

Write  $\delta X(t) = D(X_0, t) \cdot \delta X_0$ , then differentiating w.r.t. time gives,

$$\dot{D} = \begin{bmatrix} 0 & \mathbf{I} \\ \mathbf{T} & 0 \end{bmatrix} \cdot D \quad \text{with } D_0 = I$$

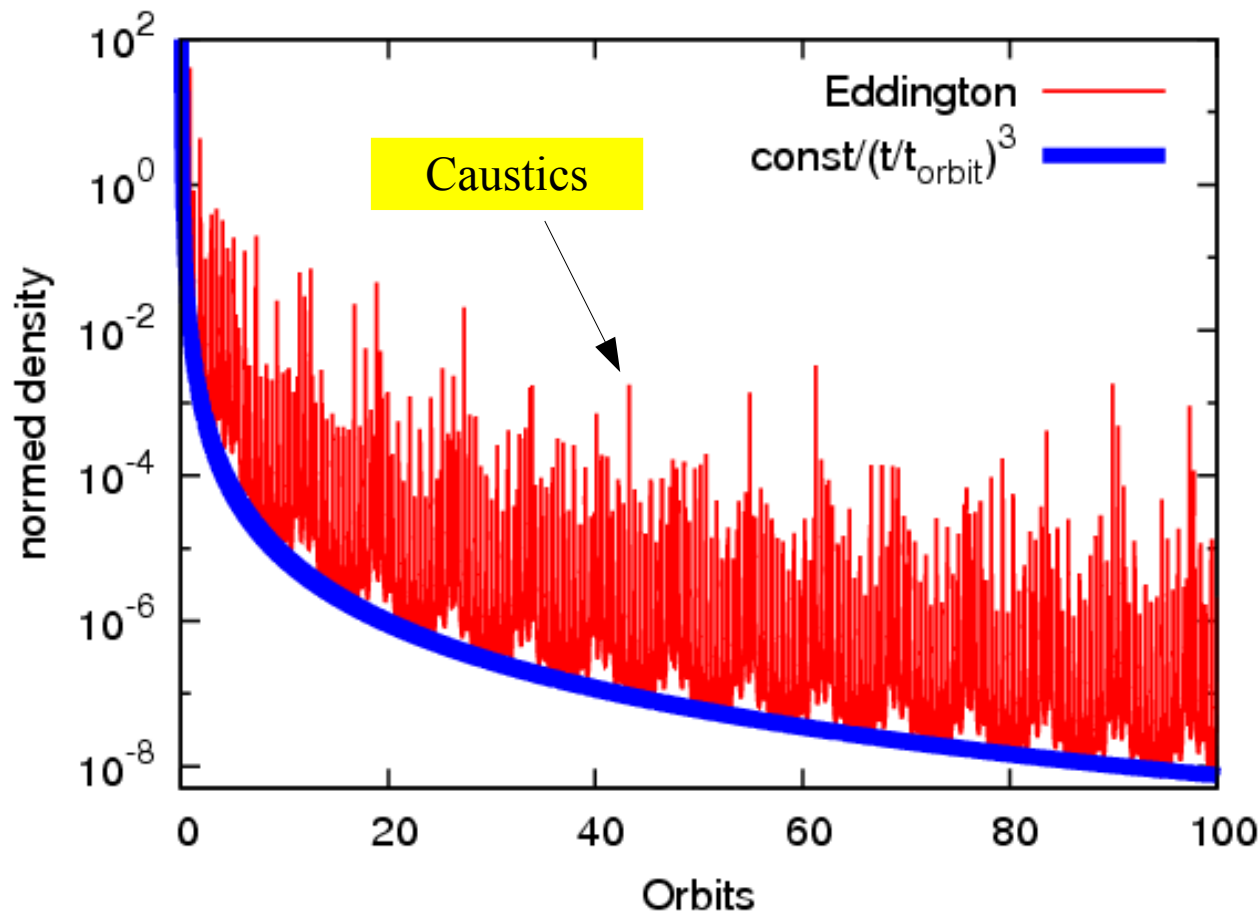
- Integrating this equation together with each particle's trajectory gives the evolution of its local phase-space distribution
- No symmetry or stationarity assumptions are required
- $\det(D) = 1$  at all times by Liouville's theorem
- For CDM,  $1/|\det(D_{\mathbf{xx}})|$  gives the decrease in local 3D space density of each particle's phase sheet. Switches sign and is infinite at caustics.

# Static symmetric potentials

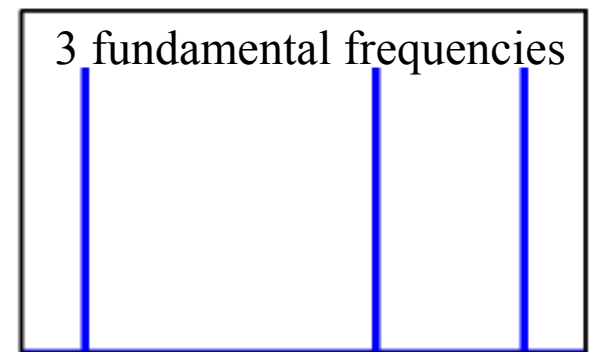
Mark Vogelsberger, Amina Helmi, Volker Springel

Axisymmetric Eddington potential

$$\Phi(r, \theta) = v_h^2 \log(r^2 + d^2) + \frac{\beta^2 \cos^2 \theta}{r^2}$$



Spectral analysis of orbit:



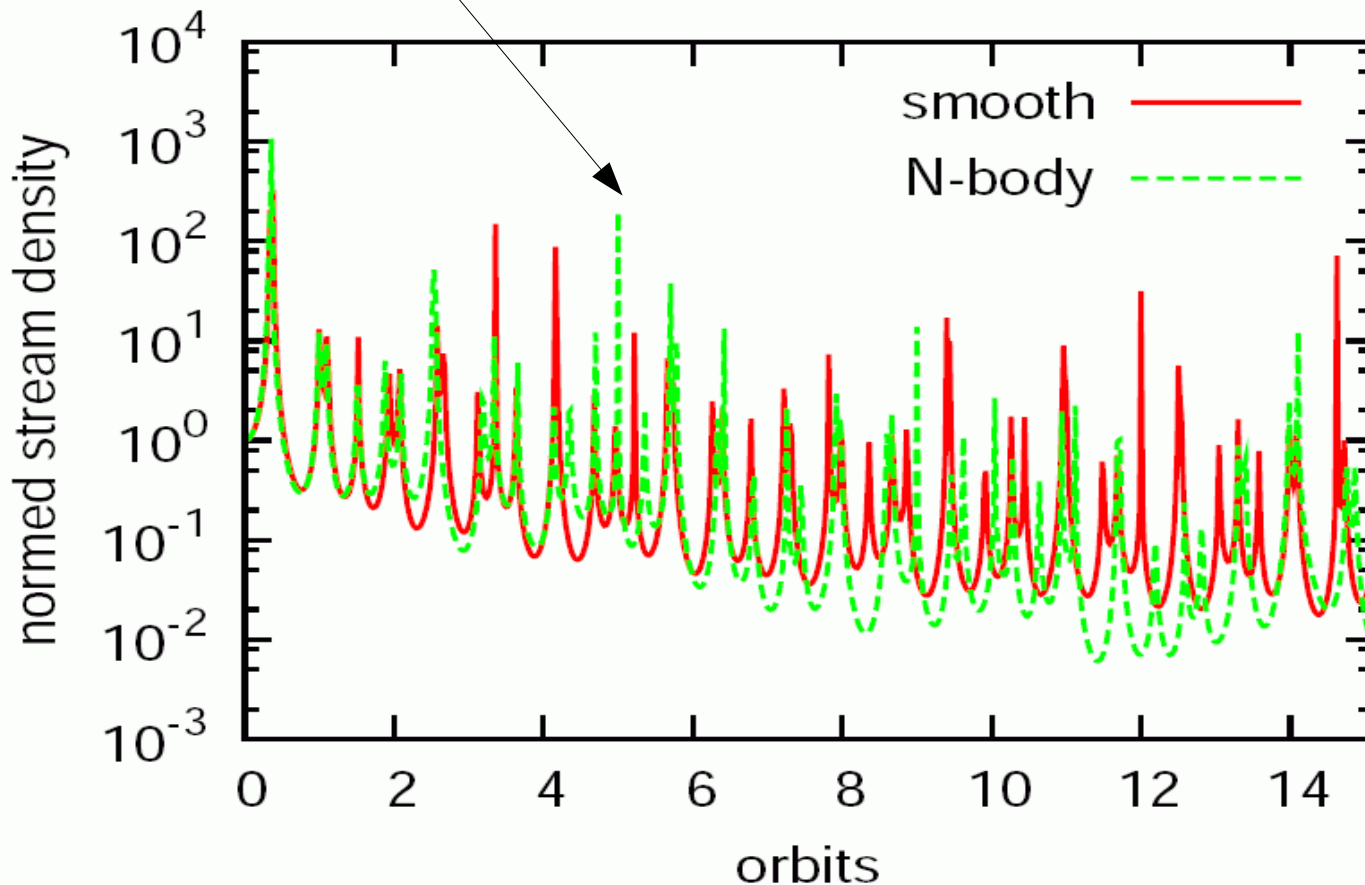
density decreases like  $1/t^3$

# A particle orbit in a live Halo

spherical Hernquist  
density profile

caustics resolved in N-body live  
halo!

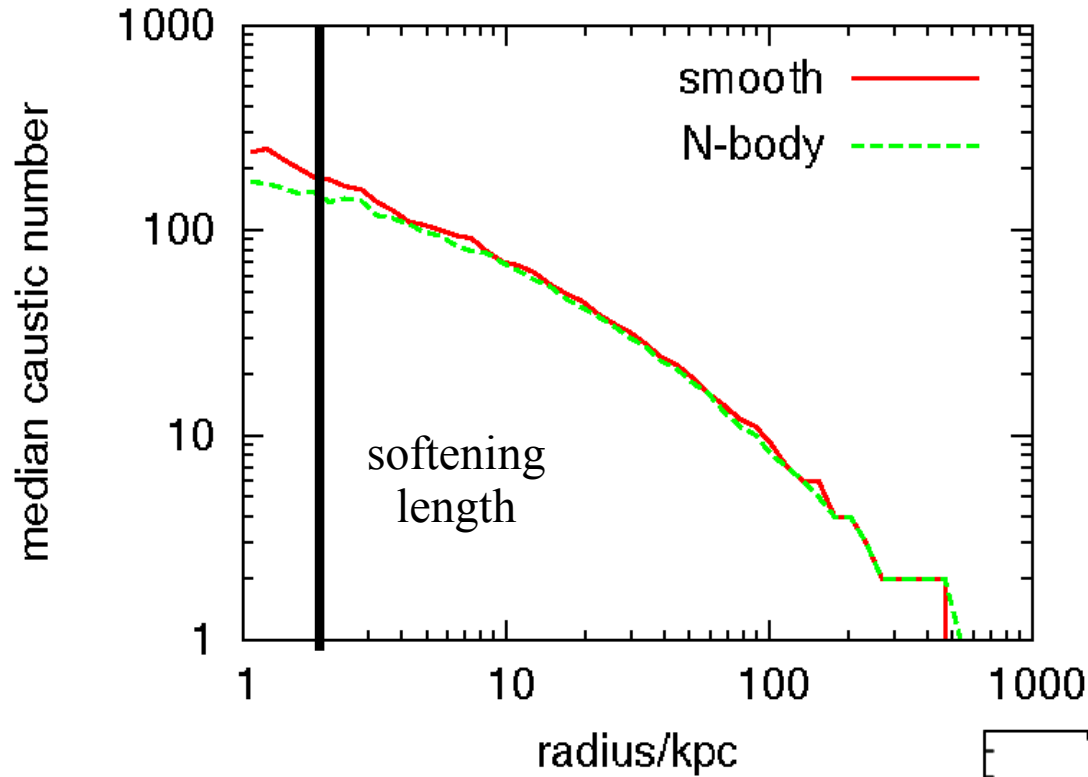
$$\rho(r) = \frac{M}{2\pi} \frac{a}{r} \frac{1}{(r+a)^3}$$



general shape and  
caustic spacing/number  
very similar!

phase-space density  
conservation:  $10^{-8}$

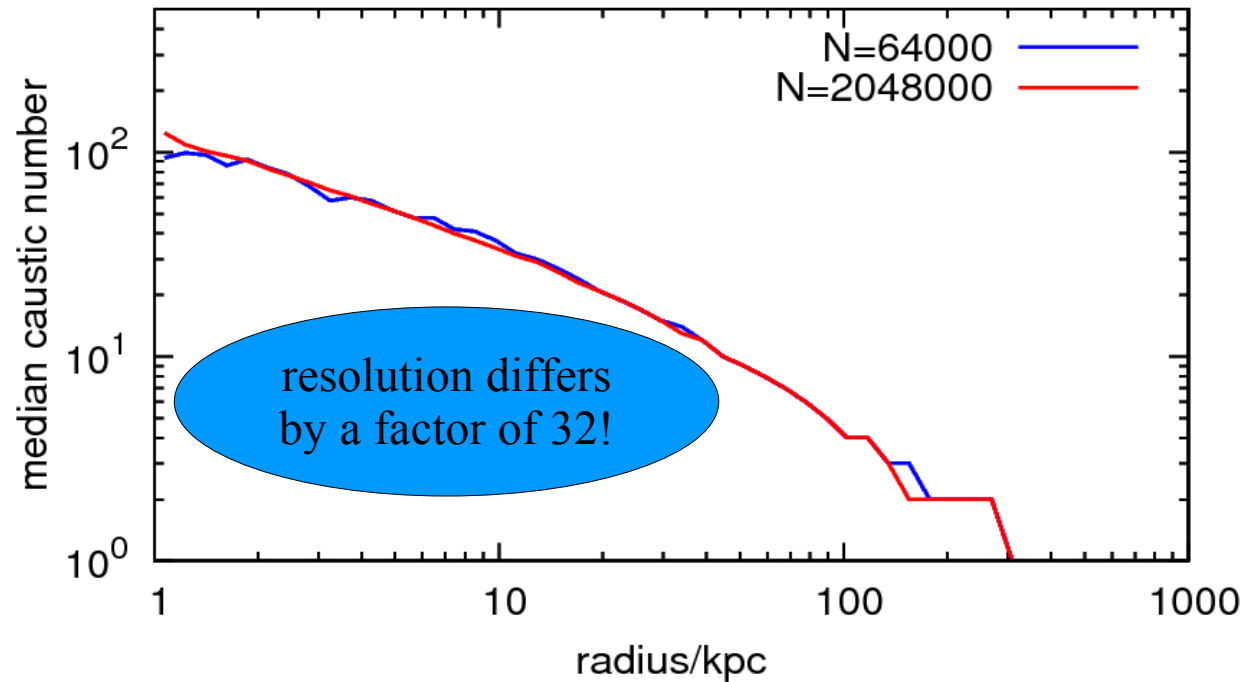
# Number of Caustic Passages



analytic and N-body  
results nearly the same!

**Annihilation boost  
factor estimates  
due to caustics  
should be very robust!**

**Very stable against  
particle number  
and softening length!**



# Conclusions about streams and caustics

- GDE robustly identifies caustic passages and gives fair stream density estimates for particles in fully 3-D CDM simulations
- Many streams are present at each point well inside a CDM halo (at least 100,000 at the Sun's position)
  - quasi-Gaussian signal in direct detection experiments
- Caustic structure is more complex in realistic 3-D situations than in matched 1-D models but the caustics are weaker
  - negligible boosting of annihilation signal due to caustics

# Myths about small-scale structure and DM detection

- Halo DM is mostly in small (e.g. Earth mass?) clumps
  - ▶ direct detectors typically live in low density regions
- DM streams —▶ non-Maxwellian, “clumpy”  $f(\mathbf{v})$ 
  - ▶ direct detectors will see an irregular energy distribution
- Small (Earth-mass?) clumps dominate observable annihilation signal
- Dwarf Spheroidals/subhalos are best targets for detecting annihilation (and are boosted by sub-substructure)
- Smooth halo annihilation emission is dominated by caustics

# Myths about small-scale structure and DM detection

- Halo DM is mostly in small (e.g. Earth mass?) clumps
  - direct detectors typically live in low density regions
- DM streams → non-Maxwellian, “clumpy”  $f(\mathbf{v})$ 
  - direct detectors will see an irregular energy distribution
- Small (Earth-mass?) clumps dominate observable annihilation signal
- Dwarf Spheroidals/subhalos are best targets for detecting annihilation (and are boosted by sub-substructure)
- Smooth halo annihilation emission is dominated by caustics